2011-08-04

Characterization of the Desorption Electrospray Ionization Mechanism Using Microscopic Imaging of the Sample Surface

Michael Craig Wood
Brigham Young University - Provo

Characterization of the Desorption Electrospray Ionization Mechanism

Using Microscopic Imaging of the Sample Surface

Michael Wood

A dissertation submitted to the faculty of
Brigham Young University
in partial fulfillment of the requirements for the degree of

Doctor of Philosophy

Paul Farnsworth, chair
Matthew Asplund
David Dearden
Milton Lee
Eric Sevy

Department of Chemistry and Biochemistry

Brigham Young University

December 2011

ABSTRACT

Title: Characterization of the Desorption Electrospray Ionization Mechanism Using Microscopic Imaging of the Sample Surface

Michael Wood
Department of Chemistry and Biochemistry, BYU
Doctor of Philosophy

Desorption electrospray ionization (DESI) is an ambient ionization technique for mass spectrometry. This solvent based desorption ion source has wide applicability in surface analysis with minimal sample preparation. Interest in improving detection limits, broadening applications, and increasing the spatial resolution for chemical imaging has led to studies of the DESI mechanism. An inverted microscope has been used to image interactions between the DESI spray and test analytes on a glass surface. Microscopic images recorded with millisecond time resolution have provided important insights into the processes governing analyte transport and desorption. These insights are the basis of a rivulet-based model for desorption that differs significantly from the widely-accepted momentum transfer model.

Keywords: [DESI, Desorption Electrospray Ionization, Microscopic, Imaging, Real-time, Mechanism, Fluorescence, Absorption, Coating, Rivulets, Mass Spectrometry]

ACKNOWLEDGEMENTS

This entire experience was realized through an extensive network of support. I would like to thank:

1) Dr. Farnsworth, for taking me as a student.

2) My family, especially Steve, for keeping me motivated, and my parents for never giving up on me

3) My lab mates for their loyalty and keeping me organized, devoted, and positive.

4) My close friends: Jared, Josh, and Roman for their extreme faith.

5) My committee for their patience and willingness to help with my project.

6) The Precision Machine Shop, Instrument Shop and Department Staff for amazing work.

7) The Chemistry department and BYU for providing the opportunity.

Table of Contents

1 Introduction

1.1 Mass Spectrometry

Modern mass spectrometry (MS) is the culmination of many generations of scientific research to produce a powerful tool capable of enhancing the chemical understanding of the world around us. As a tool which measures the mass of atoms and molecules, MS provides a quick and definitive way for chemists to identify the compounds they have used for centuries. Mass spectrometry's variety of uses for both quantitative and qualitative analyses cannot be overstated. As the field of MS has grown, it has unlocked the doors to many areas of research outside chemistry, including life sciences, healthcare, energy research, manufacturing, material science, natural science, and the environmental sciences. New applications of MS to current problems are discovered constantly. Because MS plays an integral part in so many cutting edge fields, it is a significant contributor to modern economic growth. It could be argued that an understanding of the molecular world through MS is necessary for continued progress in these areas.

Considering the scope of MS today, it is intriguing to note that it started with a very controlled set of operating conditions that greatly limited the capabilities of the first mass spectrometers. Such limitations included operating within a vacuum and low (<100 m/z) molecular weight ions. Chemists have long sought ways to expand the operating conditions, and in doing so opened doors that pushed the technique into new areas and applications. While physicists, chemists, and engineers have expanded MS by removing many of the

limitations of the original instruments, there continue to be constraints on the technique that warrant further research. Due to the innumerable benefits of MS, mankind has a vested interest in the pursuit of expanding its capabilities. Therefore, it should be no surprise that many government and private organizations have made significant financial investments in the growing research in MS.

Significant financial backing has allowed researchers to focus on every aspect of MS for potential areas of improvement, creating a positive feedback cycle as it drives research to explore and discover new applications. Continuing application research can improve understanding of fundamental mechanisms of MS. This in turn would fuel new ideas for optimizing the use of MS while extending its limits. A significant fraction of recent and current research efforts reflect both a rapid expansion in the field of novel ionization sources and a need to understand the fundamental aspects of said ionization sources for further improvement in sensitivity and application.

1.1.1 The Art – Theory of Separating Ions

The theory of the atom was created based on evidence gathered through research, observation, and induction. Since the inception of the atomic theory, scientists have wanted to 'see' an atom. While our understanding of matter has progressed rapidly from the early beginnings in alchemy, few things give evidence of atoms and molecules as strong as that provided by MS.

1.1.1.1 Atomic and Molecular Theory

The word atom is derived from the ancient Greek word 'Atomos' meaning indivisible. It was theorized that matter could be broken down to a point, into individual atoms, after which it could not be further broken down. John Dalton is the father of modern atomic theory. Using various gases, Dalton was able to show that the compounds in his experiments combined in specific ratios. He proposed 5 rules, taught in freshman chemistry courses today, and summarized below:

1. Elements are made of tiny particles called atoms.
2. Atoms from an element are indistinguishable from each other.
3. Atoms from one element are distinguishable from atoms of another element.
4. Atoms from different elements can combine to form compounds, and a given compound is always formed with the same combination of atoms.
5. In a chemical reaction, atoms are neither created nor destroyed.

These rules established the basis upon which modern chemistry is built. Atomic theory states that matter is composed of atoms. Atoms can be combined at specific ratios to produce molecules. These theories were necessary for the rapid discovery and identification of elements as well as the assembly of the periodic table.

1.1.1.2 Ionization

Ionization is the process by which an atom or molecule gains an electric charge, usually through the loss or gain of an electron. For many years following Dalton's proposal of the atomic theory, scientists held that the atom was indivisible. J.J. Thomson first demonstrated the existence of

the electron through his famous experiments with cathode ray tubes.[1] In these experiments he demonstrated the ability to deflect electrons with an electric or magnetic field. He proposed that the electrons were generated from the atoms themselves in the gas and as such indicated that the atom was divisible. Being divisible and typically of neutral charge, Thomson also proposed the atom must contain a positive counterpart to the electron.

The discovery of the electron was a critical step in the development of the mass spectrometer. The discovery led researchers to understand the duality of an atom's charge; the nucleus is positive while the electron shell is negative. Since electrons are far smaller and found outside the nucleus they can easily be added or removed. While atomic ionization involves the removal or addition of electrons, molecular ionization can also occur through addition of other charged species, such as protons.

1.1.1.3 Transport of Ions

Ions play a fundamental role in MS. MS focuses on ions due to their ability to respond to an electric (or magnetic) field. The force a charge experiences in the presence of another charge is given by equation 1:

$$\vec{F} = k_e \frac{q_1 q_2}{r^2} \vec{v} \qquad (1)$$

where k_e is Coulomb's constant, q_1 and q_2 are the individual charges, and r is the distance between the charges. A negative value for force indicates an attraction and a positive value for force indicates repulsion. Thus, particles with like charges will repel each other. Charged particles generate electric fields. The strength of an electric field generated by a charged particle is given by equation 2:

$$E = k_e \frac{q}{r^2} \quad (2)$$

where k_e is Coulomb's constant, q is the charge on the particle and r is the distance from the particle. While both of these equations are defined for fixed or slow moving particles, they indicate that it is possible to control the movement of charged particles. A more complete equation for the instantaneous force a particle experiences while moving through both electric and magnetic fields is given by the Lorentz equation:

$$\vec{F} = q\vec{E} + q\vec{v} \times \vec{B} \quad (3)$$

where q is the charge on the particle, E is the electric field at the particle's location, v is the velocity of the particle, and B is the magnetic field at the particle's location. Thus, a charged, free standing particle can be directed between any two points by controlling the electric and magnetic fields which surround it. Careful manipulation of charged molecules and atoms is necessary for separation and measurement by MS. This fundamental difference between charged particles and neutral particles is necessary for molecular measurements by MS and the basis upon which all mass spectrometers are constructed.

1.1.1.4 Fundamentals of a Mass Spectrometer

Mass spectrometers perform three major functions with each analysis: (1) ionization, (2) mass selection, and (3) detection. Typically each function is performed by a separate component of the mass spectrometer. Some mass spectrometers have interchangeable components, especially in the case of the ion source. Over the years, improvements have been made in each of the three areas. As with any field that matures, there are theoretical limits to the

improvements that can be made, and MS is no exception. Research continues in each of the major areas of MS.

Traditionally MS techniques were classified by the component that performed the mass selection. However, with the realization that any ion that could be manipulated by a mass selector could be detected, the true limit to developing new analyses became the dependence on analyte ionization and transport. This dependence has given rise to the practice of identifying MS techniques by their ion source as well as their mass selector. It is increasingly common to refer to a technique solely by its ion source.

1.2 Ambient Ionization

While significant progress has been made in the areas of separation and detection, the limiting factor in many modern analyses remains the method of ionization. This limitation has largely been due to the necessity of operating in a vacuum. All mass spectrometers must operate within some form of vacuum to increase the mean free path of ions and preserve charge on the ions by reducing collisions. Early ion sources were not excluded from this limitation and were designed and constructed with the vacuum in mind. Operating an ion source in a vacuum requires varying degrees of sample preparation and is not conducive to volatile samples, labile samples, *in vivo* samples, or time sensitive samples. These limitations have driven researchers to look for ways to reduce the influence the vacuum has on an analysis, and to develop ambient ionization.

Ambient ionization sources have provided a way to avoid the problems presented when working with a vacuum system through ionization of the sample at ambient pressure, typically outside the mass spectrometer, before the ionized sample is transported into the vacuum for

analysis. The ability to analyze a far wider range of samples through ambient ionization has fueled the recent, rapid growth of research in this area.

It is important to note that the development of ambient ionization sources occurred gradually, preceded by many successive improvements in non-ambient ionization sources. Early sources, such as chemical ionization and electron impact, were contained within a controlled environment within the mass spectrometer. Later sources such as electrospray ionization and atmospheric pressure chemical ionization were developed to operate at atmospheric pressure. While these and other sources, such as inductively coupled plasma, can be operated at ambient pressures, they are not considered ambient ionization techniques due to significant sample preparation requirements. As summarized by Harris et al., "ambient ionization is characterized by operating in the open air, and with the ability to probe the surface of samples of any size and shape."[2]

Currently, ambient ionization chiefly consists of two main groups of ion sources: solvent-based ion sources and plasma-based ion sources. Rapid development is occurring in both areas and in many cases the two groups are complementary, working with different classes of molecules. This complementary nature is most likely due to the very different ionization mechanisms that are theorized to be at work.

1.2.1 Solvent Based

Solvent based ion sources are derived from the electrospray ionization (ESI) source, first demonstrated by Jon Fenn et al.[3] In this technique the analyte molecule is dissolved and transported by a solvent. While the general ESI mechanism has never been fully explained, droplets produced by any of the solvent-based ambient ionization methods undergo a size

reduction process, such as fragmentation, fission, or evaporation, producing charged molecules from the analyte that was in solution. The ESI source was the first source that could be operated at ambient pressures. It is one of the most widely used ion sources today. Currently, the fastest growing and most widely published ambient desorption ionization source is desorption electrospray ionization (DESI).

1.2.2 Plasma Based

Researchers have been experimenting with plasmas for decades. Plasmas are generated by ionizing gases. Ambient ionization sources typically use helium for plasma generation. Plasma-based ambient ion sources have surged in popularity in recent years. The first major source to see commercial success was direct analysis in real time (DART) developed by the Cody research group.[4] A variety of plasma sources have since been described, varying in operating parameters such as gas flow rate, power, frequency, alternating or direct current, and operating distance. Investigation into plasma source ionization has yet to conclusively identify the mechanisms by which analytes are ionized. It remains the focus of continued research.

1.3 Desorption Electrospray Ionization

Desorption electrospray ionization (DESI) was first reported by the Cooks research group in 2004 in *Science*.[5] The DESI source was a variant of the ESI source, with the addition of a nebulizing gas jet placed around the solvent capillary. Initially, Cooks' group employed a setup similar to one designed in the '90s called the sonic spray ion source (SSI). They demonstrated a very simple and economical construction using Swagelok fittings for the analysis of amino acid clusters.[6] Shortly thereafter the group applied voltage to the SSI setup and declared the

creation of a new ion source termed the electrosonic spray ionization (ESSI).[7] While nearly identical to the ESSI source in construction, the DESI operating parameters were specifically optimized for surface analysis, unlike ESSI and SSI, in which the analyte is introduced through the solvent stream.

1.3.1 Design - DESI

The DESI source is fairly simple. It is constructed from two capillaries and a housing connected to a high pressure gas line. The inner and outer diameters of the capillaries are chosen such that the smaller diameter capillary can be run through the larger diameter capillary. The smaller inner capillary is connected to a syringe pump for the delivery of solvent. The larger outer capillary is for the transport of the nebulizing gas. A high voltage (3-5 kV) is applied to the solvent. Figure 1-1 illustrates the basic components of the DESI source: an inner capillary inserted into a larger outer capillary. The dotted arrows represent the flow of the nebulizing gas, while the solid arrow represents the flow of the solvent. The DESI source is typically angled toward a flat surface placed in front of an inlet to the mass spectrometer.

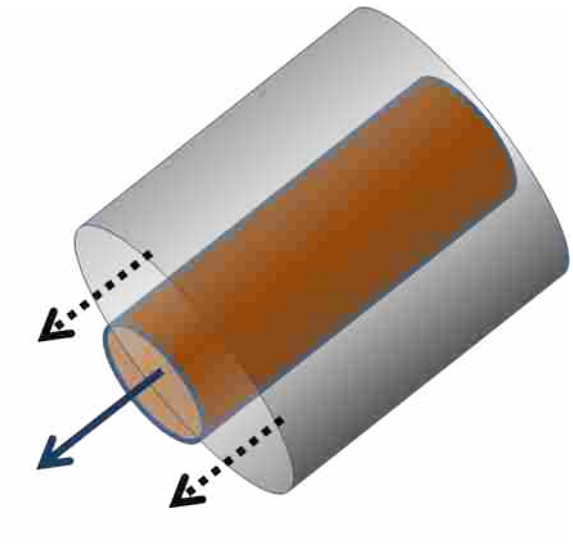

Figure 1-1 DESI emitter tip. Dotted arrows represent nebulizing gas; the solid arrow represents the flow of solvent. (Not to scale)

Unlike previous solvent-based ion sources, analyte is not present in the solvent itself, but desorbed from a surface. This seemingly minor difference is important in the context of sample preparation, in many cases requiring absolutely no sample preparation. Desorption of an analyte directly into the mass spectrometer without sample preparation makes it possible to analyze many things that were previously outside the realm of other ion sources. This novel difference has largely been the reason for the rapid growth of ambient ionization sources in recent years, and DESI in particular. Wide acceptance of the DESI source can also be attributed to the many applications that have been demonstrated since it was first developed. Some of the more prominent applications, such as detection of pharmaceuticals or explosives, fall within areas that are well funded, providing a strong feedback cycle for more investment into the DESI source.

1.3.2 Variations of DESI

Variants of the DESI technique have been introduced in the last few years, expanding DESI capabilities and possible analyses using a DESI source. Other variations have been presented to further simplify the experimental process. A brief overview of some of the most pertinent DESI variants is listed below.

1.3.2.1 Non-proximate

Typically, DESI is operated a few centimeters or less from the inlet of the mass spectrometer to optimize signal. Such a setup reduces collisional loss of charge and diffusion by reducing the travel distance into the instrument. The Cooks group demonstrated[8-9] that it was possible to operate much further from the instrument by employing a transfer line between the instrument and the collection location. They showed that the DESI source itself can be operated at an extended distance from the mass spectrometer, and that while the corresponding signal generated in the instrument is orders of magnitude smaller than when the sample is close to the inlet, the noise is diminished as well. There are many obvious applications for non-proximate detection. The most obvious application is when the sample is not easily placed near the mass spectrometer, for example, when an analysis must be done in a public location while simultaneously allowing the mass spectrometer to be kept at a distance from non-technical personnel. Non-proximate detection has been shown to be effective at up to 3 meters in distance from the mass spectrometer.[8]

1.3.2.2 Reactive DESI

A major breakthrough for desorption electrospray ionization came with the incorporation of additional compounds into the solvent spray to increase sensitivity. Reactive DESI works by selecting a target molecule that has poor response to standard DESI, and incorporating adducts that will selectively react with the target analyte, similar to many of the adducts found with common cations present in electrospray. This is a direct way to increase selectivity and sensitivity to target molecules. Reactive DESI was first mentioned in the original DESI paper as a way to introduce substrates to enzymes, and in more detail later by Cooks' group for decreasing detection limits of explosives.[10] Reactive DESI was also briefly mentioned in the same journal issue for improved detection of pharmaceuticals.[11] Reactive DESI has been shown to be useful for distinguishing isomers,[12] oxidizing analyte compounds,[13] oxime formation of metabolites in urine,[14] and adduct formations with triperoxide triacetone.[15]

1.3.2.3 Geometry Independent DESI

Geometry independent(GI) DESI was introduced by Venter and Cooks as a convenient fixed orientation DESI to improve the ease of use over traditional DESI.[16] The GI setup secures both the spray capillary and the sampling capillary in an open ended chamber. Applying the opened end of the chamber to a surface seals the chamber while the spray capillary and the sampling capillary are both 90° from the surface. This setup suffers from lower sensitivity but increases the ease of use by removing the need to optimize the spray angle.

1.3.2.4 Transmission Mode DESI

Transmission mode DESI was proposed by Chipuk and Brodbelt as an alternative to traditional desorption electrospray ionization in an effort to reduce the number of operating parameters.[17] A standard DESI analysis includes many parameters that must be optimized for ideal results. These include angle of the spray, distance the emitter tip is from the sample, angle of the sample with regard to the mass spectrometer, and material upon which the sample is placed. By introducing a mesh barrier containing the analyte, transmission mode DESI removes these parameters and simplifies the operating conditions by allowing the DESI source to point directly at the mass spectrometer, passing through the analyte coated mesh, instead of being deflected off a surface. Despite the removal of spray parameters such as spray angle and sample angle, the spray plume still needs to be optimized for maximum interaction with the mesh.[18]

1.3.2.5 Nanospray DESI

Roach et al. first described the nanospray-desorption/electrospray ionization source in 2010 as surface liquid extraction method.[19] The nanospray DESI does not use a nebulizing gas or concentric capillaries. The source instead uses two separate capillaries connected by a solvent bridge that is in contact with the surface. The first capillary delivers a charged solvent to the surface, dissolving the analyte, while the second capillary draws the solvent up from the surface via capillary action and sprays the sampled analyte toward the mass spectrometer inlet similar to an electrospray.

1.3.2.6 Large Area DESI

In 2009 Cooks' research group developed the 'large area DESI' for detection of trace analytes spread over large surface areas.[20] Besides the increased size of the components, the large area DESI is constructed different than the traditional DESI in several key ways. The outer 'capillary' is a metal tube with a diameter of 1 cm and the inner metal tube is capped with a septum. Both the solvent and the nebulizing gas are allowed to mix in the annular region between the two tubes and sprayed from the effective ring at the opening between the tubes.

Not only is the large area DESI constructed differently, but it is operated in a closed chamber to assist in droplet transport into the mass spectrometer. The applied pressure is close to 300 psi and the angle of operation is somewhat shallower at 40° as opposed to the steeper 55° of traditional DESI. An advantage of the large area DESI was demonstrated in a subsequent paper by Cooks' group showing that swabs could be sampled after wiping large surface areas for analyte.[21] Wiping a large area is useful in cases where low concentrations of the analyte can be concentrated on the swab, or when the analyte is non-uniformly distributed, making sampling with DESI impractical.

1.3.2.7 MALDESI & ELDI

DESI can be combined with other ionization techniques for special applications. Matrix assisted laser desorption electrospray ionization (MALDESI) [22] and electrospray-assisted laser desorption ionization (ELDI)[23] are fundamentally similar hybrid ion sources that combine laser desorption and solvent based ionization. In both cases, a laser is focused on a sample to produce a high energy plume which interacts with the electrospray. The interaction of the plume with the spray generates charged particles that undergo electrospray-like processes to

produce the final ions. The difference between MALDESI and ELDI is that the former employs an analyte within a matrix while the latter does not.

1.3.3 Mechanisms

A common goal with any new analytical technique is broadening the application of the technique. While experimentation is a valuable approach for identifying areas of improvement, a fundamental understanding of the mechanisms behind an ionization technique is critical for improving an ion source. Despite the relatively simple design of the DESI ion source, the mechanism by which it operates is poorly understood. Even the mechanism for ESI, upon which DESI is based, is only partially understood many years after its introduction.[24] There is evidence supporting two different models for ion creation in the gas phase of ESI: the ion ejection model and the charged residue model, both of which should be applicable to DESI as well as ESI. Considering the lack of understanding of the separation of gas phase ions from the liquid phase, DESI has an added level of complexity inherent in sample transport that does not exist in ESI where the sample is dissolved in the solvent.

Current research into the mechanisms of DESI has focused on analyte removal through surface desorption, assuming that the ionization mechanism is similar to electrospray. Initially this assumption was difficult to make because it was not known how much solvent/analyte interaction actually occurred. With increased inspection, it became apparent that the solvent was dissolving analyte on the surface and transporting it into the gas phase. Due to the microscopic nature of DESI, non-invasive analysis of sample transport is difficult. However, improving our understanding of the mechanism on the surface is one way in which we can attempt to improve DESI-MS.

1.3.3.1 Initially Proposed Mechanisms

The Cooks group initially proposed three different mechanisms for possible analyte transport from the surface.[11, 25 26] They were: charge transfer, neutral volatization, and droplet pick-up. Charge transfer consisted of charged particles transferring charge to analyte, which was removed through static repulsion or sputtering into the gas phase. Neutral volatization consisted of volatile analyte molecules leaving the surface, interacting with the spray itself, and picking up a charge through collisions or charge transfer. The third mechanism, droplet pick-up, was the process of larger droplets making contact with the surface, dissolving the analyte and then producing ions through ESI like mechanisms.

While evidence for each of the three mechanisms existed, the droplet pick-up mechanism had some very definitive examples. It is possible to analyze proteins with DESI, but proteins could not undergo much of a sputtering affect and the vapor pressure of proteins is so low that it is unlikely that they would be volatile under DESI conditions. The ability to detect multiply charged ions existed in DESI, unlike any other desorption technique at the time, and similar to ESI.[26] Finally, some groups including the Van Berkel group coined the term 'washing affect', which could be visually detected on surfaces when the analyte had little affinity for the surface on which it was placed.[27]

1.3.3.2 Advances on the Droplet Pick-up Mechanism

As the droplet pick-up mechanism became more widely accepted, researchers used high magnification to inspect the desorption region as it was being sprayed. The Van Berkel group described the spray footprint, illustrating the central elliptical region that acted as the area of

most effective desorption and ionization.[27-28] They further concluded that solvent flow lines formed jets originating outward from the central elliptical region.

To investigate the various suggested mechanisms, the Cooks group used Doppler particle analysis to look at droplets leaving the surface during the desorption process.[29] By measuring droplet velocity and size, it was relatively easy for them to exclude chemical sputtering from the mechanism. They noted that "some droplets appear to roll along the surface, increasing contact time and presumably the amount of material that is taken up in the droplets during conditions typical of the DESI experiment." This paper further showed that the droplets leaving the DESI source were traveling at a mean velocity of 140 m/s and that the sheer gas itself prevented the formation of a stable Taylor cone, broadening the size distribution of droplets formed in the process. Their conclusion summarily ended most research into the other mechanisms by stating: "The evidence acquired in this study supports the droplet pick-up model as the major process leading to ionization of the analytes considered in the conditions studied here."

The Cooks group took data from the Doppler particle analysis results and used them to model droplets from DESI. They came to the conclusion that the high velocity droplets were creating micro splashes in a thin solvent film that formed on the surface containing the dissolved analyte.[30-31] Droplets that were splashed into the air from the thin film then contained dissolved analyte, carrying a charge which underwent ESI ionization processes to produce charged analyte.

In studying the capability of DESI for nucleotide analysis, Qui and Luo identified nucleotide clustering, similar to the clusters found in ESI, as evidence of momentum transfer.[32]

They showed that an increase in the acidity of the solvent increased the protonated guanine signal as well as clustering. The increased signal from clustered guanine was then used as supporting evidence for the formation of a thin film and momentum transfer.

1.3.3.3 Problems with the Droplet and Thin Film Splashing Mechanism

The thin film droplet ejection model suffers from a few significant problems that cannot easily be dismissed. In the modeling paper it states,[31] "Two of these simulations are emphasized here. They both include the collision of a 3.7 μm^3 [sic] in diameter fluid droplet with velocity 120 m/s impacting a thin fluid layer (1 μm in depth) on a flat surface in three dimensions." There is no statement about the velocity of the solvent on the surface. A high velocity droplet would make far less of a splash if it came in contact with a fast moving film as opposed to a free standing film. It is hard to imagine a free standing film in conjunction with fast moving nebulizing gas and collisions from high velocity droplets.

These simulations also do not take into consideration the fact that the ideal surface under which DESI is performed is Teflon. A rough Teflon surface is unlikely to have a flat film forming on the surface, but is more likely to have the solvent fill the grooves on the surface. Costa and Cooks cite a paper by Bereman and Muddiman[33] suggesting that there is a 1-2 second 'solvation delay.' They use this as a justification for the formation of the thin film over this time.[31] They state that "when spraying on glass, for instance, an easily visible surface layer is immediately evident," but go on to state that on Teflon no such film is observed. No further discussion is given to the topic as the researchers hypothesize that a thin film is formed. The conclusion section of the paper does however recognize the possibility of other mechanisms, but only after claiming that the droplet splashing from a thin film is a dominant factor in analyte

transfer: “The dominant hydrodynamic force is certain to be the momentum-transfer event. However, as previously noted, other non-hydrodynamic processes are possible in the gas phase and through chemical sputtering events.”

Transmission mode DESI poses yet another problem for the droplet splash model. A thin mesh of between 200-250 µm could easily support a 1 µm film, but fast moving jets most likely ‘blow’ the bulk of the solvent off the mesh into the air. Analyte at the front of the edge would quickly migrate around to the back side of the edge where direct momentum transfer would not occur.

The paper by Qui and Luo[32] suffers from a similar lack of evidence. An increase in solubility of the analyte in the solvent does not implicitly lead one to conclude that there must be a thin film of solvent on the surface. When considering the similarity of DESI to ESI it is reasonable to conclude that increased solubility would lead to increased analyte transfer and detection. A sample that was completely insoluble would most likely not interact with the analyte in any significant way and could theoretically be treated similarly to the rest of the substrate the analyte was placed on for analysis.

The Zare research group published a paper[34] that further calls into question the validity of droplet expulsion by exploring the limitations of DESI rapid sampling. The experiment was designed to see how quickly an area could be sampled with DESI. They constructed a spinning disk and used a Sharpie™ to draw alternating patterns onto the disk. By attaching the disk to a motor, they exposed the spray to alternating samples at high rates. With the disk divided into 8 wedges, they resolved sample variations at frequencies as high as 75 per second. At this rate,

the thin films would need to form much faster than a second (the time suggested by Bereman and Muddiman) to support the occurrence of droplet splashing and momentum transfer.

1.3.3.4 Further Mechanistic Research

Other approaches have been employed to better explain the sample transport in an effort to improve signal. Fluorescent dye has been instrumental as an analyte, allowing the collection of spatial data along with mass spectra. The Bereman and Muddiman paper[33] was the first to note that even removal of attomole amounts of dye could be tracked over time. Green et al. [35] used rhodamine B dye to analyze the spot size and shape created on a surface with regards to the signal. This characterization showed how the solvent behaved on the surface during ideal and non-ideal sampling.

Further research showed that varying the solvent composition with the analyte played an important role in sensitivity.[36] It was shown that solubility plays an important role in analyte transfer and that increasing the mole fraction of organic solvent over the conventional 0.5 with each analyte tested improved the signal. The optimal organic solvent mole fraction was found to be 0.8. Green et al. suggested that increasing the amount of organic solvent generated smaller droplets (visible on the surface) which were more effective for analyte transfer into the mass spectrometer. They defined DESI efficiency as:

$$E = \frac{I(M+H)}{A} \qquad (4)$$

where I(M+H) is the intensity of the mass peak of interest with an attached hydrogen and A is the area of erosion by the DESI spray. The group plotted DESI efficiency vs. droplet size

(volume) but did not address other possibilities, such as increasing volatility of the solvent, nor did they explain why a pure organic solvent is not optimal.

Cooks' research group demonstrated that additives to the solvent other than reactive molecules can improve signal as well.[37] In a demonstration of a non-reactive mix, different surfactants were tested for increase in signal. Many of the analytes showed an increased signal when sampled with a solvent containing a 20 μM surfactant while other solvents produced better results with lower (2 μM) concentrations of surfactant. They attributed the gain in signal to a decrease in the surface tension, resulting in smaller droplets generated from thin film surface splashing.

Both studies conclude that smaller droplet size plays an important role in the ionization process. The latter makes the assumption based on calculations using surface tension and constants used to calculate droplets from electrospray[36], while the former publication[37] uses water sensitive paper to look for droplet spots.

1.3.4 Applications

The Cooks group demonstrated the versatility of DESI by using it to detect explosives on common surfaces, biological molecules in plant tissues, and anti-histamines directly from the skin.[5] Introduced in 2004, the DESI source has seen many additional applications presented within the last 6 years.

1.3.4.1 Pharmaceuticals

After publishing their initial paper in *Science*, Cooks' group published an article in *Analytical Chemistry* focused entirely on the analysis of pharmaceuticals.[11] The article showed that many

common drugs such as Claritin and Excedrin could be rapidly identified by their active ingredient when directly spraying the tablets placed on a conveyer belt. This study also included the analysis of eye drops applied directly to filter paper, indicating that liquid samples could be analyzed directly from paper surfaces after drying. Shortly thereafter, Weston et al.[38] demonstrated that DESI could be used in conjunction with ion mobility spectrometry to analyze a variety of pharmaceutical tablets and creams. The creams were spotted on filter paper, further demonstrating the types of analyte that would respond to DESI.

Rodriguez-Cruz demonstrated[39] the applicability of DESI to compounds in illicit drugs and commonly abused prescription drugs that are normally analyzed with ESI. She further demonstrated the ability of DESI to detect the active ingredient, cannabis, in dried marijuana leaves. The analysis of marijuana is especially significant due to the limited amount of sample preparation required when compared to what is necessary for electrospray. The Hopfgartner group further demonstrated[40] the capability of the DESI source by analyzing more than 20 different illicit drugs directly, including Ecstasy. They demonstrated that powder analysis was possible through creation of pellets using a pellet press. They noted that the analysis time of almost all samples took less than 10 s.

Many drug samples contain a variety of compounds, both acidic and basic. Some compounds may respond better in either the positive or negative ion mode. In a demonstration of the versatility of DESI in rapid, mass analysis, Williams et al. showed that DESI was capable of simultaneous analysis of pharmaceuticals in both the positive and negative ion modes through the use of polarity switching.[41] Further development with pharmaceuticals has shown that DESI is capable of in situ analysis of drugs in tissues, covered in the imaging section below.

One of the most important pharmaceutical applications of DESI with immediate benefit for the public is the identification of counterfeit anti-malarial drugs. In many developing countries, malaria poses a serious threat to the population. Anti-malarial tablets are available, but are prime targets for counterfeiters. Identification of the false tablets has become increasingly difficult, especially with the counterfeiters adding small amounts of the active ingredient, artesunate, to fool traditional detection methods. The Fernandez group demonstrated the capability of DESI to identify fake anti-malarial drugs using reactive DESI.[42] DESI vastly reduced the time to identify fake anti-malarial tablets over conventional liquid chromatography.

1.3.4.2 Imaging

Surface techniques such as secondary ion mass spectrometry (SIMS) and matrix assisted laser desorption ionization (MALDI) are important tools in mass spectrometric imaging. Chemical imaging is a quantitative technique, producing images based on the spatial variations in the concentration of the analyte. From the beginning, imaging has been one of the intended uses of DESI. DESI imaging relies on efficient and consistent ion transport to construct a proper image. Certain DESI parameters play a critical role in ion transport with minor variations resulting in large differences in signal. These parameters are usually held constant during analyses. Because imaging does not always occur on perfectly flat surfaces, variations in surface to capillary height are difficult to maintain throughout an imaging experiment and introduce variations in detected signal based on height instead of concentration.

In the first DESI paper, Cooks' group briefly described the possible use of DESI for 'the spatial analysis of surfaces' with an example of ion intensities of coniceine in poison Hemlock sampled across the stem.[5] In 2005, the group demonstrated the ability of DESI to identify

proteins in various animal tissue samples.[43] The tissues were prepared as thinly sliced (16 µm) cross sections of mouse pancreas, rat brain, and human liver. While no actual imaging was presented in this preliminary paper, important aspects of the imaging technique were addressed including spot size based on the source construction and the capability to identify an increase in cancer related proteins based on lateral distance traveled when sampling the tissue.

The following year the Cooks group published the 'first 2D images taken using ambient mass spectrometry'.[44] In the study DESI was used to map lipid distribution found in a rat brain, producing images showing the distributions of each and drawing connections based on the types of tissues present. They reported a resolution of 500 µm and recognized that while not providing resolution equal to that provided by MALDI or SIMS, the advantages of DESI outweigh the lower resolution in certain cases, with the possibility for improvement in the future. At nearly the same time, the Cooks group also submitted a paper to the *International Journal of Mass Spectrometry* with experiments to 'test the feasibility of performing molecular imaging studies using DESI.'[45] This paper took a more fundamental look at DESI imaging using dyes printed on glossy paper. Using a traditional printer, they were able to produce images with precise spacing to examine the imaging capabilities of DESI with a known sample. By spacing lines of varying width 1 mm apart and monitoring the selected ion monitoring (SIM) signal as the lines were scanned, they showed that none of the sample signals from the lines crossed into each other. They then demonstrated the capability of DESI to image different components simultaneously and reconstructed the printed image. They reported a lateral resolution of 200 µm.

While Cooks' group has taken an applications based approach to imaging, the Van Berkel group has investigated the nature of the spray on the surface and how it influences DESI as an imaging source. In 2005, the Van Berkel group laid their groundwork for DESI imaging research using thin layer chromatography (TLC) plates.[46] This paper reported three dyes separated chromatographically and then scanned along the separated components while monitoring the signal in the mass spectrometer. The effect of washing the analyte outside the sampling region and the effects on sampling resolution due to the size of the DESI plume were noted. Kertesz and Van Berkel published their first TLC imaging paper in 2006 using the signal from a mass spectrometer recorded through an automated process.[47] They configured the Handsfree™ software used with TLC to map the ion content as they rastered the DESI source over the individual ion spots and compared it to images taken with the CCD.

The Van Berkel group took another important step in DESI imaging by investigating the spray on planar arrays of TLC plates.[27] This study was one of the first to address the nature of the 'impact plume region,' citing the lack of research at the time. They defined the most effective desorption area and identified the presence of solvent flow lines. They also addressed resolution by comparing the impact region (footprint) with the spot size of samples. It was shown that the direction of approach when moving across a sample had an effect on the resolution due to solvent spreading the analyte. The best results were produced when the sample was moved into the spray from the sides, away from the solvent flow lines (denoted spray to capillary S-C in the paper). This finding was critical in imaging because it suggested that it is better to image a region by approaching it first with the most effective desorption region before disturbing it by solvent flowing from the central impact region.

In early 2008, the Van Berkel group published a paper on the investigation of image quality based on scanning methods and source to surface distance.[48] The paper compared rastering to unidirectional scanning and found unidirectional scanning to consistently give better results. When the sampling surface was set at an incline, slightly angled at 1.35°, it had a negative effect on the imaging quality. As the sample was rastered, the highest part imaged without any loss in quality. However, as rastering continued at a gradient, the effective distance between the sample and the capillary increased and the image quality deteriorated. This loss in quality is attributed to the increase in sample-to-capillary distance. They concluded the paper showing that an automated software process can compensate for variations in surface height to maintain a consistent inlet and spray distance from the surface.

Later the same year, Van Berkel and Kertsz published a paper on methods for improving imaging resolution with a reported resolution of 40 μm.[28] This resolution was achieved by focusing on the various spray factors and identifying which of these played the most important role in resolution. The most important factor in increasing resolution was minimizing the spray plume impact region. The parameters that had the greatest effect on minimizing the impact region were distance between surface and tip, solvent flow rate, and scan lane spacing. Another important factor in resolution reported in the paper was choosing solvent and surface interactions to minimize the spread of solvent on the surface. Somewhat surprisingly, they also reported that changing the capillary size used in the DESI source did not improve the size of the plume and, therefore, the resolution.

Research continues on a variety of DESI applications. The Van Berkel group produced images showing drug distribution in a full body cross section of a rat 60 minutes after

administering the analyte.[49] The cross section presented in the image contained various organs including the brain, liver, lung, kidney and stomach, displaying where the drug migrated after ingestion. The Cooks group published a paper on rat spinal tissue Imaging showing the distribution of a large number of compounds in both the white and gray matter and reported a sub 200 µm resolution.[50] DESI has also been used to image the surface response of seaweed to fungal pathogens.[51] The possibility for DESI imaging in natural products has been investigated[52] suggesting that while not as robust as MALDI, the potential for future applications is large.

1.3.4.3 Homeland Security

With the rise in demand for increased national security created by 9/11, rapid explosive detection quickly became one of the central focuses of security experts. The Cooks group examined the effects of DESI on many major explosives such as RDX, HMX, PETN, and TNT.[10] They showed that although there is little to no sample preparation involved with DESI, these analytes are so responsive that they were detectable when mixed with other chemical matrices such as cleaners, lubricants, and diesel fuel. Furthering explosive research, the same group also showed that through reactive DESI, triacetone triperoxide could be detected despite the lack of the nitro groups that are important for other detection methods.[15]

1.3.4.4 Other

Many other applications have been outlined using DESI. DESI has been used to analyze industrial polymers,[53] to measure sealant age for propellants in rocket fuel,[54] and alkaloids in dietary supplements.[55] DESI has also been used to measure diterpene glycosides in Stevia Leaves.[56]

1.4 References

1. Falconer, I., Corpuscles, Electrons and Cathode Rays: J.J. Thomson and the Discovery of the Electron. *The British Journal for the History of Science* **1987,** *20* (03), 241-276.
2. Harris, G. A.; Nyadong, L.; Fernandez, F. M., Recent Developments in Ambient Ionization Techniques for Analytical Mass Spectrometry. *Analyst* **2008,** *133*, 1297-1301.
3. Fenn, J.; Mann, M.; Meng, C.; Wong, S.; Whitehouse, C., Electrospray Ionization for Mass Spectrometry of Large Biomolecules. *Science* **1989,** *246* (4926), 64-71.
4. Cody, R. B.; Laramee, J. A.; Durst, H. D., Versatile New Ion Source for the Analysis of Materials in Open Air under Ambient Conditions. *Analytical Chemistry* **2005,** *77* (8), 2297-2302.
5. Takats, Z.; Wiseman, J. M.; Gologan, B.; Cooks, R. G., Mass Spectrometry Sampling Under Ambient Conditions with Desorption Electrospray Ionization. *Science* **2004,** *306* (5695), 471-473.
6. Takats, Z.; Nanita, S. C.; Cooks, R. G.; Schlosser, G.; Vekey, K., Amino Acid Clusters Formed by Sonic Spray Ionization. *Analytical Chemistry* **2003,** *75* (6), 1514-1523.
7. Takats, Z.; Wiseman, J. M.; Gologan, B.; Cooks, R. G., Electrosonic Spray Ionization. A Gentle Technique for Generating Folded Proteins and Protein Complexes in the Gas Phase and for Studying Ion Molecule Reactions at Atmospheric Pressure. *Analytical Chemistry* **2004,** *76* (14), 4050-4058.
8. Cotte-Rodríguez, I.; Cooks, R. G., Non-proximate Detection of Explosives and Chemical Warfare Agent Simulants by Desorption Electrospray Ionization Mass Spectrometry. *Chemical Communications* **2006**, 2968-2970.
9. Cotte-Rodríguez, I.; Mulligan, C. C.; Cooks, R. G., Non-Proximate Detection of Small and Large Molecules by Desorption Electrospray Ionization and Desorption Atmospheric Pressure Chemical Ionization Mass Spectrometry: Instrumentation and Applications in Forensics, Chemistry, and Biology. *Analytical Chemistry* **2007,** *79* (18), 7069-7077.
10. Cotte-Rodríguez, I.; Takáts, Z.; Talaty, N.; Chen, H.; Cooks, R. G., Desorption Electrospray Ionization of Explosives on Surfaces: Sensitivity and Selectivity Enhancement by Reactive Desorption Electrospray Ionization. *Analytical Chemistry* **2005,** *77* (21), 6755-6764.
11. Chen, H.; Talaty, N. N.; Takats, Z.; Cooks, R. G., Desorption Electrospray Ionization Mass Spectrometry for High-Throughput Analysis of Pharmaceutical Samples in the Ambient Environment. *Analytical Chemistry* **2005,** *77* (21), 6915-6927.
12. Chen, H.; Cotte-Rodríguez, I.; Cooks, R. G., cis-Diol Functional Group Recognition by Reactive Desorption Electrospray Ionization (DESI). *Chemical Communications* **2006**, 597-599.
13. Nefliu, M.; Cooks, R. G.; Moore, C., Enhanced Desorption Ionization Using Oxidizing Electrosprays. *Journal of the American Society for Mass Spectrometry* **2006,** *17* (8), 1091-1095.
14. Huang, G.; Chen, H.; Zhang, X.; Cooks, R. G.; Ouyang, Z., Rapid Screening of Anabolic Steroids in Urine by Reactive Desorption Electrospray Ionization. *Analytical Chemistry* **2007,** *79* (21), 8327-8332.
15. Cotte-Rodríguez, I.; Chen, H.; Cooks, R. G., Rapid Trace Detection of Triacetone Triperoxide (TATP) by Complexation Reactions During Desorption Electrospray Ionization. *Chemical Communications* **2006**, 953-955.

16. Venter, A.; Cooks, R. G., Desorption Electrospray Ionization in a Small Pressure-Tight Enclosure. *Analytical Chemistry* **2007,** *79* (16), 6398-6403.
17. Chipuk, J. E.; Brodbelt, J. S., Transmission Mode Desorption Electrospray Ionization. *Journal of the American Society for Mass Spectrometry* **2008,** *19* (11), 1612-1620.
18. Chipuk, J. E.; Gelb, M. H.; Brodbelt, J. S., Surface-Enhanced Transmission Mode Desorption Electrospray Ionization: Increasing the Specificity of Ambient Ionization Mass Spectrometric Analyses. *Analytical Chemistry* **2009,** *82* (1), 16-18.
19. Roach, P. J.; Laskin, J.; Laskin, A., Nanospray Desorption Electrospray Ionization: an Ambient Method for Liquid-extraction Surface Sampling in Mass Spectrometry. *Analyst* **2010,** *135* (9), 2233-2236.
20. Soparawalla, S.; Salazar, G. A.; Perry, R. H.; Nicholas, M.; Cooks, R. G., Pharmaceutical Cleaning Validation Using Non-proximate Large-area Desorption Electrospray Ionization Mass Spectrometry. *Rapid Communications in Mass Spectrometry* **2009,** *23* (1), 131-137.
21. Soparawalla, S.; Salazar, G. A.; Sokol, E.; Perry, R. H.; Cooks, R. G., Trace Detection of Non-uniformly Distributed Analytes on Surfaces using Mass Transfer and Large-area Desorption Electrospray Ionization (DESI) Mass Spectrometry. *Analyst* **2010,** *135* (8), 1953-1960.
22. Sampson, J. S.; Hawkridge, A. M.; Muddiman, D. C., Generation and Detection of Multiply-Charged Peptides and Proteins by Matrix-Assisted Laser Desorption Electrospray Ionization (MALDESI) Fourier Transform Ion Cyclotron Resonance Mass Spectrometry. *Journal of the American Society for Mass Spectrometry* **2006,** *17* (12), 1712-1716.
23. Shiea, J.; Huang, M.-Z.; HSu, H.-J.; Lee, C.-Y.; Yuan, C.-H.; Beech, I.; Sunner, J., Electrospray-assisted Laser Desorption/ionization Mass Spectrometry for Direct Ambient Analysis of Solids. *Rapid Communications in Mass Spectrometry* **2005,** *19* (24), 3701-3704.
24. Kebarle, P.; Verkerk, U. H., Electrospray: From Ions in solution to Ions in the Gas Phase, What We Know Now. *Mass Spectrometry Reviews* **2009,** *28* (6), 898-917.
25. Takáts, Z.; Cotte-Rodriguez, I.; Talaty, N.; Chen, H.; Cooks, R. G., Direct, Trace Level Detection of Explosives on Ambient Surfaces by Desorption Electrospray Ionization Mass Spectrometry. *Chemical Communications* **2005**, 1950-1952.
26. Takáts, Z.; Wiseman, J. M.; Cooks, R. G., Ambient Mass Spectrometry using Desorption Electrospray Ionization (DESI): Instrumentation, Mechanisms and Applications in Forensics, Chemistry, and Biology. *Journal of Mass Spectrometry* **2005,** *40* (10), 1261-1275.
27. Pasilis, S. P.; Kertesz, V.; Van Berkel, G. J., Surface Scanning Analysis of Planar Arrays of Analytes with Desorption Electrospray Ionization-Mass Spectrometry. *Analytical Chemistry* **2007,** *79* (15), 5956-5962.
28. Kertesz, V.; Van Berkel, G. J., Improved imaging resolution in desorption electrospray ionization mass spectrometry. *Rapid Communications in Mass Spectrometry* **2008,** *22* (17), 2639-2644.
29. Venter, A.; Sojka, P. E.; Cooks, R. G., Droplet Dynamics and Ionization Mechanisms in Desorption Electrospray Ionization Mass Spectrometry. *Analytical Chemistry* **2006,** *78* (24), 8549-8555.
30. Costa, A. B.; Cooks, R. G., Simulation Of Atmospheric Transport and Droplet-Thin Film Collisions in Desorption Electrospray Ionization. *Chemical Communications* **2007**, 3915-3917.

31. Costa, A. B.; Graham Cooks, R., Simulated Slashes: Elucidating the Mechanism of Desorption Electrospray Ionization Mass Spectrometry. *Chemical Physics Letters* **2008,** *464* (1-3), 1-8.
32. Qiu, B.; Luo, H., Desorption electrospray ionization mass spectrometry of DNA nucleobases: implications for a liquid film model. *Journal of Mass Spectrometry* **2009,** *44* (5), 772-779.
33. Bereman, M. S.; Muddiman, D. C., Detection of Attomole Amounts of Analyte by Desorption Electrospray Ionization Mass Spectrometry (DESI-MS) Determined Using Fluorescence Spectroscopy. *Journal of the American Society for Mass Spectrometry* **2007,** *18* (6), 1093-1096.
34. Barbula, G. K.; Robbins, M. D.; Yoon, O. K.; Zuleta, I.; Zare, R. N., Desorption Electrospray Ionization: Achieving Rapid Sampling Rates. *Analytical Chemistry* **2009,** *81* (21), 9035-9040.
35. Green, F. M.; Stokes, P.; Hopley, C.; Seah, M. P.; Gilmore, I. S.; O'Connor, G., Developing Repeatable Measurements for Reliable Analysis of Molecules at Surfaces Using Desorption Electrospray Ionization. *Analytical Chemistry* **2009,** *81* (6), 2286-2293.
36. Green, F. M.; Salter, T. L.; Gilmore, I. S.; Stokes, P.; O'Connor, G., The Effect of Electrospray Solvent Composition on Desorption Electrospray Ionisation (DESI) Efficiency and Spatial Resolution. *Analyst* **2010,** *135* (4), 731-737.
37. Badu-Tawiah, A.; Cooks, R. G., Enhanced Ion Signals in Desorption Electrospray Ionization Using Surfactant Spray Solutions. *Journal of the American Society for Mass Spectrometry* **2010,** *21* (8), 1423-1431.
38. Weston, D. J.; Bateman, R.; Wilson, I. D.; Wood, T. R.; Creaser, C. S., Direct Analysis of Pharmaceutical Drug Formulations Using Ion Mobility Spectrometry/Quadrupole-Time-of-Flight Mass Spectrometry Combined with Desorption Electrospray Ionization. *Analytical Chemistry* **2005,** *77* (23), 7572-7580.
39. Rodriguez-Cruz, S. E., Rapid Analysis of Controlled Substances using Desorption Electrospray Ionization Mass Spectrometry. *Rapid Communications in Mass Spectrometry* **2006,** *20* (1), 53-60.
40. Leuthold, L. A.; Mandscheff, J.-F.; Fathi, M.; Giroud, C.; Augsburger, M.; Varesio, E.; Hopfgartner, G., Desorption Electrospray Ionization Mass Spectrometry: Direct Toxicological Screening and Analysis of Illicit Ecstasy Tablets. *Rapid Communications in Mass Spectrometry* **2006,** *20* (2), 103-110.
41. Williams, J. P.; Lock, R.; Patel, V. J.; Scrivens, J. H., Polarity Switching Accurate Mass Measurement of Pharmaceutical Samples Using Desorption Electrospray Ionization and a Dual Ion Source Interfaced to an Orthogonal Acceleration Time-of-Flight Mass Spectrometer. *Analytical Chemistry* **2006,** *78* (21), 7440-7445.
42. Nyadong, L.; Green, M. D.; De Jesus, V. R.; Newton, P. N.; Fernandez, F. M., Reactive Desorption Electrospray Ionization Linear Ion Trap Mass Spectrometry of Latest-Generation Counterfeit Antimalarials via Noncovalent Complex Formation. *Analytical Chemistry* **2007,** *79* (5), 2150-2157.
43. Wiseman, J. M.; Puolitaival, S. M.; Takáts, Z.; Cooks, R. G.; Caprioli, R. M., Mass Spectrometric Profiling of Intact Biological Tissue by Using Desorption Electrospray Ionization. *Angewandte Chemie International Edition* **2005,** *44* (43), 7094-7097.

44. Wiseman, J. M.; Ifa, D. R.; Song, Q.; Cooks, R. G., Tissue Imaging at Atmospheric Pressure Using Desorption Electrospray Ionization (DESI) Mass Spectrometry13. *Angewandte Chemie International Edition* **2006,** *45* (43), 7188-7192.
45. Ifa, D. R.; Wiseman, J. M.; Song, Q.; Cooks, R. G., Development of Capabilities for Imaging Mass Spectrometry Under Ambient Conditions with Desorption Electrospray Ionization (DESI). *International Journal of Mass Spectrometry* **2007,** *259* (1-3), 8-15.
46. Van Berkel, G. J.; Ford, M. J.; Deibel, M. A., Thin-Layer Chromatography and Mass Spectrometry Coupled Using Desorption Electrospray Ionization. *Analytical Chemistry* **2005,** *77* (5), 1207-1215.
47. Van Berkel, G. J.; Kertesz, V., Automated Sampling and Imaging of Analytes Separated on Thin-Layer Chromatography Plates Using Desorption Electrospray Ionization Mass Spectrometry. *Analytical Chemistry* **2006,** *78* (14), 4938-4944.
48. Kertesz, V.; Van Berkel, G. J., Scanning and Surface Alignment Considerations in Chemical Imaging with Desorption Electrospray Mass Spectrometry. *Analytical Chemistry* **2008,** *80* (4), 1027-1032.
49. Kertesz, V.; Van Berkel, G. J.; Vavrek, M.; Koeplinger, K. A.; Schneider, B. B.; Covey, T. R., Comparison of Drug Distribution Images from Whole-Body Thin Tissue Sections Obtained Using Desorption Electrospray Ionization Tandem Mass Spectrometry and Autoradiography. *Analytical Chemistry* **2008,** *80* (13), 5168-5177.
50. Girod, M.; Shi, Y.; Cheng, J.-X.; Cooks, R. G., Desorption Electrospray Ionization Imaging Mass Spectrometry of Lipids in Rat Spinal Cord. *Journal of the American Society for Mass Spectrometry* **2010,** *21* (7), 1177-1189.
51. Lane, A. L.; Nyadong, L.; Galhena, A. S.; Shearer, T. L.; Stout, E. P.; Parry, R. M.; Kwasnik, M.; Wang, M. D.; Hay, M. E.; Fernandez, F. M.; Kubanek, J., Desorption Electrospray Ionization Mass Spectrometry Reveals Surface-mediated Antifungal Chemical Defense of a Tropical Seaweed. *Proceedings of the National Academy of Sciences* **2009,** *106* (18), 7314-7319.
52. Esquenazi, E.; Yang, Y.-L.; Watrous, J.; Gerwick, W. H.; Dorrestein, P. C., Imaging Mass Spectrometry of Natural Products. *Natural Product Reports* **2009,** *26*, 1521-1534.
53. Nefliu, M.; Venter, A.; Cooks, R. G., Desorption Electrospray Ionization and Electrosonic Spray Ionization for Solid and Solution Phase Analysis of Industrial Polymers. *Chemical Communications* **2006**, 888-890.
54. Venter, A.; Ifa, Demian R.; Cooks, R. G.; Poehlein, Sara K.; Chin, A.; Ellison, D., A Desorption Electrospray Ionization Mass Spectrometry Study of Aging Products of Diphenylamine Stabilizer in Double-Base Propellants. *Propellants, Explosives, Pyrotechnics* **2006,** *31* (6), 472-476.
55. Van Berkel, G. J.; Tomkins, B. A.; Kertesz, V., Thin-Layer Chromatography/Desorption Electrospray Ionization Mass Spectrometry: Investigation of Goldenseal Alkaloids. *Analytical Chemistry* **2007,** *79* (7), 2778-2789.
56. Jackson, A. U.; Tata, A.; Wu, C.; Perry, R. H.; Haas, G.; West, L.; Cooks, R. G., Direct analysis of Stevia Leaves for Diterpene Glycosides by Desorption Electrospray Ionization Mass Spectrometry. *Analyst* **2009,** *134*, 867-874.

2 Real Time imaging on Glass

2.1 Introduction

Desorption electrospray ionization was introduced by the Cooks group in late 2004.[1] DESI was one of the first ionization sources to figuratively 'open the door' for ambient sampling in mass spectrometry. Like many other research groups, we looked at DESI as an opportunity to work with something on the cutting edge of new analytical techniques. As a spectroscopy group with imaging experience, we felt that we could offer additional insight into the technique, providing information to the field that would complement research from traditional mass spectrometry laboratories. One of the appealing aspects of DESI as an ion source is the interaction with the surface. We believed that examination of the surface would provide important information about the DESI process.

Because a DESI footprint ranges from a few hundred nanometers to a few millimeters, microscopic imaging is the best method for investigating the surfaces used in DESI analyses. It is fairly simple to place a surface, post analysis, on a microscope and look at displaced analyte. Looking at a surface under a microscope seems like a fairly logical step to take for anyone interested in the DESI process and mechanism. We suspected that many researchers working with DESI would publish magnified pictures taken of a DESI surface, and some did.[2-3] Such images provided an idea of what was occurring on the surface, but could not be relied upon for an accurate picture of what was occurring in real time.

When we took up DESI studies, our group had recently purchased an inverted microscope from Nikon. These microscopes are designed for imaging fluorescent species.

Fluorescence imaging is an extremely sensitive technique, illuminating the sample with laser light to produce detailed images of microscopic, fluorescent samples. An inverted microscope is also useful for performing experiments above a sample that is illuminated from below. This advantage does not exist in overhead microscopes, which position the optics directly above the sample.

The characteristics of an inverted microscope lend themselves to looking at DESI. DESI operates near the sample surface, making it impossible to be used with the optics of a top-down microscope. The inverted geometry allowed us to look at a DESI surface in real time. After Cooks' group published a paper on non-proximate detection,[4-5] we realized that we could combine real time imaging with real time sampling through the use of a transfer line. The combination of DESI-MS and an inverted microscope is the basis of our research into this budding field.

2.1.1 Goals

One of our primary goals in combining microscopic imaging with DESI was to obtain real time images of analyte removal. We were certain that microscopic images of displaced analyte provided far less information than images recorded during sampling. We also believed that these images would yield results that could be used to elucidate the desorption mechanism.

Our goals were to:

1. Design a mounting system for the DESI source for precision positioning over the microscope.
2. Design a non-proximate detection adaptation for the mass spectrometer to use over the microscope.

3. Design experimental methods for obtaining real time images of analyte removal and transport by DESI.
4. Correlate images from sample removal with changes in signal detected by the mass spectrometer.
5. Identify the mechanism responsible for analyte desorption and ionization on DESI.

Despite never having operated a DESI source, we were confident that microscopic imaging would provide information useful to the mass spectrometry community. The success of the latter two goals depended on the initial goals. This meant that a well designed hardware setup would have a significant impact on future experiments.

2.1.2 Implementation

The simplest implementation of DESI involves placing an analyte on a surface and sampling it in close proximity to the inlet capillary of the mass spectrometer. In order to accomplish our goals we needed to greatly expand on this implementation without compromising the DESI setup in a way that would prevent the results from being comparable with work from other groups.

Surface selection was the first setup issue we addressed. The most common sampling surfaces for DESI are Teflon and glass. Because Teflon is not transparent, it is not an option when working with the inverted microscope. We made the design decision that our experimentation would focus entirely on glass and that any inherent differences in behavior or mechanism from Teflon would need to be investigated in later experiments.

DESI is useful for a wide range of compounds. However, the requirements for this experiment meant that analyte selection was an important part of the implementation. The

most important characteristics for the analyte were that it was easily sampled by DESI, including detection, and that it was useful for imaging. Other important qualities we considered included: cost, ease of handling, shelf life, reactivity, solubility, quantum efficiency, spectral absorptivity, and toxicity. Molecular dyes matched many of our requirements in these areas. We chose to work with the dyes Rhodamine B Base (RBB) and Crystal Violet (CV).

RBB was chosen as an ideal dye for fluorescence imaging because it is highly fluorescent, gives a very strong signal in the mass spectrometer, is fairly cheap and has a free amine group for binding H^+. Unlike rhodamine B, RBB is not a salt. This removed issues that might have arisen due to differences in salt concentration in the system. CV was chosen as the dye for absorption experiments. CV absorbs light well, is highly soluble in water and methanol, and produces a strong ion signal. Because we chose to work with dyes, any variations that might exist due to differences in sample would need to be investigated in later experiments.

Brigham Young University houses a Precision Machining Laboratory (PML) with which the Department of Chemistry and Biochemistry has a contract for design and machining of specialized parts. The Department employs electronics specialists in an instrument shop whose employees also design electronic setups for research purposes. Both of these groups were invaluable in instrumental design and implementation.

2.2 Hardware Design

2.2.1 DESI Source

2.2.1.1 Design Considerations

Our DESI source was designed after the manner of the ESSI source by the Cooks group using 1/16" stainless steel Swagelok™ fittings.[6] This design was fairly durable, inexpensive, and easily constructed. This in-house design was similar to that used by other groups and was functionally identical to the commercial DESI source offered by Prosolia.

Most DESI sources are mounted on a mass spectrometer in a fashion similar to conventional removable ESI and MALDI ion sources. The spray capillary is mounted just above the intake orifice of the mass spectrometer and the sample is placed just in front of the same orifice. These DESI sources allow control in the X, Y, and Z directions for signal optimization as well as spray angle. The sample surfaces are removable, allowing for quick sample switching without disturbing the optimized position of the DESI source.

To operate over the microscope, significant design changes were required. The source itself could not come in contact with the microscope stage. Such contact would interfere with translation of the microscope stage. This meant that the DESI source necessarily extended over the microscope stage on an arm and was attached to the 'breadboard' table. Attachment to the table meant that the source needed to be elevated 13 inches, so that it could be positioned over the microscope stage. The X, Y, and Z stages could not be positioned over the microscope due to size. A rotational stage was necessary to allow for control of the DESI angle. A special

brace was designed and manufactured by the PML to connect the rotational stage to the DESI source.

For convenience, we defined the X axis as the axis along which the DESI source pointed when it was parallel to the microscope stage, typically mounted on the right side of the microscope pointing left. The Z axis was elevation with the remaining horizontal axis was the Y axis. Thus the DESI capillary rotated in the XZ plane.

2.2.1.2 Source Construction

The source used for all investigations was constructed using a 1/16" stainless steel T-union. Approximately 0.5m of 75 µm inner diameter (ID)/150 µm outer diameter (OD) fused silica (FS) capillary was used for the inner capillary and approximately 2 cm of 200 µm ID/400 µm OD fused silica capillary was used for the outer capillary. An SGE Vespel reducing ferrule with 0.2 mm ID was used to secure the smaller capillary and a Supelco Supeltex M-2A ferrule with 0.4 mm ID was used to secure the larger capillary. 1/8" perfluoroalkoxy (PFA) tubing and stainless steel ferrules were used to deliver gas to the T-union through a reducing union and a 1/16" male port connector. The inner capillary was connected to a 250 µL Hamilton carbon analysis syringe with metal end cap using zero dead volume PEEK adapters and a PEEK sleeve. Voltage was applied with a custom power supply built by the BYU instrument shop using alligator clips and conductive copper tape attached to the metal cap of the syringe. The syringe was driven by a Harvard Apparatus PHD 2000 syringe pump. Figure 2-1 illustrates the overall mounting setup.

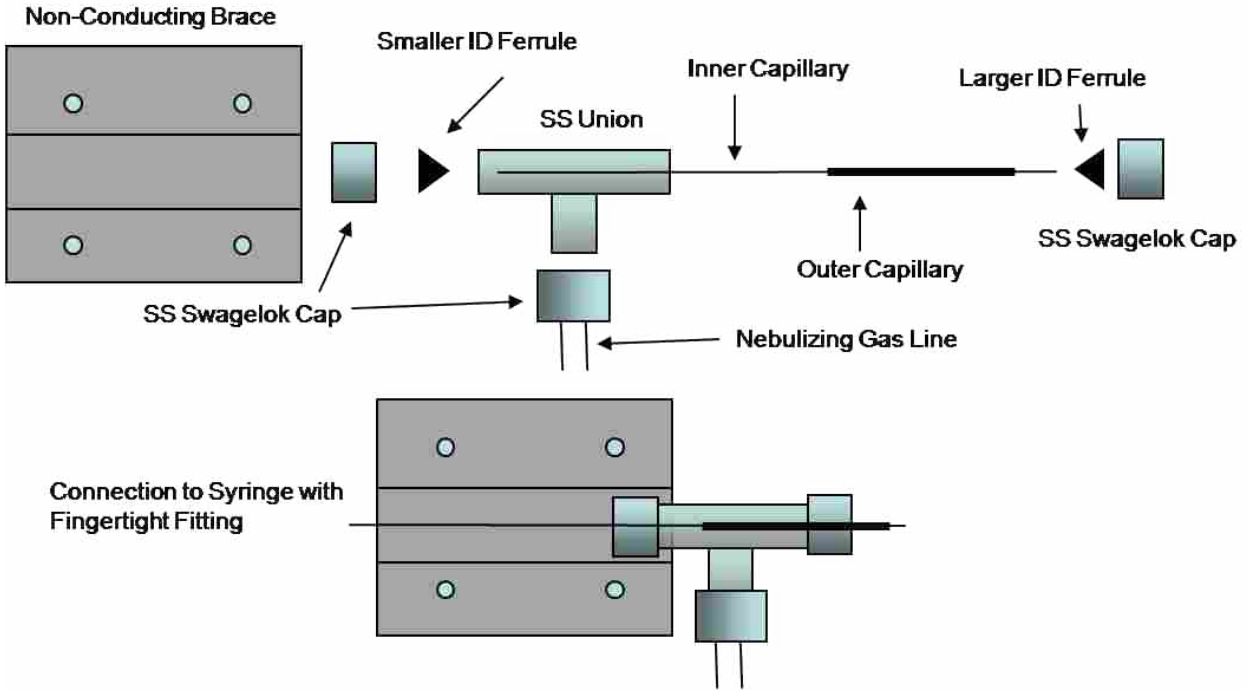

Figure 2-1 DESI source construction.

The DESI source was mounted in a custom brace built by the BYU PML. This mount was bolted to a Melles Griot 365° 40 mm diameter rotational stage, which was in turn bolted to an aluminum arm secured to the X, Y, and Z Melles Griot stages. These stages consisted of an X, Y stage bolted on top of a Z stage with ¼-20 screws. The Z stage was secured to a flat aluminum plate with ¼-20 screws. This plate had 2" grooves cut in each of the corners for course adjustment along the Z axis. The entire stage was set upon a plate that was supported by four, 1" diameter x 10" long aluminum rods bolted to the large bread board in the lab. This entire setup was mounted over a Nikon TE-2000U microscope. To improve the ease of use and reduce the amount of smaller capillary needed, the syringe pump was also elevated to the height of the source using plastic stands. An LCQ classic ion trap with custom built transfer line sampled

from the spraying location over the microscope. Figure 2-2 illustrates the mounting and overall setup used in the DESI experiments.

2.2.1.3 DESI Mounting

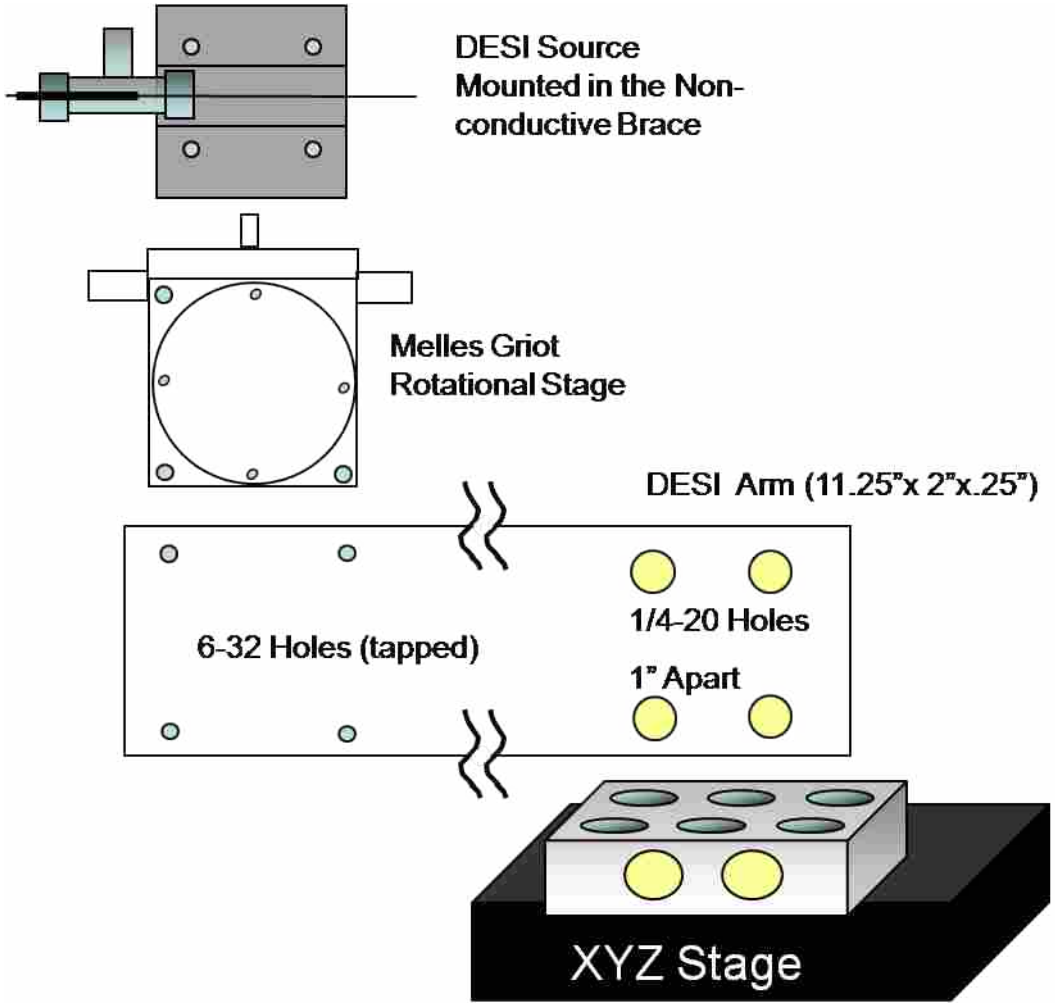

Figure 2-2 DESI Source Mount

2.2.1.4 Fluid Delivery

Our original DESI design was implemented with a zero dead volume 1/16" stainless steel union for solvent delivery. The union served two purposes. The first purpose was as an adaptor for solvent delivery between the syringe and the DESI source. One side of the union was connected to 1/16" polypropylene (PP) tubing that fit over the syringe needle containing the DESI solvent. The opposite side of the union was connected to a PEEK adapter securing the 150 µM OD fused silica solvent capillary. The second purpose for the union was to act as a connection to the high voltage source.

This design proved to be problematic for a number of reasons:

1.) Our mount had originally been designed to support the DESI and the union, but proved very difficult to remove as the weight of the union would occasionally be inadvertently applied to the FS capillary, resulting in a break.
2.) Construction of the source required very precise measurements for capillary length so that it could properly be seated in the PEEK tubing.
3.) Despite the fact that the channel mount block was designed to be non-conductive, voltage was still applied to the protruding SS union, creating a potential high voltage hazard when operating the rotating stage.
4.) The syringe itself used a sharp needle which required fitting with the PP tubing each time the syringe needed to be refilled. This led to wear of the tubing, creating folds that in turn resulted in poor fit. The poor fit caused leaks and lower back pressures, contributing to inconsistent solvent delivery. This could be solved by cutting off the

damaged PP tubing, reducing the operating length of the system. In addition to tubing damage, the process often introduced bubbles into the line

5.) The large volume of the 1/16" PP tubing made it very difficult to flush bubbles out of the line using the typical 250 µL syringe.

After visiting Cooks' lab, I noted that they had adopted a setup in which the voltage was applied directly to the needle of the syringe. It dawned on me that a bubble in the line would cause a break in applied voltage. I realized that I could attach the fused silica capillary to the syringe directly, bypassing the needle, union, and the PP tubing entirely. Such a setup also benefitted from a smaller tubing volume, making it very easy to expel bubbles in the line with minimal solvent waste.

The original source design employed 1/16" stainless steel tubing for the nebulizing gas. I did not investigate plastic tubing because the pressure tolerances for the tubing available in the stockroom fell below operating conditions we originally thought were necessary. Stainless steel tubing is difficult to work with due to its rigidity. The short length that we used initially required us to move the nitrogen gas tank on a cart up to the DESI source. Visiting the Cooks lab, I noted that they used flexible plastic tubing without any problems. Further research led me to find that PFA tubing (PFA-T2-030-100) could withstand pressures above 250 psi at 70 °C and was available through Swagelok.

2.2.2 Mass Spectrometery

2.2.2.1 Design considerations

We purchased the LCQ Classic for the DESI imaging project. The LCQ Classic worked well because it has an open interface for sampling that is designed for interchangeable ion sources. The LCQ Classic has a 'nanospray ion source mode', which is designed for use with third party ion sources and is ideal for the DESI setup.

Because the microscope was on a rail system with our DESI source, the mass spectrometer needed to be elevated to the proper height. This height was critical to allow the transfer line to extend over the microscope stage for mass analysis. In order to facilitate changing of the ion source, as well as maintenance of the mass spectrometer, the design included a rotating stage and bearings.

2.2.2.2 Mounting

To allow the mass spectrometer to sample from the microscope stage, additional hardware was required for positioning on the rail system. A large rotational stage was built for the mass spectrometer, complete with bearings for translation along the rail system. Figure 2-3 provides a 3-dimensional drawing of the stage. The base of the stage has grooves cut into it to accommodate 4 sets of roller bearings, positioned at the ends of the grooves. A rotational stage is mounted in the center of the base. The upper section of the stage is attached to the rotational stage, along with 4 removable footrests upon which the mass spectrometer can be placed. Each of the footrests is center tapped and bolted to the upper plate. Grooves are cut in each footrest to prevent the mass spectrometer from sliding. The footrests can be replaced to

vary the height of the mass spectrometer relative to the microscope. Handles were attached on two sides to allow easy positioning and rotation. A clamp is attached to the rail and then connected to a large threaded bolt with a handle for fine control in translation. When coarse translation is needed, the clamp can be loosened and slid along the rail with the stage.

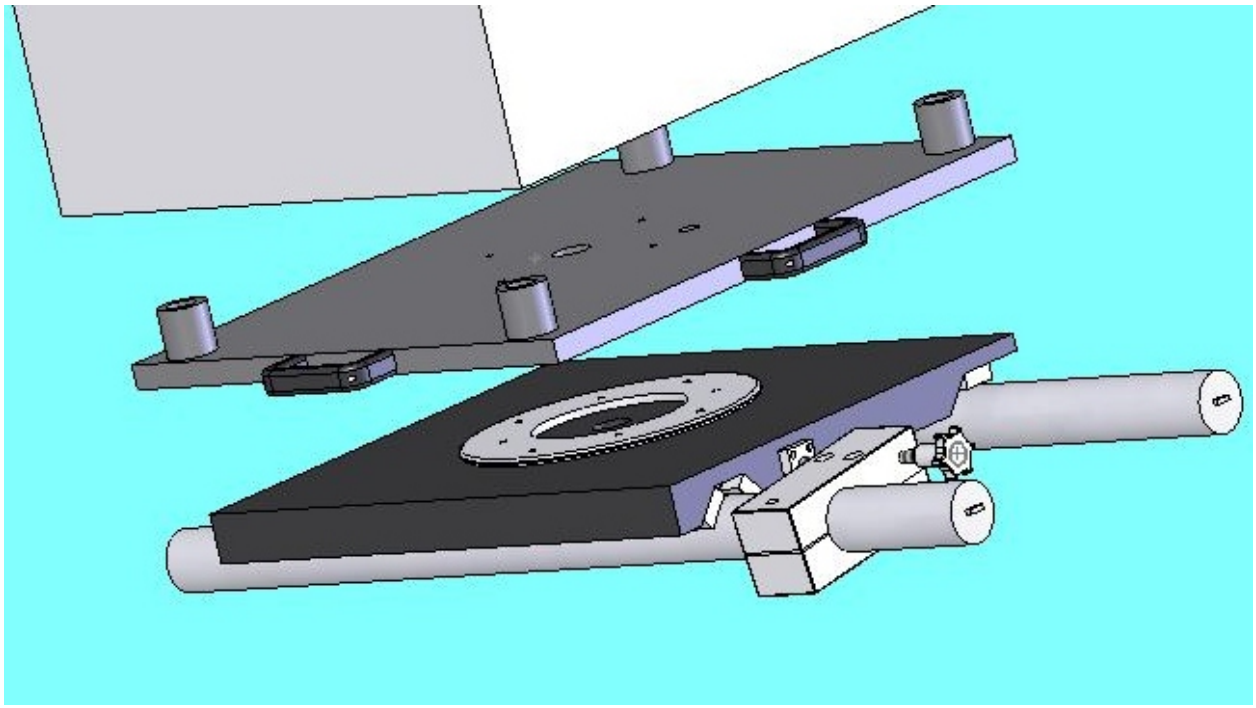

Figure 2-3 3-D drawing of the MS Stage.

2.2.2.3 Transfer Line

A transfer line, based upon the research[4] of the Cooks group, was constructed for analyte sampling over the microscope. The transfer line assembly was composed of 4 parts: the bridge, mount, extension, and transfer line. Figure 2-4 shows the design of the transfer line setup and mount.

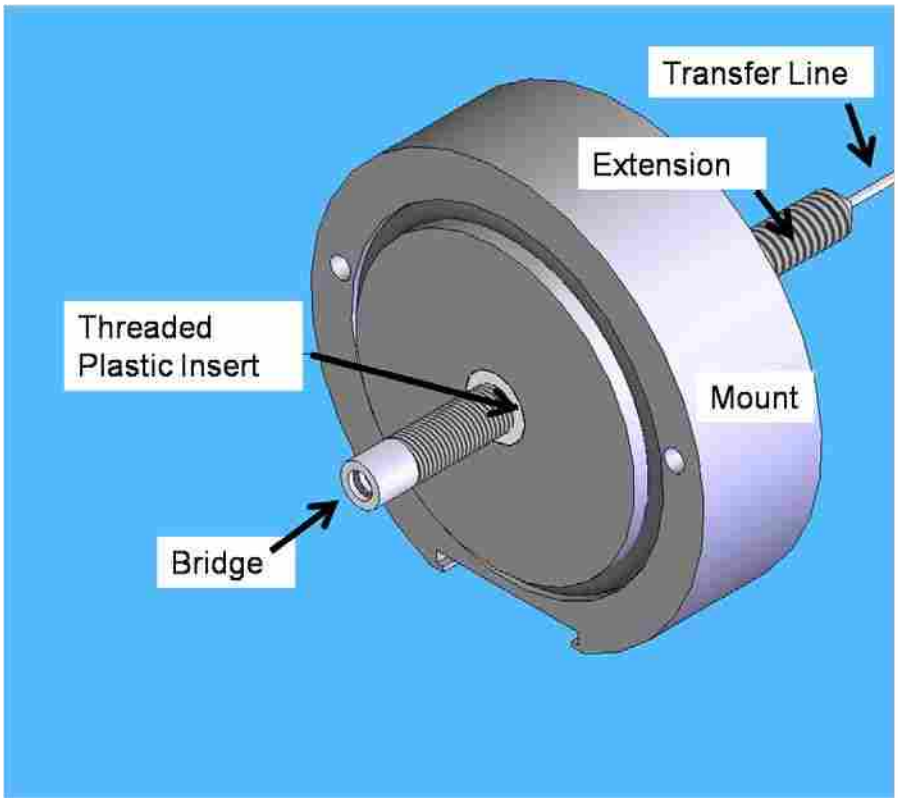

Figure 2-4 Transfer line Setup

The mount was designed to sit on the sliding stage built for commercial ion sources, such as the ESI and APCI ion sources provided by the manufacturer of the mass spectrometer. It can be locked in place with a dovetail joint using a groove machined in the base. When bolted to the spray shield of the mass spectrometer, the Teflon o-ring forms a seal with the faceplate of the mass spectrometer. A Teflon cylinder insert has been threaded through the center of the mount, to provide electrical isolation from the bridge and extension. The bridge and extension are both threaded into the Teflon insert in the mount, butting against each other within the center of the mount. The bridge itself has an o-ring that forms a seal with the heated capillary in the inlet of the mass spectrometer. A 0.550 mm hole cut in one end matches the hole in the

heated capillary. A 41 cm stainless steel tube with 1.8 mm ID/2.3 mm OD can then be inserted into the extension and through to the far side of the bridge. Voltage applied to the heated capillary is carried throughout the bridge and extension, charging the transfer line while allowing the mount to remain grounded.

2.2.2.4 Operational Parameters

All data collection, calibration, and tuning were performed using the Tuneplus™ software included with the Xcalibur 2.1 package. The mass spectrometer was calibrated with the standard calibration procedure using the recommended solution of caffeine, MRFA, and Ultramark 1621 as described in the LCQ Classic hardware manual. Injection times were left at 50 ms using 1-3 microscans. The heated capillary was set at 200 °C and between +5 and +30 V.

2.2.3 Imaging

2.2.3.1 Design Considerations

The overall imaging scheme consisted of a light source, imaging optics (microscope), and detection tools (CCD). This experiment was designed to take both fluorescence images and absorption images. We used a laser for fluorescence imaging and the incandescent lamp of the microscope for absorption imaging.

2.2.3.2 Laser

We used an argon Ion laser from Melles Griot, Model: 35-lap-321-120 for fluorescent imaging. The laser was tuned to 488 nm with power supply set to ½ – ¾ maximum capacity. The laser needed to be properly aligned to homogenously illuminate the sample. The laser was aligned to

enter the microscope by first passing the beam through a periscope, followed by a rotating diffuser and finally through a focusing lens. The periscope set the beam to the correct height. The beam struck a custom built, sandblasted, rotating diffuser which created a large laser spot. This spot was focused by the focusing lens through the opening at the back of the microscope.

2.2.3.3 Microscope

A Nikon TE-2000U inverted microscope was used for magnifying and imaging samples. When performing fluorescence imaging, laser light from the argon ion laser was passed through a 488 dichroic mirror into a microscope objective. The objective height was varied to focus on a sample placed on the microscope stage. DESI on a microscope slide was best imaged with the 2x or 4x objective when imaging the entire spray footprint. Light from Fluorescent samples passed through the same objective and was redirected by the dichroic mirror to the CCD, which we mounted on the left port.

2.2.3.4 CCD

We first attempted to image DESI using a PI-Max Gen II CCD. The sampling rate was ~3.5 Hz due to a very low analog to digital conversion rate. We needed a CCD that was capable of imaging at higher frequencies for real time imaging. The Andor Luca S was designed for fluorescence imaging on inverted microscopes. The CCD had 658 x 496 pixels. Each square pixel was 10 x 10 µm. DESI fluorescence images using the CCD were taken with a gain of 50 and an exposure time of 10-20 s. Higher gain levels of 100-250 produced images that were too noisy for imaging. For absorption imaging, either room light or the incandescent microscope lamp was employed with

no gain, and with exposure times from 0.0001 to 0.1 s. The Andor CCD operated at the default temperature of -20° C.

2.2.4 Coating Hardware

2.2.4.1 Design Considerations

Standard preparation of DESI samples includes spotting or wiping the analyte onto a slide. Our imaging goal was dependent on disruption of a dye on the surface. To be an effective technique, even small quantities of solvent on the surface would need to be detected. Not only would single spots of dye show limited solvent interaction, but it would be impossible to create a reproducible sample. We needed a method for coating a microscope slide in a highly reproducible manner for fluorescence imaging.

A paper by Hanley and Harris described quantitative dosing of surfaces with a sub-monolayer of fluorescent dye.[7] The paper described a technique of withdrawing a slide from a solution at a constant rate to create a homogenous coating. Through experimentation, we found that we could produce a sub-monolayer coating at a range of concentrations that was both homogenous and reproducible. Despite the visual appearance of a complete coating, Dr. Farnsworth calculated that these coatings were still sub-monolayer.

Figure 2-5 is a fluorescence image of a dye coating on a clean glass slide taken with the Andor CCD. The black area to the left is the uncoated portion of the slide. The leading edge of the dye coating typically contains slightly more dye and, thus, is slightly brighter than the rest of the coating. Minor blemishes can be seen in the coating, but are small in comparison to the size of the spray on the surfaces. The Hanley and Harris paper reported that a pure methanol

solvent and a withdrawal rate of 0.5 cm/s were ideal for coating. We also found that methanol was the best solution for coating homogenously. Water produced various defects in the coating with concentration build-up lines across the slide due to slower evaporation rates. Changing the withdrawal rate also produced poor results. Slower rates caused the dye to dry unevenly, leaving varying concentration contour lines along the surface and faster rates caused the solvent to run down the slide.

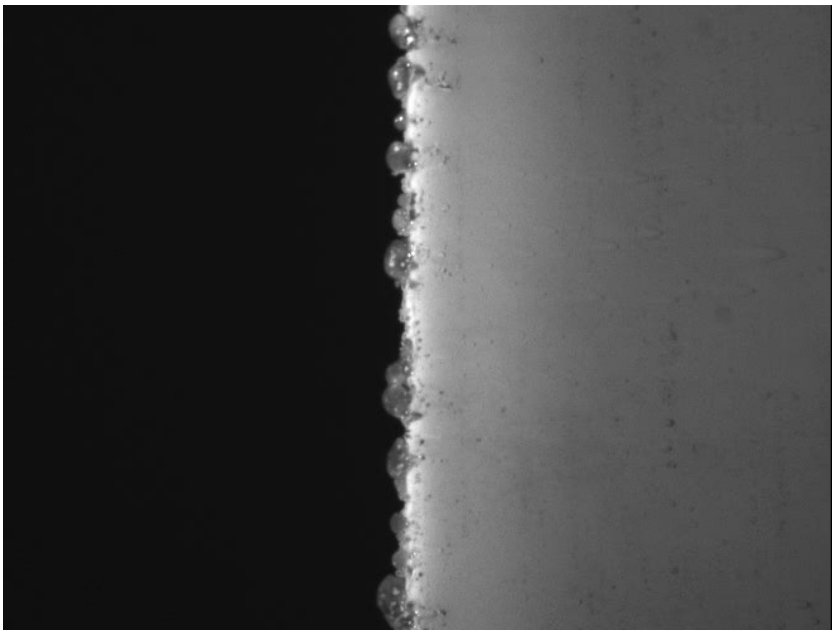

Figure 2-5 Fluorescence image of the edge of a RBB coating used to focus the microscope.

2.2.4.2 Coating Setup

Slides used in fluorescent imaging experiments were coated through a dipping process. A cleaned glass slide was secured with a rubber coated aluminum claw attached to an Aerotech Zeta 100 motorized stage. The stage was mounted with a Plexiglass base built by the instrument shop in an upright position, allowing the stage to travel vertically. The motorized stage was controlled by a Dynatech stepping motor control box using a Labview program called

"Slide Dipping.vi." The program was written by Jeff Macedone, a former post-doc in our lab. For coating, a standard clean slide would be lowered into a dye solution of methanol contained in a 30 mL beaker. The slide would then be withdrawn from the methanol at 0.5 cm/s. After the slide was allowed to dry, it was removed and one side of the slide was wiped clean of the dye coating using Kimwipes and methanol. Figure 2-6 shows the dye dipping setup.

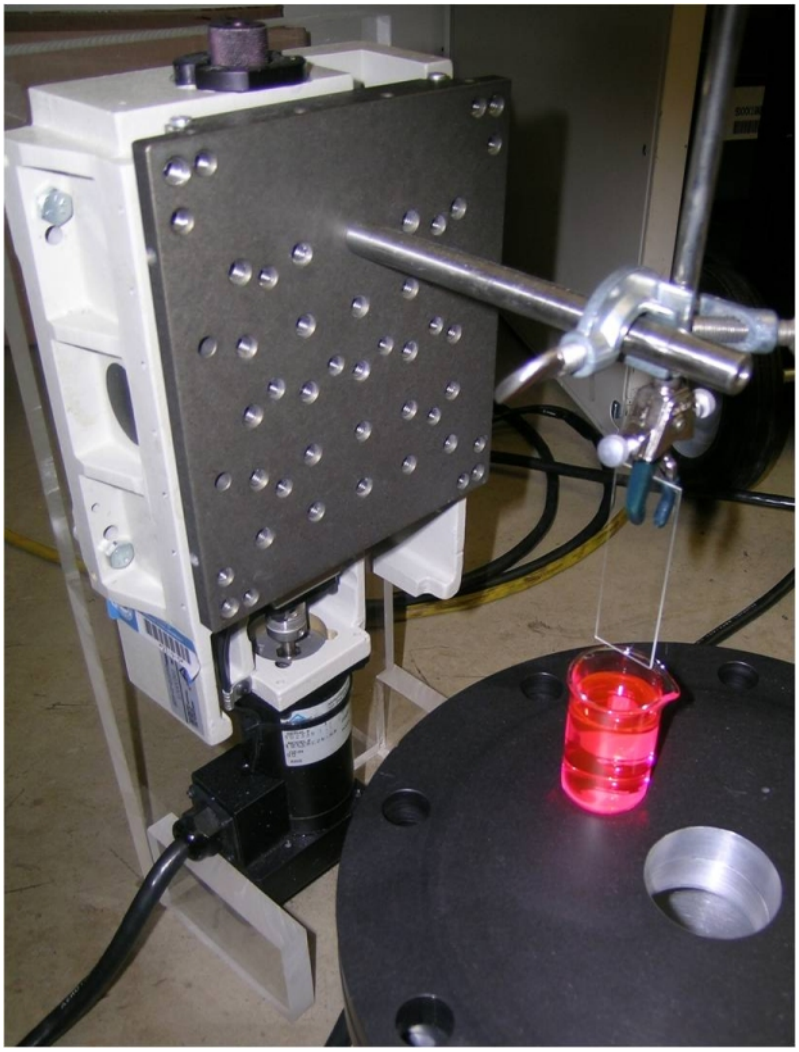

Figure 2-6 Slide dipping setup

2.2.4.3 Fluorescence Calibration Curve

A calibration curve of fluorescence signal vs. dye concentration was constructed from coated slides. Each slide was dipped in a different concentration of dye and removed at 0.5 cm/s. Each slide was then imaged for 20 s. The fluorescence signal from the coating was averaged at 3 different locations on each slide and plotted against concentration. The fluorescence signal was linear between 1.0 μM and 10. μM, beyond which self quenching occurred.

2.2.4.4 CV Samples

CV has solubility similar to RBB in methanol, and proved to coat out relatively well. However, even with a concentrated solution, the absorbance was too low to provide useful absorption images. To produce a less transparent coating, concentrated solutions of CV in methanol were added drop-wise to microscope slides until the entire slide was covered. This solvent layer was then allowed to evaporate. The solvent evaporated from the edges until a thick spot remained in the middle of the slide. This was repeated (re-dissolving the previous coating) several times until the desired opacity and consistency were created on the microscope slide.

Devin, an undergraduate in our laboratory, discovered that by placing the slide on different surfaces, he could change where the dye/methanol solution would pool. We found that by placing the slide on two flat metal one-inch risers, the entire slide could be covered in dye, but would quickly gather in the center of the slide, naturally increasing the concentration. Using this technique, we could make reproducible slides with thick coatings for absorption experiments. The dye on the surface crystallized in various fashions. Of the many slides created there were always a few slides with patches of fairly homogenous coatings for spraying.

2.2.5 Shutter Hardware

2.2.5.1 Design Considerations

With some preliminary work with the DESI and coated surfaces, it became apparent that we needed a way to control when the spray made contact with the surface for several of reasons:

1.) It was impossible to start both the gas and spray solvent simultaneously with a single person.
2.) The DESI source itself often needed time to reach equilibrium due to air bubbles in the line or the ramp-up time of the gas pressure.
3.) Positioning of a slide while spraying reduced the amount of useable coating due to premature removal.
4.) There was no accurate way to generate reproducible removal of analyte.

We realized that we needed to build an electronic shutter to instantaneously start and stop the spray from reaching the surface. The shutter needed to operate 1 mm above the sample slide without damaging the coating on the slide. In addition to operating above the slide, the shutter needed to pass under the DESI tip without coming in contact with it. The shutter also needed to be compact enough to fit beneath the DESI mount arm. Finally, the shutter needed to be computer controlled with very fast response times.

We approached Bart Whitehead in our instrument shop with these requirements and he designed the electronic shutter. The shutter was designed with a thin, flat piece of plastic that could pass back and forth over a glass microscope slide with roughly 100 µm tolerance. To achieve short duration exposures (less than 50 ms) two solenoids were necessary, one for

opening and the second for closing the shutter. The solenoids are mounted on thin flat Teflon plate and secured with metal rods.

2.2.5.2 Hardware Setup

The shutter was constructed with a Teflon base. Long metal rods were attached to the base to stabilize the Teflon and to mount two solenoids for driving the shutter. The shutter itself was made of a hard, thin plastic sandwiched between grooves cut in the base. The shutter was designed to be used with a standard 75 mm x 25 mm x 1 mm microscope slide. The shutter sat less than 1 mm above the slide and below the 1.5 mm operating height of the tip of the DESI source. Included with the shutter was a control box which triggered signals and converted them to the correct voltage to activate the solenoids.

Bart Whitehead also wrote a program called 'shutter.vi' to control the shutter with a National Instruments 6034-e PCI card. The PCI card sent signals to a National Instruments BNC-2110 control box, which was connected to the shutter control box. Figure 2-5 shows the shutter.

Figure 2-7 Electronic shutter

2.2.5.3 Operational Details

The jolt from either solenoid on activation was strong enough to cause the electronic shutter to jump slightly along the microscope stage. We solved this problem by taping the system to a microscope plate so that the shutter covered the hole over the objective while the back end hung over the plate and rested on the microscope stage. The back end of the shutter was then taped to the top of the microscope stage to prevent the microscope plate, with the attached shutter, from rotating. The jolt could also cause the microscope stage to move. This movement was visible (1-4 pixels) in images taken before and after triggering the shutter.

Slight movements in the stage were not a problem for real time imaging because we were interested in the time resolved images and not in comparing individual frames before and after triggering. When necessary, this slight movement could be overcome by securing the microscope stage with the set screws positioned on the sides or the long screw from the

motorized translational stage. Taping the sample slide to the microscope stage also prevented movement of the slide.

Occasionally, the shutter would come in contact with the top of the sample slide. This always occurred toward the solenoid side of the shutter. We added a small amount of tape to the underside of the shutter frame to elevate it slightly, with extra tape placed beneath the solenoids toward the back to prevent contact with the slide surface

It should be noted that it took about 13 ms for the shutter to make a complete cycle. Any attempts to reduce the time resulted in activation of the solenoid that shut the shutter before it was completely opened. Based on the position of the spray tip relative to the shutter, the time for the spray to actually reach the surface on a 13 ms cycle could be much shorter. The time necessary to open and close completely in one direction was between 5 ms and 10 ms.

Due to the way the shutter program was written and the shutter hardware was designed, there was a small set of exposure times in which the shutter could not properly function. If the shutter was set to 150 ms ± ~13 ms, the shutter opened but did not close properly. Bart explained that this was due to a signal being processed while the solenoid that closes the shutter is being activated. He offered to rebuild the control box, but we declined and have simply avoided working in this time frame.

Bart chose a reflective plastic for the shutter material, which proved problematic with reflected and scattered laser light, notwithstanding the dichroic cube in the microscope. We chose to use a black Sharpie™ to 'paint' the underside of the shutter, reducing the amount of non-fluorescent light seen in the microscope. This made a large improvement. However,

despite nearly homogenous coatings with ink, imperfections in the surface and the edge of the shutter could still be seen in the microscope.

2.2.6 Barrier Setup

2.2.6.1 Design Considerations

Dr. Farnsworth suggested that we find a way to construct a barrier that could be placed in front of the DESI source. This barrier could block potential secondary droplets from thin film splashing and would be useful for investigation into rivulet based ionization. Devin Busby, an undergraduate in our research group designed a setup with which we could block any spray solvent that left the surface before reaching the ends of the rivulets.

2.2.6.2 Experimental Setup

This barrier consisted of a microscope cover slip held in place by a rubber coated 'claw' positioned using the large 4-dimensional stage. The 4 dimensional stage (X, Y, Z, and rotational stage) was elevated to the height of the microscope with aluminum rods and placed on top of an aluminum plate. The claw was secured by right angle braces attached to an aluminum rod that was secured to the stage with an in-house designed mount (see Figure 2-8). The cover slip was positioned less than 150 µm above the surface to reduce the chance of any droplets passing underneath.

Dipped slides were positioned beneath the barrier along the X axis with the coated and uncoated sides separated by the barrier. The coated side was placed on the same side as the transfer line while the non coated side was placed on the side with the DESI source. When

sampling, the rivulets ran underneath the barrier and came in contact with the analyte on the opposite side.

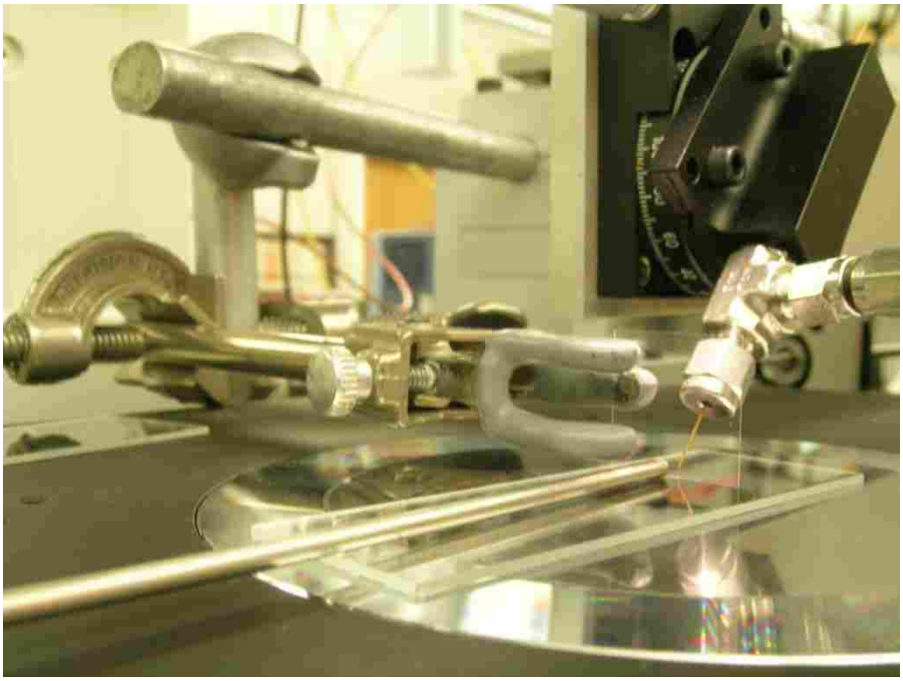

Figure 2-8 DESI barrier setup

2.3 Experimental Methodology

Much of my effort was focused on the design and implementation of the instrumentation for the project. Experimental design required consistent operating parameters that would work with the DESI source, mass spectrometer, and the microscope. For example, there are many instances of experiments in which DESI is operated at flow rates higher[1, 8-11] and lower[12] than our 2 µL/min, with some as high as 30 µL/min.[13] With our setup, the flow rate could be increased, but the resulting spray spot when viewed with the microscope would be far too large

to image. We have thus stayed within a limited operating range for our DESI source, similar to that first proposed by Cooks' group. The results should still be applicable to larger scale spraying parameters.

2.3.1 Samples

2.3.1.1 Sample Preparation

RBB was prepared as a stock solution using pure methanol at a concentration of 500 µM in a 100 mL volumetric flask. This solution was then diluted to make the 10 µM solution used for coating and any other solutions as necessary. CV was prepared as a stock solution of 100 µM and used to prepare solutions at varying concentrations for coating.

2.3.1.2 Slide Cleaning

We found that the 'pre-cleaned slides' purchased from any of the standard suppliers were not sufficiently clean for our imaging needs. The slides were cleaned by applying a small drop of liquid dish soap and rubbing both surfaces between the fingers (using nitrile gloves). Each slide was then rinsed with tap water, methanol, and finally deionized water. The slides were then allowed to air dry and placed in a separate container for future use.

2.3.2 DESI Positioning

The standard DESI analysis is typically performed at an angle between 50° and 60°. We chose 55° as an operating angle for all DESI experiments to reduce the number of variables between experiments. The angle was set by leveling the needle so that it was parallel to the microscope stage and then turning the rotational stage 55° toward the microscope stage. Care was taken

when mounting the DESI brace arm to ensure that it was level. If the arm was not tightened sufficiently, it would sag slightly. When the DESI source was mounted to a 'sagging' brace arm, spacing was insufficient to operate at the correct angle and height above the microscope stage.

After correctly setting the angle, coarse adjustments were made to the bolts securing the base of the stage to the aluminum posts. With a lowered DESI source, the capillary was positioned visually as seen through the microscope eye pieces using the fine adjustment knobs on the XY stage. To position the height correctly, the capillary was lowered slowly using the Z stage until it made contact with a standard glass microscope slide on the microscope stage. The capillary was then raised 1.5 mm off the stage using the vernier scale on the knob of the Z stage.

Once the capillary was adjusted to the proper height we started the DESI spray. We then adjusted the XY stage to center the spray footprint within the viewing area of the microscope using the eyepieces. The spray could then be further positioned using the XY stages and the CCD.

When setting up an experiment that used both the shutter and the transfer line, it was important to take extra care with the transfer line positioning to prevent the shutter from hitting the transfer line when it closed. This was especially important when hunting for a homogenously coated region on the sample slide. Because the transfer line worked better closer to the source, we found it easier to position the transfer line with respect to the shutter at a fixed location, and then hunt for a homogenous spot on the slide by moving the slide back and forth (as opposed to the microscope stage). This approach worked as long as the slide extended to the opposite side of the hole in the microscope plate. If the slide did not extend to

the end of the hole it would not be level. Non-level slides were problematic for imaging because they were not in focus over the entire slide.

2.3.3 Imaging Methodology

Coated slides typically did not exhibit a perfect coating, even when thoroughly cleaned prior to being dipped. Because the spray area was only a couple of square millimeters in size, many images could be taken on a single coated slide. When performing imaging experiments it was necessary to choose the spray location based on surface coating uniformity. The steps for setting up a fluorescence imaging experiment with the shutter follow:

1. Start the laser, rotating diffuser, and the CCD. Turn off the room lights.
2. Secure the shutter to the microscope plate so that that it opens directly over the hole in the microscope plate.
3. Place a coated slide beneath the shutter. The uncoated part of the slide should be positioned closest to the transfer line.
4. Set the CCD exposure time to 0.3 s. Change the optical pathway to the left port.
5. Using video imaging mode, check for high light intensity and find the edge of the dye coating on the slide.
6. Set the CCD exposure time to 10 s. Take individual images at 10 s exposures, adjusting the focus with each image.
7. Close the shutter. Find a homogenously coated spot on the slide using video imaging mode in Solis with a 0.3 exposure time. Tape the slide to the microscope stage to prevent movement by the shutter.

8. Perform imaging experiments using 10 s exposures. Move the microscope stage as necessary for additional spraying locations.

Focusing on the slide prior to the beginning of a run was very important. This was done with the shutter open because blemishes on the underside of the shutter made focusing difficult due to scattered laser light. Because small droplets splashed downfield from the spraying location, spraying always began close to the uncoated edge. We found that spraying along the Y direction before moving the microscope stage in the X direction produced the best results. Care was taken not to move the microscope stage too far in the X direction because the open shutter could affect the DESI spray. In these cases, it was better to remove the tape securing the microscope slide and shift the slide downfield so that the point of exposure was close to the edge of the shutter when closed and many millimeters from the shutter edge when open.

A similar procedure was required for imaging crystal violet coated slides. Because the slides were coated by spotting, the slide positioning was based entirely on the spot location. The incandescent microscope lamp was switched on and adjusted to low power, approximately 10-20%, with no gain on the CCD. The exposure time and lamp light were then adjusted in video mode while monitoring the data histogram to prevent over exposure. For image acquisition that required experiments longer than a few seconds, the CCD was set to sample at a rate much slower than the actual acquisition rate. This was done by setting the kinetic cycle time in the kinetic imaging mode.

For acquiring video data using the kinetic imaging mode, it was extremely important to take the computer hardware capacity into consideration. The Andor Solis software took a long

time to allocate the memory for a large file. This sometimes resulted in timing issues if the CCD and mass spectrometer or the CCD and the shutter were activated simultaneously. We were not able to run Labview and take video images simultaneously on a single computer because both programs competed for processor time. Small quantities of computer RAM also limited the size of the data file. Future users of the system can take advantage of the spooling feature of the Andor Solis software to report how much disk space a video image will require. On the spooling tab, clicking the 'enable spooling' check box generates a data report for the amount of memory necessary to record a file at the given settings. Since data that is not spooled directly to the hard drive is recorded in the .sif file format, it takes roughly double the space in RAM as a binary file, and can be seen by checking the .sif radio button.

2.3.4 MS Methodology

The mass spectrometer was set up so that the sampling orifice was approximately the same height as the microscope stage. When the transfer line was connected, it extended over the microscope stage. The transfer line was made from stainless steel tubing and was easily bent so that the tip of the transfer line came in contact with the microscope slide. If the transfer line was bent too far downward the pressure it exerted on the slide was enough to hold the slide in place during stage translation. A slight bend in the transfer line afforded enough pressure to maintain surface contact while still permitting the slide to move freely when the stage was moved. Because contact from the transfer line scratched the dye on the slide, the slide was always shifted down field of the spray.

Before each experiment, the alignment and functionality of the mass spectrometer setup was tested using a test slide. The transfer line was positioned 2-3 mm from the spray

position while viewed through the microscope eye-pieces. The test slide was made by spotting a clean slide with either experimental dye or marked with a Sharpie™ pen. Tuneplus was used in scan mode to monitor signal from the test slides. Any problems identified in the process were then fixed prior to exposing the sample slide to the spray.

2.4 Experimental

Unless otherwise noted, the DESI source was operated at a nebulizing pressure of 150 psi, solvent flow rate of 2.0 µL/min, and potential of 4900 V. These parameters were chosen to be similar to parameters from some of the original Cooks' publications[14-16] and produced detectable signal with our system. Other pressures, flow rates, and potentials were tested, but did not produce any noteworthy visible changes within the levels we were capable of imaging during these experiments. The solvent for our experiments was a 50/50 mix of water/methanol (18 MΩ from a Millipore water purification system, and spectroscopic grade respectively).

2.4.1 Fluorescence Imaging and the Electronic Shutter

In order to ensure that the fluorescence intensities recorded in the microscopic images were proportional to dye concentrations on the surface, we coated a series of slides with RBB by dipping them in solutions with concentrations ranging from 1×10^{-6} M to 1×10^{-5} M. The slides were then imaged with the CCD, and the average intensities plotted as a function of the original solution concentration. The fluorescence signal was linear up to a dye concentration of 1×10^{-5} M. An increase in dye concentration over this led to a decrease in the fluorescence due to self absorption.

A slide dipped in 1.0 x 10^{-5} M RBB was mounted with the shutter device and exposed to the DESI spray at standard conditions for 30 s. The DESI source was shut off (solvent, nebulizing gas, and potential) without removing the slide or the shutter. The slide was then imaged using 4x objective and the planar imaging mode of the microscope, with excitation by the argon ion laser at 488 nm. Images were taken with 20 s exposures. The images were stitched together using Microsoft PowerPoint (Figure 2-9) and shown in the results and discussion.

Additional images were taken using the shutter, both before (Figure 2-11a) and after (Figure 2-11b) 30 ms of exposure. The position was then moved to an undisturbed location and exposed to 200 ms of spray and then imaged (Figure 2-11c); the same location was then exposed for an additional 200 ms and imaged a second time (Figure 2-11d). The shutter, spray, and a coated slide were mounted on the microscope stage. Evenly coated locations on the slide were selected by watching the uniformity of the coating with the real time imaging (0.3-0.5 s exposures) of the CCD and while slowly moving the microscope stage. The selected spot was then imaged with an exposure of 20 s while the shutter was closed.

2.4.2 High Speed Imaging

To increase the sampling rate of the CCD, a custom sized sub array was chosen for sampling, permitting the maximum sampling rate for the sub-array to be set at 144.5 Hz. With the gain disabled, the incandescent lamp of the microscope was slowly adjusted in video mode to allow the desired amount of light for imaging on the CCD. Slides coated with CV were prepared, the most homogenous coating being selected for a high speed experiment. Using the CCD in video mode the slide was positioned over an area that had no visible deformations in the coating. The shutter was then moved to the closed position before starting the spray.

The DESI spray was allowed to spray for 5 min with the shutter closed to equilibrate and to remove any bubbles in the solvent line. Using two people, the CCD was activated, and followed immediately by the shutter. This entire process lasted approximately 5 s, producing roughly 3 s of images.

2.4.3 Simultaneous Imaging Experiment

A thick coating of CV was prepared by spotting multiple aliquots of 4×10^{-5} M CV on a slide with successive evaporation, resulting in crystallization of the dye on the slide. This coated slide was mounted on the microscope along with the shutter. A location on the slide was selected for spraying and the shutter was closed. The CCD exposure time was set for 0.1 s exposures with a kinetic cycle time of 2 Hz. The number of images was set to 360 for a total of 3 min of imaging. The DESI source was allowed to spray for 5 min to equilibrate and remove bubbles from the line. The mass spectrometer was set to acquire data for 4 min.

Data acquisition on the mass spectrometer was initiated with the shutter closed for 30 s as a blank. At the 30 s mark the CCD was started and the shutter was opened. The shutter was closed after 3 min. This process was repeated 7 times at different locations on the slide.

2.4.4 Rivulet Experiment

A glass cover slip was mounted to a translational stage and positioned over the microscope so that the cover slip was orthogonally oriented to the microscope stage and to the DESI tip, creating a barrier between the spray and the transfer line of the mass spectrometer. The cover slip was positioned to be 2 mm from the DESI tip and 3 mm from the transfer line. The lower edge of the cover slip was positioned using the translational stage to be approximately 0.3 mm

above a slide. This positioning allowed for the DESI spray to impinge directly on the microscope slide and the rivulets formed during the process to pass under the cover slip.

A slide partially coated in 9.2 x10^{-4} M CV was placed on the microscope stage so that the coated portion of the slide was on the side of the barrier opposite the DESI source, several mm away from the cover slip. The uncoated side was then sprayed for 30 s while being imaged with the CCD. After 30 s, the microscope stage was repositioned to bring the coated portion of the slide to the edge of the cover slip, but still on the side opposite the DESI emitter. The only contact between the DESI spray and the sample was via the flow of the rivulets underneath the barrier. The experiment was started with the dye positioned downstream from the cover slip and spray footprint. The slide was then moved with respect to the spray until the rivulets came in contact with the dye by running under the barrier. The time-dependent signal from the CV was recorded by the mass spectrometer during the entire experiment.

2.5 Results and Discussion of the DESI Mechanism

From the first moment that the DESI source was properly mounted over the microscope, we could easily see the formation of a spray footprint with streaming rivulets breaking off from all sides of the central region and washing across the slide. Our first attempt at fluorescence imaging consisted of spotting the surface with concentrated dye, letting it dry, and then exposing it to DESI. While the spot was too thick to produce fluorescence, we could visually see the rivulets rolling across the sample, picking up dye, and fluorescing brightly. This confirmed droplet pickup as a possible mechanism for desorption and ionization due to the analyte being dissolved in the solvent.

2.5.1 Fluorescence Experiments

Real time imaging of the surfaces used with DESI required some form of separation of the spray and surface to gain an accurate picture of the changes that took place on a short time scale when the surface was exposed to the spray. The electronic shutter was a crucial component for imaging the surface. The shutter allowed us to precisely control spray exposure, limiting the volume of liquid delivered.

A coating of RBB on a clean glass slide was exposed to the DESI spray for 30 s and provided insight regarding the nature of the DESI spray (shown in Figure 2-9**).** The individual images were all taken on the same scale and are shown in the false color option 'glow' of the Solis software. The false color makes it possible to see the small droplets outside the main spraying region. Despite a uniform coating, the image edges are slightly darker due to the beam profile of the laser. The white line to the left of the image is the edge of the shutter, which was left in place while the images were taken.

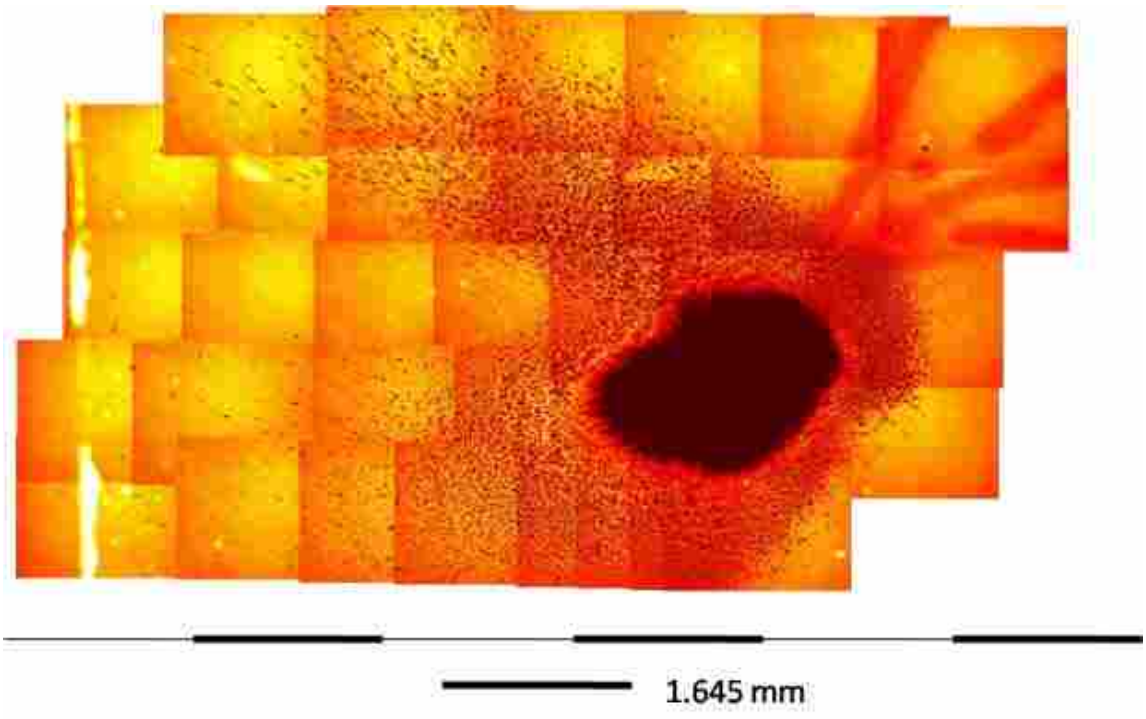

Figure 2-9 DESI Stitched image from 30 s exposure.

The displaced dye in the center is what we refer to as the 'footprint' region of the sample. Unexpectedly, the footprint region is not symmetrical, despite the fact that the source was constructed from two standard fused silica capillaries. This is common in DESI spray, and is due to minor variations in the construction of the needle tip, e.g., distances between the inner and outer capillary ends as well as how smoothly the capillaries have been cut.

Close inspection of an individual frame of the image above provides additional insight into the nature of the spray. Figure 2-10 shows the upper region of the spray footprint using a single frame. The dye itself has been removed from the central region. At the edges of the footprint there is an uneven removal of the dye, resulting in 'fingers' of dye pointing toward the center. This is caused by the solvent washing the dye to the edges of the footprint before evaporating. Further outside the footprint, we see the formation of spots on the coating from

droplet collisions. An increase in the intensity of color indicates a dye build up in the direction of the momentum of the individual droplets. The more elongated droplets to the left of the image suggest higher velocities. Because these image were taken from 30 s of spray exposure, the droplets indicate a certain level of randomness, especially where some of the coating remains undisturbed on the far left edge of the image.

What the images do not show is the behavior of the spray over a short period of time. High speed exposures to the solvent were used to investigate the spray as it briefly came in contact with the surface.

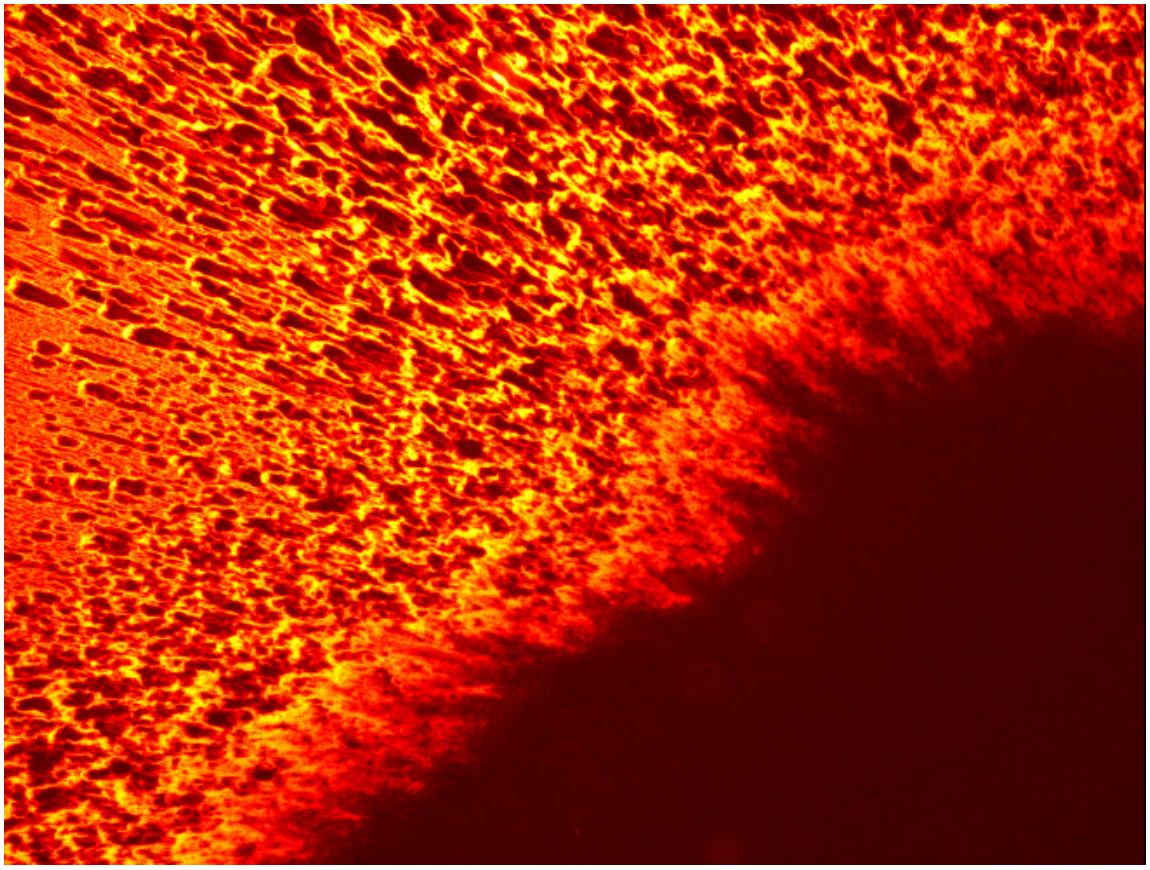

Figure 2-10 DESI footprint edge

Figure 2-11 shows the effect of various exposure times from the DESI spray. Figure 2-11A and Figure 2-11B are before and after images taken from exposure to 30 ms of spray. Figure 2-11C and Figure 2-11D show two successive DESI exposures of 200 ms on an undisturbed location. These images provide a stark contrast to the 30 ms exposure to the spray, having a very different footprint. Each image taken at 4X magnification is 1.645 mm wide, indicating that the spray footprint grew for the duration of the spray (within a limit). It can also be seen in Figure 2-11B that some displacement began by 30 ms, showing how quickly dye removal begins. The image also shows the occurrence of droplets well outside the location of the spray footprint. These droplets are present from the onset and are likely produced from the source tip itself.

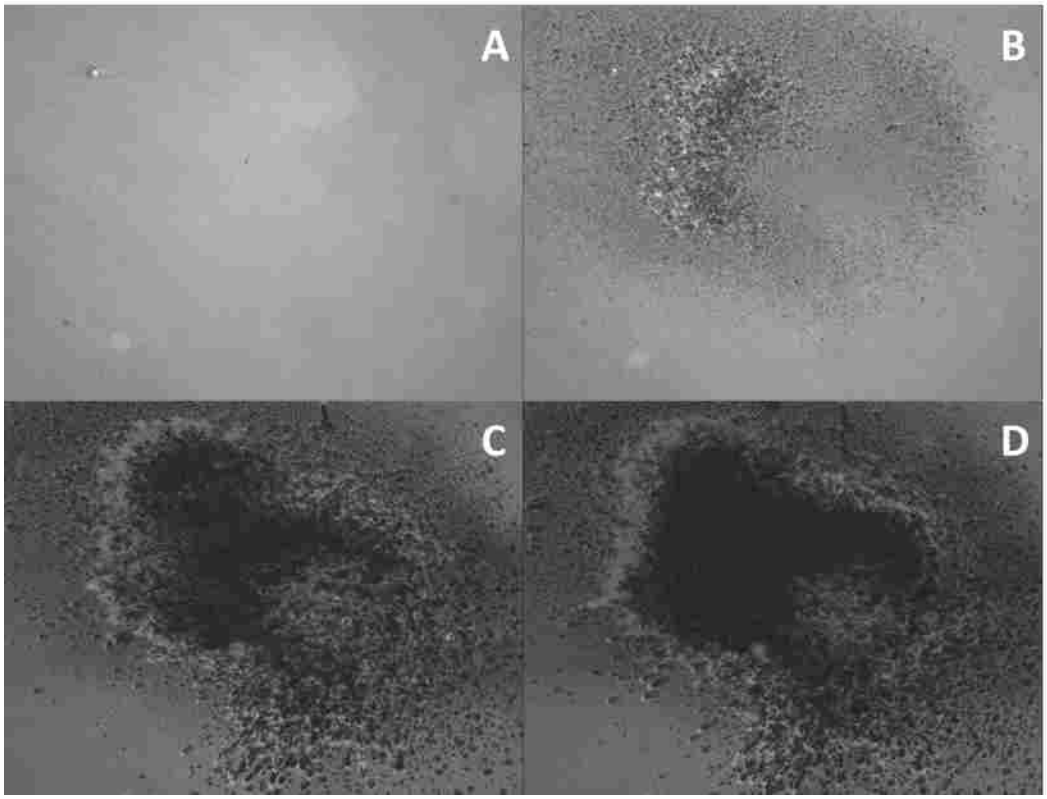

Figure 2-11 Time evolved footprints

Figure 2-11C shows that the spray itself is not symmetrical. The shape is different than that shown in the 30 s image due to the difference in the construction of the needle but has no effect on the signal from the mass spectrometer. The additional 200 ms exposure (Figure 2-11D) at the same location shows a continued expansion of the footprint. The residual dye remaining in the center of the spray footprint in frame C has been mostly pushed up to the edge of the footprint where the solvent evaporates. Additional 200 ms exposures have only a minimal effect on the shape and size of the footprint (not shown) as the footprint approaches the maximum displacement before the solvent evaporates. However, if the shutter is left open for long durations, as opposed to successive short exposures, the spot predictably gets larger. These images clearly indicate that the dye migrates across the slide as it is dissolved and transported by the solvent. The droplets on the outside of the spray footprint are present regardless of the duration of the spray, suggesting that they are generated by the source and not from splashing off of a thin film on the surface.

2.5.2 High Speed Experiment

The interactions of a DESI spray with a surface occur on a range of time scales. The CCD itself was limited to 37 Hz when using the entire chip for data collection. This corresponded to a 27 ms exposure per frame, which was far too long in comparison to the rate at which the dye was removed. Since the shutter itself opened at around 10 ms, we needed a way to image faster to obtain a picture of the spray as it made contact with the surface. The binning tab of the Andor Solis software has an option that can be used to choose a subarray of pixels. The limiting factor is the analog to digital conversion, resulting in a linear relationship between the number of

pixels and readout time. By selecting a smaller area we were able to image at a much faster frequency while still imaging a sizable fraction of the spray footprint.

Fluorescent coatings were not useful for fast, real-time imaging because they needed many seconds exposure per frame. Dr. Farnsworth suggested that high speed images be taken using absorbance measurements. Even with very thick coatings RBB was a poor absorber, so we decided to experiment with the quenching dye, crystal violet. After some work, we were able to produce fairly opaque coatings using a spotting technique with CV (see Section 2.2.4.4).

Figure 2-12 shows select individual frames taken from the video of the high speed experiment. The images were taken at a frame rate of 144.5 Hz or approximately 6.9 ms exposures. Because the CCD recorded images from the onset of the shutter opening, we can see the initial effects of the spray on the surface from the moment it made contact. The formation of the central elliptical region can be seen in the first images as the removal of the dye is represented by lighter colors.

Figure 2-12A shows digitally magnified images of the formation of the spray footprint in successive time steps approximately 6.9 ms apart. From the moment the spray hits the surface, the dye begins to be displaced. There are noticeable formations of rivulets on the surface that are removing the dye, with a buildup of dye as the darker rivulets break free from the leading solvent edge of the footprint. By the second frame, an elliptical region has begun to form where a majority of the dye has been removed due to the majority of the solvent passing over this location. By the third frame, the flow lines from the remaining dye in the solution have begun to disappear leaving the classical elliptical spray footprint.

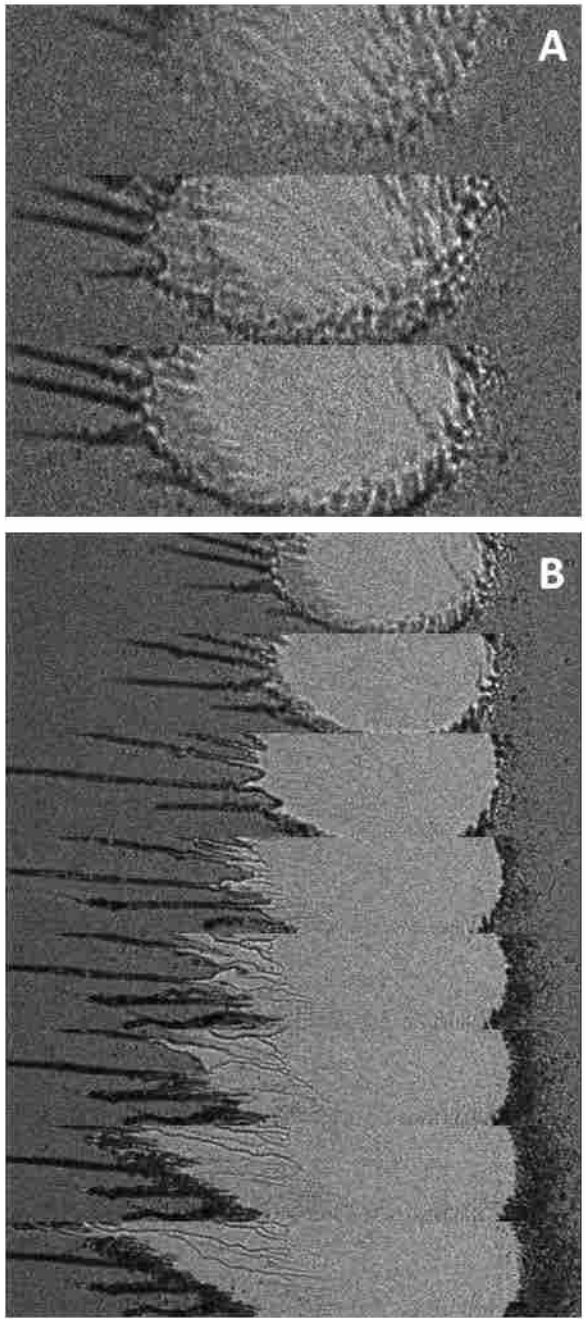

Figure 2-12 High speed images taken immediately after exposure to the DESI spray. The first 7 ms are shown in A. Selected frames over the next 3 seconds are shown in B.

The frames in Figure 2-12B are nonconsecutive and show the progress of the spray in removing dye. A thin film of solvent forms that reaches a certain size before the rivulets break from it, making their way to the analyte. The thin film remains fairly uniform in size as the

rivulets move about, dissolving dye and depositing it further downstream as they evaporate. While the images confirm the formation of a thin film, the images do not support the droplet splashing mechanisms proposed by Cooks' group because the analyte is completely removed from the area of the film within the first second. In most cases, signal remains for many seconds after the surface is exposed, if the analyte is quickly removed it is reasonable to conclude that the analyte must be leaving the surface from the rivulets and not from the film.

2.5.3 Simultaneous Imaging Experiment

One would expect that a correlation exists between the sample present on a surface and ion signal detected by the mass spectrometer. The combination of the microscope with the mass spectrometer gave us the capability to look at both simultaneously. We had already seen that removal from the surface of a lightly coated slide was nearly instantaneous. We had also found that thick coatings could be sampled by the mass spectrometer for many minutes. Given the fast removal seen in the previous experiment, we wondered what was causing the prolonged signal with thicker coatings. This was the first experiment where we used both the shutter and the transfer line together.

Sampling with both the shutter and transfer line in place for the thick samples produced a background signal, so we decided to start the mass spectrometer 30 s before opening the shutter to produce a baseline that could be used as a blank. The shutter was then opened for 3 min. The signal produced in this setup was very noisy so we repeated the experiment multiple times, while recording images with the microscope and CCD. The signal generated by averaging seven runs is shown in Figure 2-13.

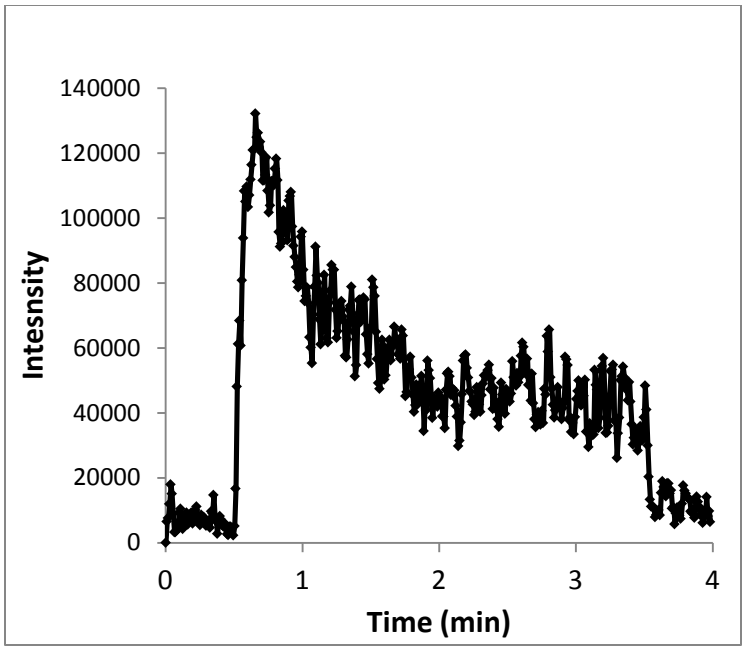

Figure 2-13 Average simultaneous imaging signal

Due to the limitation on storage capacity, it was not possible to record several minutes of video at 37 Hz. However, by looking at images sampled at a much lower frequency, the migration of analyte is more noticeable due to larger incremental changes between images. Examining the last of the videos captured at 2 Hz, we were surprised to note a very subtle change in the sample over the course of each run. There was a noticeable migration of analyte on the surface outside the spray footprint toward the center of the footprint. At first we thought this was purely a coincidence, but further examination of the other videos confirmed what we were seeing. The dye outside the spray footprint was migrating back towards the spray region.

Figure 2-14 shows a second time lapsed comparison between two images taken at the same location. After a relatively short time of less than 20 s, all the dye was removed from the spray footprint, as seen in the upper half of Figure 2-14. The dye crystals were transported to the outer edge where the dye was deposited in a darker line surrounding the edge of the

footprint. The second image was taken a minute after the first. There are visibly fewer dye crystals remaining along the dark edge. The buildup at the edge has been broken down. While not possible to show on paper, the video clearly shows the crystals migrating towards the rivulets. This migration likely comes from the external droplets that land outside the spray footprint. The dye migration provides evidence as to why the signal lasts longer than expected.

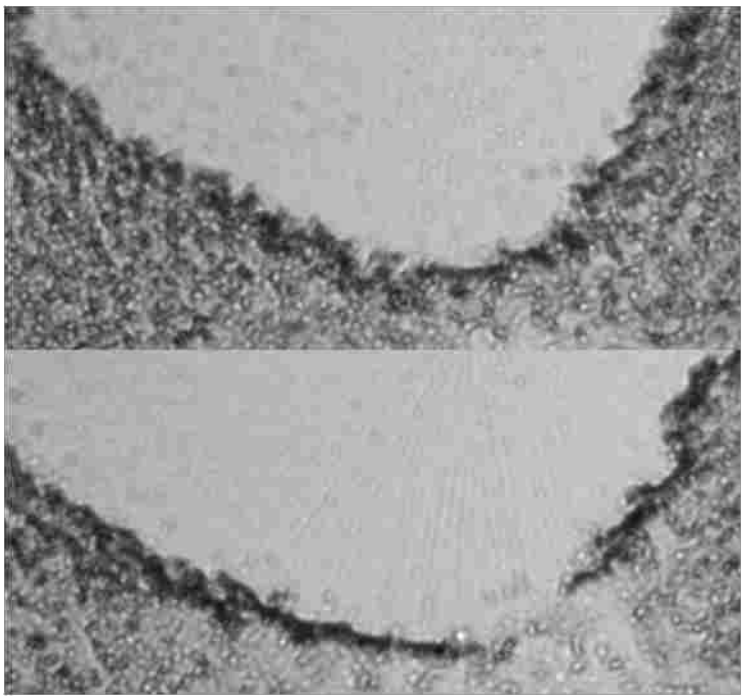

Figure 2-14 Simultaneous removal border

2.5.4 Rivulet Experiment

As noted earlier, the Cooks group had proposed a mechanism for analyte transfer through splashing of a thin film that formed on a surface from high velocity droplets generated in the spray. This mechanism is often referred to as momentum transfer and was based on data collected through Doppler anemometry[17] and theoretical simulations.[18]

After extensive work with the DESI source, and the obvious rapid removal of dye from the surface, we hypothesized that much of the ion transfer must occur somewhere other than the central spraying. Rivulet formation and subsequent transfer of analyte via the rivulets seemed a very plausible method for transition into the gas phase. Dr. Farnsworth suggested a method for testing this by introducing a simple barrier under which rivulets could pass but none of the spray could directly reach the analyte. Section 2.4.4 describes the setup for the barrier experiment. The cover slip was positioned less than 200 μm above the slide, high enough to let the rivulets to pass underneath, but low enough[17] to block any droplets generated from momentum transfer.

Figure 2-15A shows an image taken from a video recorded during the rivulet experiment with the rivulets passing beneath the cover slip. The white arrow points to the dye coating from dipping. Figure 2-15B shows the selected ion signal of RBB acquired in the rivulet experiment, as the microscope stage is moved. The dye becomes exposed to the rivulets after 20 s into the run, producing a large jump in signal.

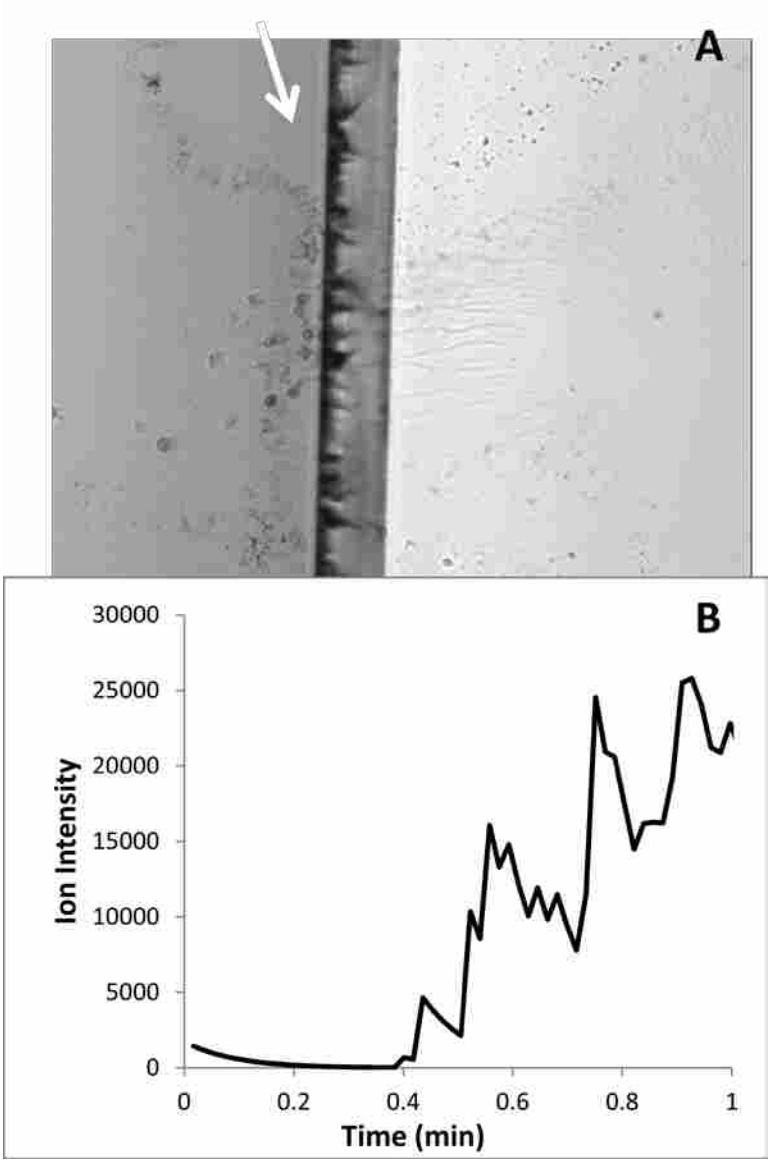

Figure 2-15 Rivulet experiment results. Image for the rivulet experiment in progress (A) and the resulting signal as analyte is moved closer to the rivulets (B).

This simple experiment demonstrates that both ionization and desorption can be accomplished solely by rivulets. While it doesn't disprove the momentum transfer mechanism, it does demonstrate a phenomenon not predicted by any of the proposed mechanisms. The rivulet experiment demonstrates that analyte outside the central elliptical spray region can be transported into the gas phase through the rivulets. Since this process is not described by any

of the previous mechanisms, it is necessary to propose an alternate mechanism that accommodates this mode of analyte transport.

2.5.5 An Alternate Mechanism

The most significant aspect of the various real time imaging experiments is the demonstration of the rapid removal of analyte from the central elliptical region. As predicted by others, a thin film forms in this region. But what is not predicted is that most of the analyte in this region is removed very quickly and, thus, not dissolved in the film. The simultaneous monitoring experiment, with prolonged ion signals, demonstrates that signal intensity does not correlate to the formation of a thin film with dissolved analyte.

Evidence suggests that rivulets play a critical role in ionization. Rivulet desorption could come about in two ways, through Taylor cones[19] or rapid evaporation. If Taylor cones are forming on the rivulets, they could be ejecting droplets similar to droplet generation in ESI. Rapid evaporation could also be used to explain analyte transport if Taylor cones are not present. In rapid evaporation, a small portion of the analyte would enter the gas phase as the rivulet rapidly evaporates due to the high velocity nebulizing gas. This process would leave a majority of the analyte deposited back on the surface.

2.6 Conclusions

The first four goals presented herein have been met with steps taken toward the fifth goal of identifying the DESI mechanism. Hardware adaptations for the DESI source and for the mass spectrometer have successfully been designed and built for combining an inverted microscope and mass spectrometer. This combination has proved useful in examining the DESI spray on

glass surfaces and examining the effects of DESI spray on the transport of the analyte during sampling. We have seen that the solvent interacts quickly with the analyte, generating rivulets that carry it downstream from the spray.

These experiments have uncovered important aspects of the DESI mechanism that are not in agreement with the proposed momentum transfer mechanism. Although a thin film has been shown to form on the surface in the area of most efficient desorption, the analyte does not remain within this region for an appreciable amount of time. We have also shown that even when the analyte has been entirely removed from this region, signal can be detected, suggesting that the detected analyte is not generated from splashes of droplets in this region. Our rivulet experiment has shown that rivulets alone are capable of ionization and need to be included in any future DESI mechanisms.

2.7 References

1. Takats, Z.; Wiseman, J. M.; Gologan, B.; Cooks, R. G., Mass Spectrometry Sampling Under Ambient Conditions with Desorption Electrospray Ionization. *Science* **2004,** *306* (5695), 471-473.
2. Green, F. M.; Stokes, P.; Hopley, C.; Seah, M. P.; Gilmore, I. S.; O'Connor, G., Developing Repeatable Measurements for Reliable Analysis of Molecules at Surfaces Using Desorption Electrospray Ionization. *Analytical Chemistry* **2009,** *81* (6), 2286-2293.
3. Bereman, M. S.; Muddiman, D. C., Detection of Attomole Amounts of Analyte by Desorption Electrospray Ionization Mass Spectrometry (DESI-MS) Determined Using Fluorescence Spectroscopy. *Journal of the American Society for Mass Spectrometry* **2007,** *18* (6), 1093-1096.
4. Cotte-Rodríguez, I.; Cooks, R. G., Non-proximate Detection of Explosives and Chemical Warfare Agent Simulants by Desorption Electrospray Ionization Mass Spectrometry. *Chemical Communications* **2006**, 2968-2970.
5. Cotte-Rodríguez, I.; Mulligan, C. C.; Cooks, R. G., Non-Proximate Detection of Small and Large Molecules by Desorption Electrospray Ionization and Desorption Atmospheric Pressure Chemical Ionization Mass Spectrometry: Instrumentation and Applications in Forensics, Chemistry, and Biology. *Analytical Chemistry* **2007,** *79* (18), 7069-7077.
6. Takats, Z.; Wiseman, J. M.; Gologan, B.; Cooks, R. G., Electrosonic Spray Ionization. A Gentle Technique for Generating Folded Proteins and Protein Complexes in the Gas Phase and

for Studying Ion Molecule Reactions at Atmospheric Pressure. *Analytical Chemistry* **2004,** *76* (14), 4050-4058.
7. Hanley, D. C.; Harris, J. M., Quantitative Dosing of Surfaces with Fluorescent Molecules: Characterization of Fractional Monolayer Coverages by Counting Single Molecules. *Analytical Chemistry* **2001,** *73* (21), 5030-5037.
8. Rodriguez-Cruz, S. E., Rapid Analysis of Controlled Substances using Desorption Electrospray Ionization Mass Spectrometry. *Rapid Communications in Mass Spectrometry* **2006,** *20* (1), 53-60.
9. Leuthold, L. A.; Mandscheff, J.-F.; Fathi, M.; Giroud, C.; Augsburger, M.; Varesio, E.; Hopfgartner, G., Desorption Electrospray Ionization Mass Spectrometry: Direct Toxicological Screening and Analysis of Illicit Ecstasy Tablets. *Rapid Communications in Mass Spectrometry* **2006,** *20* (2), 103-110.
10. Williams, J. P.; Lock, R.; Patel, V. J.; Scrivens, J. H., Polarity Switching Accurate Mass Measurement of Pharmaceutical Samples Using Desorption Electrospray Ionization and a Dual Ion Source Interfaced to an Orthogonal Acceleration Time-of-Flight Mass Spectrometer. *Analytical Chemistry* **2006,** *78* (21), 7440-7445.
11. Pasilis, S. P.; Kertesz, V.; Van Berkel, G. J., Surface Scanning Analysis of Planar Arrays of Analytes with Desorption Electrospray Ionization-Mass Spectrometry. *Analytical Chemistry* **2007,** *79* (15), 5956-5962.
12. Wu, S.; Zhang, K.; Kaiser, N. K.; Bruce, J. E.; Prior, D. C.; Anderson, G. A., Incorporation of a Flared Inlet Capillary Tube on a Fourier Transform Ion Cyclotron Resonance Mass Spectrometer. *Journal of the American Society for Mass Spectrometry* **2006,** *17* (6), 772-779.
13. Chen, H.; Talaty, N. N.; Takats, Z.; Cooks, R. G., Desorption Electrospray Ionization Mass Spectrometry for High-Throughput Analysis of Pharmaceutical Samples in the Ambient Environment. *Analytical Chemistry* **2005,** *77* (21), 6915-6927.
14. Takáts, Z.; Wiseman, J. M.; Cooks, R. G., Ambient Mass Spectrometry using Desorption Electrospray Ionization (DESI): Instrumentation, Mechanisms and Applications in Forensics, Chemistry, and Biology. *Journal of Mass Spectrometry* **2005,** *40* (10), 1261-1275.
15. Cotte-Rodríguez, I.; Takáts, Z.; Talaty, N.; Chen, H.; Cooks, R. G., Desorption Electrospray Ionization of Explosives on Surfaces: Sensitivity and Selectivity Enhancement by Reactive Desorption Electrospray Ionization. *Analytical Chemistry* **2005,** *77* (21), 6755-6764.
16. Cody, R. B.; Laramee, J. A.; Durst, H. D., Versatile New Ion Source for the Analysis of Materials in Open Air under Ambient Conditions. *Analytical Chemistry* **2005,** *77* (8), 2297-2302.
17. Venter, A.; Sojka, P. E.; Cooks, R. G., Droplet Dynamics and Ionization Mechanisms in Desorption Electrospray Ionization Mass Spectrometry. *Analytical Chemistry* **2006,** *78* (24), 8549-8555.
18. Costa, A. B.; Cooks, R. G., Simulation Of Atmospheric Transport and Droplet-Thin Film Collisions in Desorption Electrospray Ionization. *Chemical Communications* **2007**, 3915-3917.
19. HIGUERA, F. J., Flow Rate and Electric Current Emitted by a Taylor Cone. *Journal of Fluid Mechanics* **2003,** *484* (-1), 303-327.

3 Mechanistic Study

3.1 Introduction

The current and predominantly accepted mechanism for the DESI technique involves momentum transfer. In the momentum transfer mechanism, solvated water clusters are generated by high speed water droplets impacting upon a thin solvent film containing dissolved analyte. The proposed mechanism was derived from phase Doppler anemometry data taken by the Cooks group.[1] Fluid mechanical simulations were later used to model splashes of droplets from a thin film.[2-3] These simulations have been used as evidence that the droplets seen in the phase Doppler anemometry experiment are secondary droplets generated from momentum transfer collisions of primary high-speed droplets with a thin film.

A microscope is an excellent tool for visual observation of a glass surface under the effects of the DESI spray. When looking at the DESI spray profile with the microscope, I noted that the behavior can vary greatly and is often more complex than a simple thin film forming on a surface. Visual investigation suggested a different situation: the bulk of the solvent hits the surface and breaks into rivulets that spread to the edges of the sampling region. The sample is rapidly removed and transported to the edges of the solvent by rapidly evaporating rivulets. Figure 3-1 is an image taken of the DESI spray using conditions similar to those used in experiments discussed in Chapter 2. In the image it is difficult to determine the presence or absence of a thin film or even a central elliptical region.

Figure 3-1 Image of the DESI spray profile of 50:50 methanol/water on glass. Taken at 3 µL/min 150 psi, 1.5 mm above the surface. 5 ms exposure using low level lamp light and 2x magnification. Image is 3.29 mm x 2.48 mm.

The observation of rivulets and their behavior on the surface does not rule out the formation of a thin film or of a momentum transfer, but it does provide an alternate scenario that is difficult to reconcile with the generally accepted mechanism. Using information gained from a microscopic investigation, it is possible to propose a mechanism where droplet splashing may not be a significant contributor to analyte transport and ionization. If a non-splashing mechanism exists, it would need to involve the transport of analyte through the rivulets to the edge of the spray footprint. In this process some of the analyte would be liberated into the gas phase from the rivulets, while much of the analyte is dissolved and deposited downstream.

While such a mechanism is supported by observations, it does not explain the mechanics of the analyte transport from the rivulet itself into the gas phase. The physical

process may involve jetting of analyte through microscopic Taylor cones or the introduction of analyte in the atmosphere due to miniature coulombic explosions. Although it is difficult to prove the existence of either of these mechanisms, it is possible to design experiments that can confirm if momentum transfer is the sole ion production mechanism.

The easiest way to eliminate momentum transfer from the mechanism is to eliminate 'momentum' from the DESI experiment. One way this can be done is by lowering the DESI emitter to the surface, eliminating any travel by primary droplets between the emitter and the surface and, thus, any collisions that could produce secondary droplets. Contact with the surface creates uninterrupted flow of the solvent from the capillary to the surface, enhancing the rivulet nature of DESI without changing other parameters. Detection of the analyte indicates that a mechanism other than momentum transfer must be responsible for analyte transport into the mass spectrometer.

I report herein three separate experiments that were specifically designed to demonstrate splashless ionization through rivulets generated by modifications to traditional DESI. I refer to these modified variations of DESI as rivulet DESI, rivulet electrosonic spray ionization (ESSI)[4], and dual capillary DESI (dc-DESI). The modification of DESI for rivulet DESI is simply lowering of the DESI source to the surface. This produces large rivulets instead of a normal spray profile. These longer rivulets are easier to experiment with under certain conditions, and can work with a larger separation between the point at which they form and the analyte. Rivulet ESSI is functionally similar to Rivulet DESI, including the same hardware setup. However, like ESSI, the analyte is contained within the solvent instead of on the surface. Rivulet ESSI is useful for studying direct ionization of rivulets without the complication of

desorption. Dc-DESI is similar to DESI except that the solvent is introduced at the surface while the nebulizing gas position remains unchanged. This experiment demonstrates desorption ionization without the possibility of generating 'primary' droplets from contact of the solvent with the nebulizing gas as it exits the solvent capillary.

3.2 Experimental Setup

The basic DESI hardware configuration was the same as given in Section 2.2 unless otherwise noted. The nebulizing gas pressure was set to 150 psi, the solvent flow rate was set to 3 µL/min and the voltage was set to 4900 V. Samples acquired with the mass spectrometer were taken at 50 ms injections and three microscans. Figure 3-2 shows the difference between standard DESI and the rivulet setup.

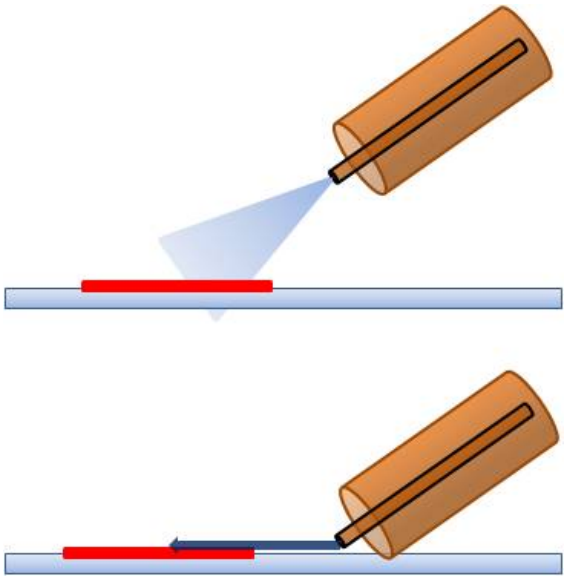

Figure 3-2 Standard DESI setup (top) vs rivulet DESI setup (bottom). The standard DESI setup creates a spray profile with many rivulets. The rivulet DESI setup creates a few large rivulets.

3.2.1 Three Dye Barrier – Rivulet DESI

3.2.1.1 Hardware Setup

The DESI source was lowered so that the tip of the source was near the surface of the microscope slide, creating a single rivulet that extended the length of the viewing area. A glass cover slip was suspended 250 µm above the surface of a microscope slide to act as a barrier facing the DESI source (see Section 2.2.6). Figure 3-3 shows the setup of the rivulet barrier experiment. The flow rate was set at 5.0 µL/min with a solvent of 60% methanol, 25% acetonitrile, 15% water and 0.75% acetic acid by volume (this is one of many alternate solvent mixtures that were tested with the barrier experiment in an attempt to produce better results. The data presented here were taken with this mixture, although other mixtures such as the 80:20 methanol/water solution produced similar results). With the solvent and nebulizing gas flowing, the DESI source was positioned away from the barrier to allow the rivulet to terminate (by evaporation) within the viewing area of the microscope.

3.2.1.2 Sample Preparation and Sampling

A straight-edge ruler was used to draw three lines on a microscope slide using red, blue, and purple Sharpie pens. The slide with the lines drawn on it was placed on the microscope, underneath the barrier, with the lines opposite the barrier from the DESI source. The lines were oriented so that they were parallel to the barrier and perpendicular to the rivulet stream. The sampling transfer line to the mass spectrometer was then positioned 3 mm from the barrier. The DESI source was activated and allowed to equilibrate. With the mass spectrometer in tune mode, the CCD was started in kinetic imaging mode. The translational stage was then used to

move the slide so that the DESI rivulet would pass underneath the barrier and make contact in succession with each of the dyes on the slide. A video of the resulting MS signal was recorded with Camstudio software from the average signal displayed in Tuneplus in real time. Subsequent mass spectra were recorded with Tuneplus using the aforementioned solution and a 80:20 methanol/water solution.

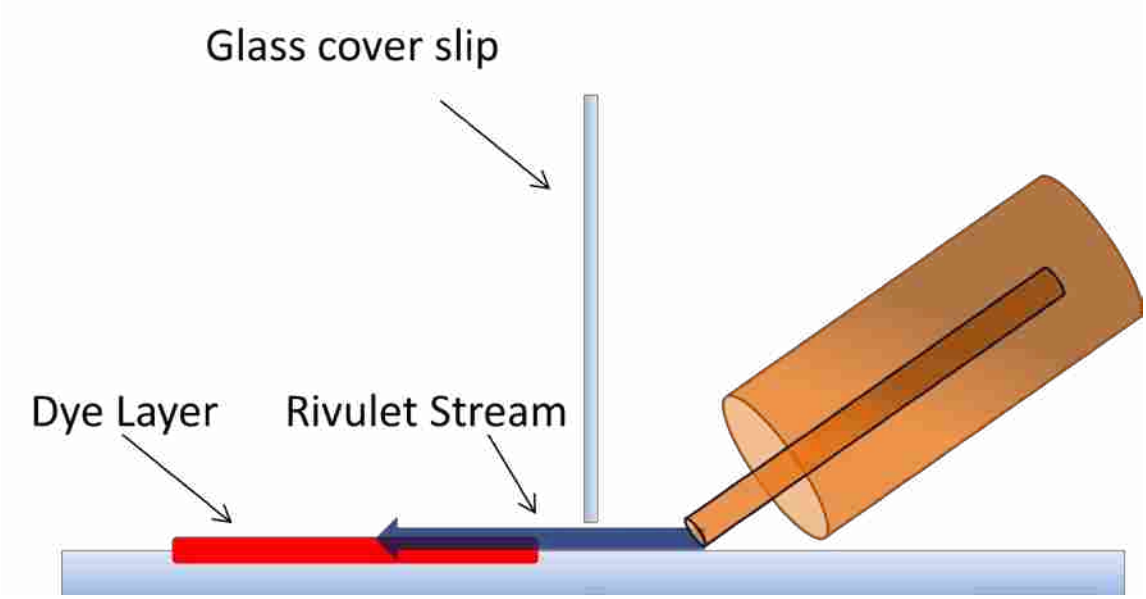

Figure 3-3 Rivulet barrier setup (not to scale)

3.2.2 Rivulet Electrosonic Spray Ionization

The DESI source was lowered so that the tip of the source was near the surface of the microscope slide, creating a single rivulet that extended the length of the viewing area. Custom made 'slides' were produced from Delrin, copper, and Teflon with dimensions similar to standard glass microscope slides. Because the custom slides were slightly thicker, the glass slide was shimmed to match the height of the custom slides (increasing the height above the stage by about 0.2 mm). When working with a copper surface, a small piece of electric tape was wrapped around the end of the transfer line to prevent current flow between conductive

copper slides and the transfer line. A solution of $1x10^{-7}$ M RBB dissolved in 80:20 methanol/water was placed in the solvent syringe and allowed to spray along the glass slide as a rivulet. The mass spectrum was recorded for one minute. This was repeated on Teflon, Delrin, and copper slides with and without the voltage applied. Pieces of masking tape were used as shims to increase the operating height of a glass slide (1 mm) to match the thickness of the other slides (1.5 mm).

A braided copper cable was connected to a ground and the other end was soldered to a metal washer. A sequence of rivulet ESSI experiments was performed as follows. With the copper slide, the experiment was run with the copper surface floating. After 20 s the grounded metal washer was placed in contact with the copper slide. After an additional 20 s of grounding the copper washer was removed. This process was repeated, recording the RBB ion intensity over 1 minute with and without a voltage applied to the DESI source.

3.2.3 Dual Capillary DESI

The DESI source was mounted in the standard operating position 1.5 mm above the slide surface. The inner DESI capillary was disconnected from the solvent syringe. A second capillary of the same dimensions as the inner capillary was taped to a microscope slide so that approximately 5 mm of exposed capillary extended past the long edge of the microscope slide. This capillary was then attached to the syringe to act as the solvent delivery line. The capillary was positioned directly beneath the suspended DESI source so that the flowing nebulizing gas would disperse solvent issuing from the capillary. This setup produced a spray footprint similar in shape to that of standard DESI. Figure 3-4 shows the dual capillary DESI (dc-DESI) setup.

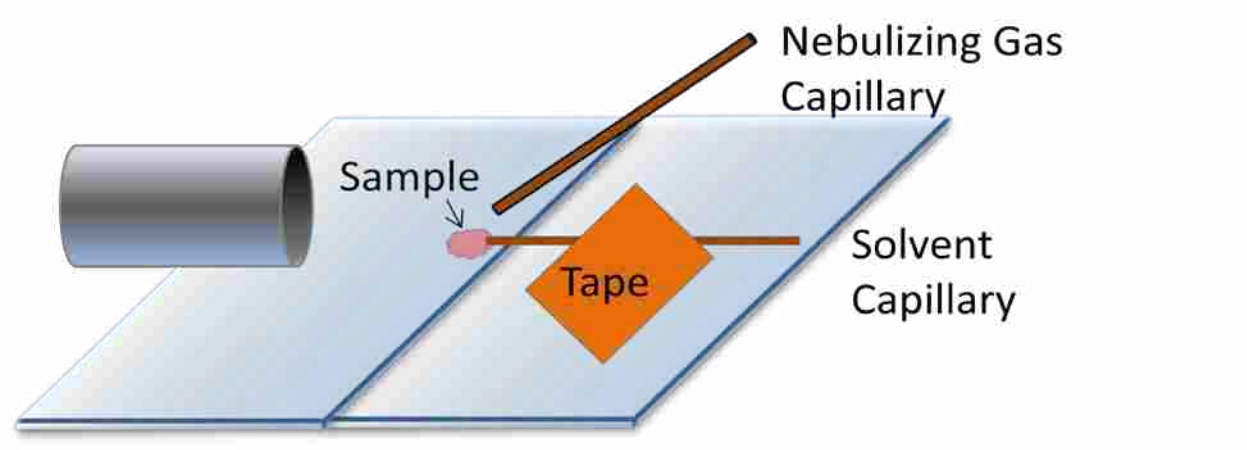

Figure 3-4 Dual capillary DESI setup (not to scale). The standard DESI setup is left intact with the exception that the solvent is introduced at the surface through a second capillary. The nebulizing gas remained unchanged.

The syringe was filled with 5 µM RBB dissolved in 75:25 methanol/water and connected to the solvent capillary. A single clean slide was placed underneath the extended solvent capillary. The syringe pump was activated and the nebulizing gas was turned on. The resulting RBB signal was recorded for 1 min using the mass spectrometer.

In a second dc-DESI experiment, concentrated RBB, dissolved in water, was spotted onto a microscope slide and dried with a heating plate. Additional drops of solution were added to the drying samples that evaporated to form 'coffee ring' spots. Figure 3-5 shows the RBB spot used in the dc-DESI experiment. The spots were intentionally created close to the edge of the microscope slide so that when the slide containing the sample was placed next to the slide with the solvent capillary, the solvent capillary extended to the sample spot on the sample slide (see Figure 3-5). With the capillary placed directly next to a sample spot, the nebulizing gas and voltage were turned on. The syringe pump flow rate was then set at 3 µL/min and the resulting mass spectra and video images were recorded over 1 min as the spot was desorbed.

Adjustments to the positioning of the sample slide were made during the run as sample was removed.

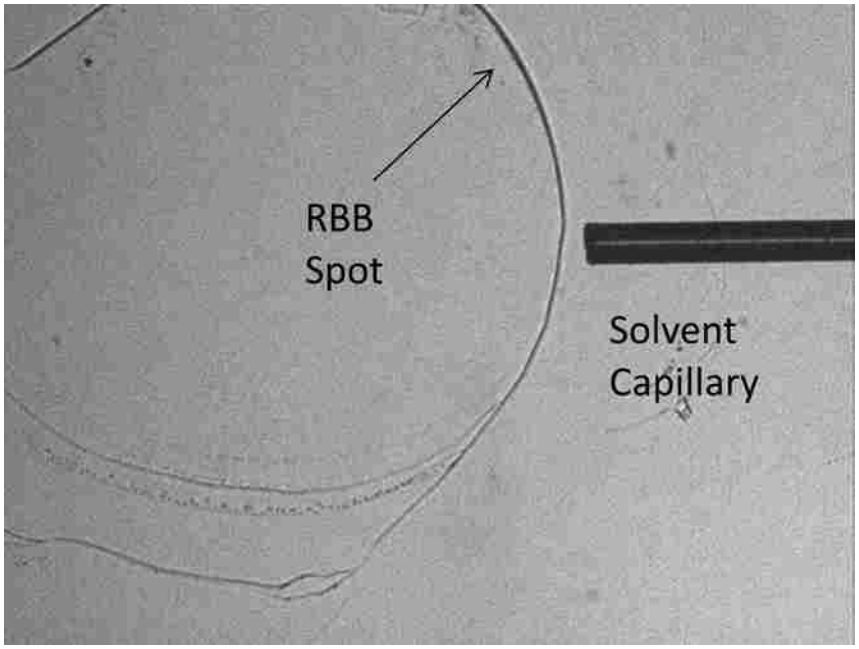

Figure 3-5 Image of surface spot used in dual capillary setup.

3.3 Results and Discussion

3.3.1 Review - Evidence of an Alternate Mechanism

Considering the amount of research that has been dedicated to the ESI mechanism, it is somewhat surprising that the research community has left the DESI mechanism largely untouched after the simulation papers by Cooks.[2-3] In our first paper on DESI, we proposed[5] the possibility of an alternate ionization mechanism, but the paper has largely been ignored. The results from the four experiments summarized below each provide evidence that the momentum transfer mechanism should be questioned as the dominant mechanism.

3.3.1.1 High Speed Shutter

The high speed shutter experiment (see Section 2.5.1) provided a detailed look at the nature of the spray as it made first contact with the surface. As we review this experiment, it is evident that there is a large number of spray droplets outside the central elliptical region. The central elliptical region has been identified as the region of most effective desorption, yet at very fast, short exposures to the spray, displacement of the dye from the central region on the surface has begun. The displacement of the dye, most of which has been pushed forward, indicates that if a thin film had begun to form on the surface, it would have had very little analyte in the most effective desorption region mere milliseconds after spraying had begun. Even with the formation of a thin film, droplet splashes in the most effective region of desorption would not contain much analyte. Traces of droplets can be seen in the fluorescence image of the 30 ms spray exposure.

The presence of these droplets without major disturbance in the middle indicates that the source of the droplets is the DESI emitter. These droplets could not have been produced by splashing from a thin film. While this does not rule out splashing from a thin film, it does provide an alternate explanation for droplet presence immediately outside the spray footprint.

3.3.1.2 High Speed Images

The high speed images taken with crystal violet show the pooling of solvent where the spray impinges on the surface. The solvent layer can be seen forming an elliptical region as the dye is pushed outward. This solvent pools as the dye is displaced in what appears to be a solvent film. Solvent rivulets break off the central elliptical film, carrying the dye from the center, displacing and depositing it downfield from the impact region. According to the momentum transfer

model, droplets produced from splashes in the thin film contain dissolved analyte. This process seems unlikely given that very little analyte is visible in the central region shortly after being exposed to the spray. Despite the lack of visible analyte in the thin film region, chemical imaging experiments have shown that this location produces the best results when sampled by DESI. When considering the results of the high speed experiment and the central elliptical region as the location in which the best results are obtained, it follows that although the analyte has been removed from the central region, it still is successfully sampled from a new location downstream. This is strong evidence for a non-momentum transfer mechanism.

3.3.1.3 Simultaneous Removal

The simultaneous imaging experiment was designed to examine a much thicker coating to see if the analyte behaved differently when it could not be removed as quickly. As expected, the MS signal from larger samples lasted far longer than the signal from a thin coating (data not shown). One would expect that the signal would drop off rapidly after the dye in the central elliptical region was completely removed. After a complete removal, it is evident that the MS signal is not generated from splashing from a thin film. The only interaction between the analyte and solvent that can occur is outside the central elliptical region (at the ends of the rivulets). These observations suggest that the ends of the rivulets themselves may be capable of generating some signal. It was observed that dye from outside the elliptical region moved towards the edges of the spray footprint. This migration is a possible explanation for the long signal duration; migrating dye can come in contact with rivulets and prolong solvent interaction with the analyte.

3.3.1.4 Barrier Experiment

The barrier experiment clearly demonstrates that rivulets alone are enough for analyte transport and ionization. While the barrier is not absolutely necessary, it eliminates the chance of stray droplets striking the analyte directly. When considering the rapid removal rates seen in the high speed imaging experiment and even the simultaneous imaging experiment, the Van Berkel scanning experiments indirectly demonstrate analyte ionization through the rivulets: scans with the sample approaching the spray profile downstream (approaching the rivulets) produce a small signal despite the fact that sample would likely be washed away before it ever reached the central elliptical region.[6]

3.3.2 Large Rivulets, DESI Parameters, and Spray Profile Behavior

Single large rivulets provide an interesting opportunity to test the effectiveness of splashless sampling. These rivulets are created by lowering the DESI source to the sampling surface. Source height above the surface is one of a few major parameters such as flow rate, angle, and potential that are optimized with each system. Because the effects of each of these parameters are dependent on each other, a discussion of their interdependence is necessary when discussing rivulet generation.

The common way to study the effects of these parameters is to track the effects that changes have on the resultant ion signal. Some of the results, however, cannot be easily explained and are not useful for predicting behavior on a surface. Again, the microscope plays a powerful role in identifying differences between these parameters as well as how they affect each other. While I have only experimented with one DESI source constructed in-house, I

suspect that a comparison of spray profiles should be considered when comparing DESI experiments between different DESI sources. It seems reasonable to believe that two different sources with different operating parameters would produce similar MS results if the spray profiles were comparable.

3.3.2.1 Terminology: Spray Profile and Spray Footprint

To properly discuss the nature of the DESI spray using images, it is necessary to distinguish the difference between the terms 'profile' and 'footprint.' The spray profile is the real time shape of the spray on the surface. The footprint is the time integrated area the solvent has covered. As an example, a single, large rivulet can move around sporadically on the surface. A short-exposure image of the rivulet will only show it in one location while the rivulet may have removed analyte such as a dye over a much larger area because its path varies with time. In many cases with DESI the two terms can be used interchangeably when the spray on the surface does not change, resulting in a footprint that is the same as the profile.

3.3.2.2 Relationship between Spray Profile and Experimental Parameters

Two of the parameters, solvent flow rate and DESI height are typically subject to a greater optimization range than the other parameters. When considering the variety of operating heights (0.4-10 mm) and solvent flow rates (0.5-30 μL/min for solvent), it is important to note that these conditions are often selected based on the dimensions of the inner and outer capillaries of the DESI source. An effective operating distance as small as 0.4 mm has been reported.[7] This height was chosen when attempting to increase the resolution by reducing the

size of the spray plume, and was accompanied by a reduction in flow rate to 1.5 µL/min from 5 µL/min.

One would guess that smaller capillaries limit the amount of solvent or gas that can be delivered. However, It has been reported that decreasing the solvent capillary diameter has no effect in reducing the size of the spray profile.[8] It is also important to note that the determining factor on nebulizing gas flow velocity is not the size of the outer capillary, but the difference in size between the two capillaries and the area of the resulting annulus.

In general, increasing the solvent flow rate increases the amount of solvent present on the surface. An increase in the nebulizing gas pressure does not have an easily distinguishable effect on the spray. The narrow gap between the capillaries can cause a choked flow, which prevents an increase in gas velocity at increasing pressure.[9] Even when overlooking a choked flow, increasing the velocity of the nebulizing gas creates two competing effects that influence the size of the spray profile. An increased gas velocity increases evaporation rates, but also increases the distance the solvent travels on a slide. Since these effects work against each other, the predominant effect is determined by DESI height from the surface and surface type.

This dependency on DESI source construction for selecting proper nebulizing gas and solvent flow rates has been given very little discussion. In almost all cases, the DESI source construction dimensions are listed as is in a publication's experimental section, and often only the easily controlled 'soft' variables (flow rates, potential, height, and angle) are tested and optimized based on a range around the detectable signal.[10] Even when pursuing improved resolution by optimizing the soft parameters, Kertesz and Van Berkel concluded their "Improved Imaging in DESI-MS" paper with the statement: "One can speculate that, *with this*

typical DESI-MS geometry, resolution might be improved somewhat further by reducing plume impact spot size (*e.g. by further optimization of the DESI sprayer*) and even better choices of analyte and surface" (emphasis added). One can speculate that this is left to the reader because of the difficulty in 'predicting' what changes to the 'hard' variables (source construction) will have on sampling. Unfortunately, optimization experiments are limited in helping us understand what physical change improves signal (or in this case resolution). Without a physical understanding, it is difficult to further optimize the DESI sprayer other than by iterative experimental trial and error.

Microscopic observation can clarify what is happening on the surface. Increasing or decreasing the height of the spray capillary outside the optimal range results in a loss of signal. Visually, this loss of signal is correlated to a decrease in the amount of analyte exposed to the solvent. The reduction in solvent at greater distances can be easily explained: increasing the DESI height results in increased evaporation of solvent as it travels to the surface. This supports the droplet pickup mechanism, but does not help in predicting a reduction in signal at closer distances. When viewed through a microscope, it can be seen that a reduction in height reduces the losses to evaporation but also reduces the area of the spray profile (ultimately creating rivulets) and the amount of analyte exposed to the solvent.

The physical behavior of spray angle can be explained in a similar fashion. A decrease in the spray angle between the source and the surface results in the formation of longer rivulets flowing toward the sampling capillary of the mass spectrometer. Increasing the spray angle produces a less elongated spray profile with more rivulets heading in all directions. A reduction in signal is the result of analyte being displaced in all directions.

3.3.2.3 Differences in Solvent Composition

Solvent composition plays an important role in DESI and is selected to produce the maximum mass spectrometric signal. As noted in the previous section, the solvent composition complicates comparison of the other soft variables (especially source height) due to different evaporation rates. Variations in the spray footprint would be expected with different solvents as well. The most commonly used solvents for DESI have been water and methanol. After the technique was introduced, most publications used 50:50 mixtures of water/methanol, some of which contained small amounts of acid to help with ionization. A more recent study[11] has concluded that the ideal solvent composition is 80:20 methanol/water due because the mixture produces the highest MS signal.

Figure 3-6 shows the effects on the spray profile of increasing the amount of methanol in the solvent. The organic/water percentages are listed in the bottom corner of each frame as methanol/water. The height above the surface is 1.5 mm, angle is 55°, flow rate is 3 µL/min, and pressure is 150 psi. Each image was part of a video, and individual frames were taken after at least 1 min exposure to the spray. Blue ellipses have been added to mark the spray profile when it differs from the spray footprint. The long individual rivulets on the edges of frames C and D are not standard rivulets but traces of a more viscous organic non-volatile liquid in the methanol. In the videos of solutions with concentrations greater than the 50:50 mix, these viscous streams grow very slowly and never evaporate, even days after spraying. The methanol used in these experiments is Omni-solv spectrometric grade methanol. The listed concentration of non-volatile organics in the methanol was less than 1 ppm. This contamination does not seem to interfere with the desorption/ionization process and was not seen in the pure water

sample. Non-volatile rivulets did not form in the 50:50 solution, but residual deposits from evaporating rivulets are left behind on the edges of the spray profile. The presence of this non-volatile liquid is unlikely to have an effect on the DESI mechanism, but it visually complicates images of the spray footprint.

Increasing the molar ratio of the methanol produces a drastic change in the spray profile at each step. The most considerable change is the reduction in the length of the rivulets due to increased evaporation rates. The 50:50 mixture appears to produce far more droplets than the other patterns (most of the dark spots in frames C and D are the tips of the slow moving non-volatile rivulets). The higher methanol concentrations exhibit droplets, but they are far smaller and due to lower surface tension, causing them to spread across the slide. This spreading likely forms a thin film as described by the momentum transfer mechanism.

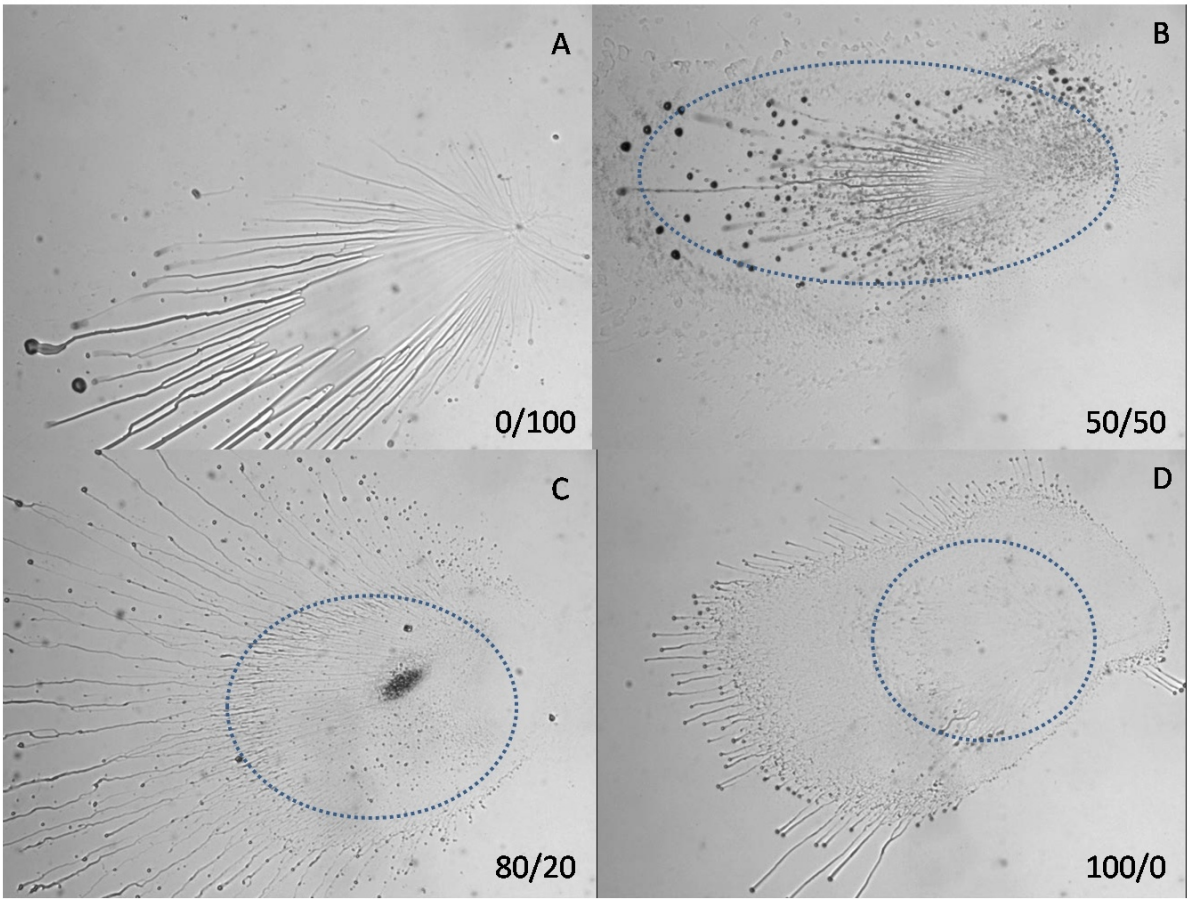

Figure 3-6 DESI spray profile with increasing methanol percentages (methanol/water). Each frame is 3.29 mm x 2.48 mm

3.3.2.4 Working with Large Rivulets

Single large rivulets provide an interesting opportunity to test the effectiveness of splashless sampling. The most basic method for generating large rivulets is to lower the DESI source to the working surface, creating a direct path for the solvent to flow. For simplicity, I refer to all forms of solvent exiting the capillary as a spray, regardless of the behavior of the solvent as seen on the surface.

Figure 3-7 shows various images of the spray profile on glass as the DESI source is lowered toward the surface of a glass slide. The image was taken using 80:20 methanol/water

flowing at 3.0 µL/min with CCD image exposure times of 1 ms taken at 4 Hz. The first image shows the spray profile at a height close to 1.5 mm from the surface with subsequent frames chosen to highlight the change in the spray profile and the onset of large rivulet formation.

While it is not technically accurate to claim that the capillary tip can be lowered below contact with the surface, lowering the DESI source causes the capillary to move forward as it bends. In Figure 3-7, the rivulet grows from the spray footprint and then begins to shrink, vanishing in frame F completely. Continued lowering of the system shows the reappearance of rivulets. The stark transformation in the behavior of the solvent on the surface at different heights can be explained by examining the construction of the DESI source.

In almost all cases, a slight offset of the inner capillary with respect to center is present and distorts the annular region between the two capillaries, allowing more nebulizing gas to exit from one side than the other. This effect contributes to the non-uniformity of a standard DESI footprint region and, in rivulet DESI, causes a single rivulet to bend to one side as it leaves the capillary. Because the inner solvent capillary protrudes from the outer capillary, initial contact with the slide shifts the orientation further. Lowering the emitter further causes the inner capillary to bend toward the mass spectrometer inlet (left in the images) and the outer capillary comes in contact with the slide surface.

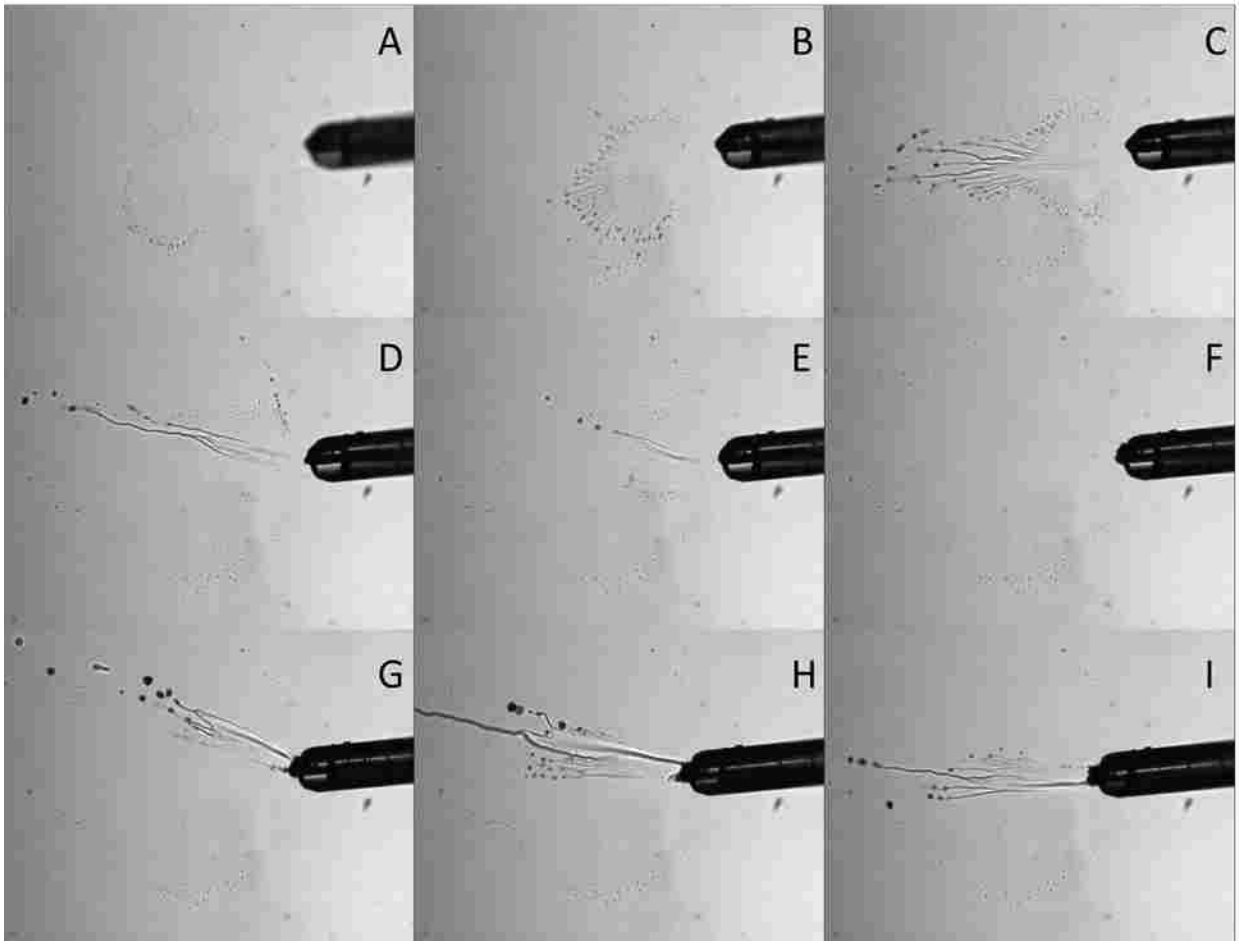

Figure 3-7 Progressive images taken from a video showing the effects of lowering the DESI needle to the surface of a glass slide.

The progressive disappearance of solvent in frames D-F is more likely due to evaporation caused by the nebulizing gas than from any blockage of solvent due to contact with the surface. With the inner capillary pushed to the 'top' of the outer capillary, the nebulizing gas exits most rapidly directly underneath the solvent, causing the majority of the solvent to evaporate. Lowering the DESI source further causes additional bending of the outer capillary as it presses against the surface and causes the solvent to begin to appear on the surface as seen in frames G-I. The bending in the capillaries reduces the effective angle to less than 55°. As seen in frame H, the rivulet extends beyond the edge of the image. As the spray angle decreased, the

rivulets traveled farther in the X direction. Rivulets generated in this state (frames G-I) usually travel farther than those generated before contact with the surface (frames D and E).

The solvents in frames D and I behave differently from each other. The solvent in frame D tends to converge onto itself so that the outer flow lines join up with the major rivulet that is produced. In frame I the solvent exits the capillary as a thin stream the same width as the inner capillary with far less convergence. The convergence toward the major flow direction was first noted by Volný et al. and was found to be caused by hydrodynamic effects.[12] Contact with the surface disrupts the nebulizing gas flow patterns, and results in additional rivulets breaking from the stream. Lowering the DESI source further has very little impact on the profile. The changes in the spray profile when lowering the DESI source can be characterized in four steps:

1. Elongation of the rivulets downstream.
2. Conversion of the longer spray profile into a single rivulet with secondary spray outside the rivulet.
3. Complete or nearly complete disappearance of solvent from the surface.
4. Reappearance of the solvent on the surface making a thin sheet about as wide as the needle that breaks into one or more rivulets.

These changes in spray profile consistently occur despite unavoidable variability in the positioning of the solvent capillary within the nebulizing capillary. Changes in positioning of the inner capillary can result in variation in direction taken by the initial single rivulet (seen in frames D and E). This variation has no notable effect on signal unless the rivulet extends beyond the front of the transfer line, evaporating to its side. Variations in solvent and gas flow rates

typically do not have an effect on the steps listed above, changing only the amount of solvent present on the surface.

When working with the barrier, I noted that the two sets of spray types (steps 2 and 4 above) that produced rivulets behaved differently. The rivulets produced in step 2 did not produce droplets at the barrier even when the emitter was very close to the barrier. In contrast, the rivulets produced in step 4 did produce droplets at the base of the barrier when the spray source was close to the barrier. In the latter case, droplets on the barrier coalesced, blocking the light from the incandescent lamp and interfering with the imaging. The droplets were most likely produced as they exited the solvent capillary and came in contact with the nebulizing gas. Due to the differences in behavior between the rivulets described in steps two and four, I characterized them as different rivulet spray types. Both spray types were used for experiments. The first type (step 2) was used in the barrier experiment because it was more likely to produce a single rivulet. The second type (step 4) was used for the rivulet ESSI experiments because the spray profile was less subject to minor differences in height when working with slides.

With these considerations, no single ideal height was chosen when setting up a rivulet stream from the DESI source. For imaging experiments, the source was lowered and solvent flow rate was chosen to produce a rivulet that evaporated within the viewable area of the microscope. Conditions varied from experiment to experiment due to variations in source construction and in the volatility of different solvents used in the experiments.

3.3.3 Three Dye Barrier Experiment

The original barrier experiment demonstrated that a sample could be analyzed without coming in contact with the 'most efficient desorption region' of the spray. We felt that we could improve upon the experiment by simplifying the process and by making it easier to see in recorded images. Lowering the DESI tip to the surface also had the added benefit of removing the possibility of splashing despite the presence of the barrier. The three dye experiment proved definitively that rivulets can generate gas phase ions from a deposited sample.

Figure 3-8 shows resulting mass spectra displayed as an ion map of the three dye barrier experiment using 80:20 methanol/water. Each of the 3 major peaks represents the mass peaks of the red, blue, and purple Sharpie markings (443, 478, and 457 m/z, respectively). The plot also shows that traces of both red and blue dye are present in the purple Sharpie, although the predominant (or most sensitive) component in the dye is a single purple compound. As would be expected, there was very little signal as the sample was being moved and the rivulet was not in contact with any Sharpie markings.

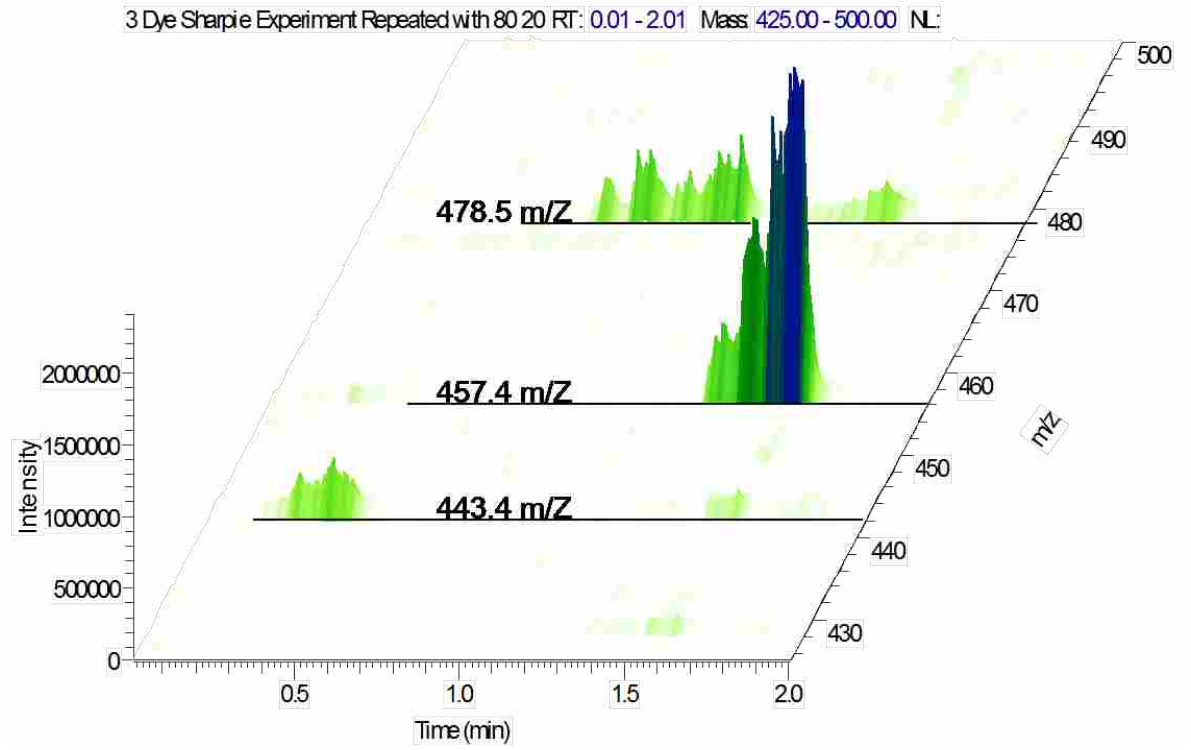

Figure 3-8 Ion map of the 3 dye sharpie experiment using 80:20 methanol water. Dye colors by m/Z: red- 443; 457-purple; 478-blue.

Figure 3-9 shows multiple images of a video taken of a DESI rivulet that was produced when the needle tip was lowered to the surface of the slide. Each frame in the figure is 3.29 mm wide. The elongated dark spot to the left of each image is the line drawn with a Sharpie pen, the vertical 'bar' to the right of each image is the underside of the glass cover slip. The DESI source was positioned to the right of the image, producing the rivulet that is seen passing underneath the cover slip. The large rivulet itself split upstream (out of frame), producing a second, smaller rivulet visible in each frame directly below the main rivulet. Figure 3-9A shows the nature of the rivulet with no potential applied to the DESI emitter. Images B, C, and D are individual frames from the video showing the behavior of the rivulet under an applied potential of 4900 V.

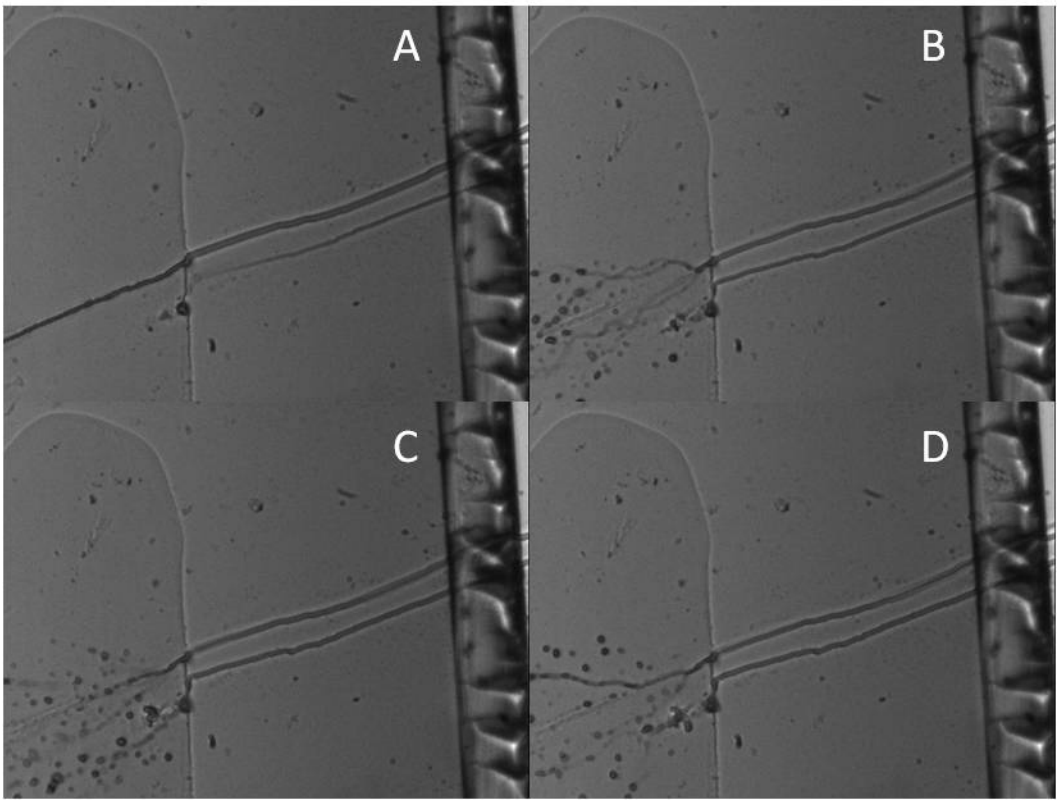

Figure 3-9 Images taken from the rivulet barrier experiment. A is taken without an applied voltage to the DESI solvent. B, C, and D were taken with an applied voltage.

The shape and length of the rivulet varied based on solvent composition as well as the nature of the surface. The length of the rivulet was much larger than the length of a conventional DESI spray profile and required that the DESI needle be moved further from the sampling location to image the interaction of the rivulet with the dye using the microscope. This additional distance from the sampling location may have had an effect on the sampling efficiency, but the tradeoff was necessary for imaging, and in some cases to prevent the rivulet from coming into contact with the transfer line to the mass spectrometer. As would be expected, more volatile solvents produced shorter rivulets and polar solvents traveled faster on hydrophobic surfaces. With the power off the solvent maintained a fairly consistent path along the slide throughout the experiment. When the voltage was activated, the terminating end of the rivulet underwent a

dramatic change in behavior: the number of forks and changes in direction increased dramatically. In addition, the ends of the rivulet fragmented into secondary droplets far more often than when there was no voltage applied.

This fragmentation is interesting because it could be a potential source of ions generated from the spray. An applied potential may cause internal repulsion and fracturing of the solvent stream similar to the reported droplet fission in ESI. In Figure 3-9, the fragmentation occurs when the charged solvent stream makes contact with the Sharpie marking on the slide. The presence of the marking on the slide is not required for the fragmentation of the rivulet, but greatly increases the chance that the solvent stream will fragment. On a clean glass surface, rivulet fragmentation still occurs. This fragmentation is different than that shown in Figure 3-9 because it occurs farther downstream from the DESI needle and produces far fewer fragments and droplets.

It is interesting to note we found no evidence prior to this experiment of a change to the rivulets induced by the application of voltage to the DESI emitter. This is remarkable because we had previously made several attempts to look for such a change. The fracturing and increased droplet production may provide some clues to the actual mechanism responsible for ionization within the rivulets in standard DESI. Whether such a behavior continues at a much smaller scale is difficult to examine using our current instruments. At higher magnification levels, it becomes increasingly difficult to image the rivulets and droplets. An increased magnification results in smaller depths of field. At the 20x magnification, there is no discernible difference between rivulets with and without an applied voltage. At 40x magnification, the shallow depth of field prevents imaging of the droplets at the end of rivulets. It is entirely

plausible that similar fracturing occurs with the smaller rivulets seen in standard DESI operation and that we are incapable of imaging the smaller structures.

Another interesting question that arises is 'why does the Sharpie marking cause rivulet fracturing?' Rivulet fragmentation on clean glass is likely caused by an increase in charge density with decreasing rivulet size due to evaporation. Increasing charge density would cause the rivulet to undergo fission, similar to what is thought to occur in ESI droplets that undergo evaporation. If charge repulsion is the cause, a disruption in the flow would create turbulence for rivulet fission to begin. By prematurely splitting the flowing solvent, new droplets and rivulets would rapidly separate from each other due to coulombic repulsion.

A coulombic repulsion-induced separation due to turbulence would have an interesting implication for rough surfaces. If increased turbulence due to obstructions that prevent laminar flow induces fragmentation, then surfaces that are rough would be expected to increase the amount of fragmentation that would occur. If the droplet generation from rivulet fragmentation plays a significant role in the mechanism, then a rough surface would promote ionization over a smooth surface like glass.

3.3.4 Rivulet ESSI

Rivulet ESSI is another way to investigate possible mechanisms that do not rely on droplet splashing for analyte transport to the mass spectrometer. If a single rivulet can be used to detect analyte on a surface, then it should also be possible to detect an analyte dissolved in a rivulet. Rivulet ESSI has a couple of advantages over rivulet DESI. First, having the analyte entrained in the solvent, there should be little change in signal over time that is inherent in DESI

due to removal of deposited analyte. Second, surface contributions can be investigated without the difficulties presented by variations in coating.

The major disadvantage of Rivulet ESSI is the added dependence on capillary positioning on the surface. Very minor differences in surface height can greatly change the spray profile. Small changes in height can cause the signal to vary by as much as a factor of three. Irregularities in the spray profile can be identified using the microscope when operating on glass, but cannot be seen on opaque materials.

Rivulet ESSI produced a strong signal with a 100 nM RBB solution on glass. Because the second rivulet spray type (see Section 3.3.2.4) was chosen to reduce the amount of variation in the spray profile, alignment was first performed on a glass slide with shims and adjusted to reduce the number of droplets generated from the capillary tip by the nebulizing gas. It was not possible to distinguish between ions that are generated directly from the source and ions that were generated after being transferred from solvent on the surface. This problem did not prevent us from drawing some conclusions about ionization from rivulets. Any undesired signal that was generated from the source would have been consistent with any surface, meaning any variations in signal arose from differences in the surface.

Figure 3-10 shows the difference between signal intensity of RBB on glass with and without an applied potential. Each run was taken using a 50 ms injection time and 3 microscans. The variations in signal at these settings without averaging were similar to signal in DESI. An increase in signal was always observed with an applied voltage. The running average signal did not change significantly during the experiment, suggesting that the buildup of dye on the surface had little contribution to the resulting ion signal.

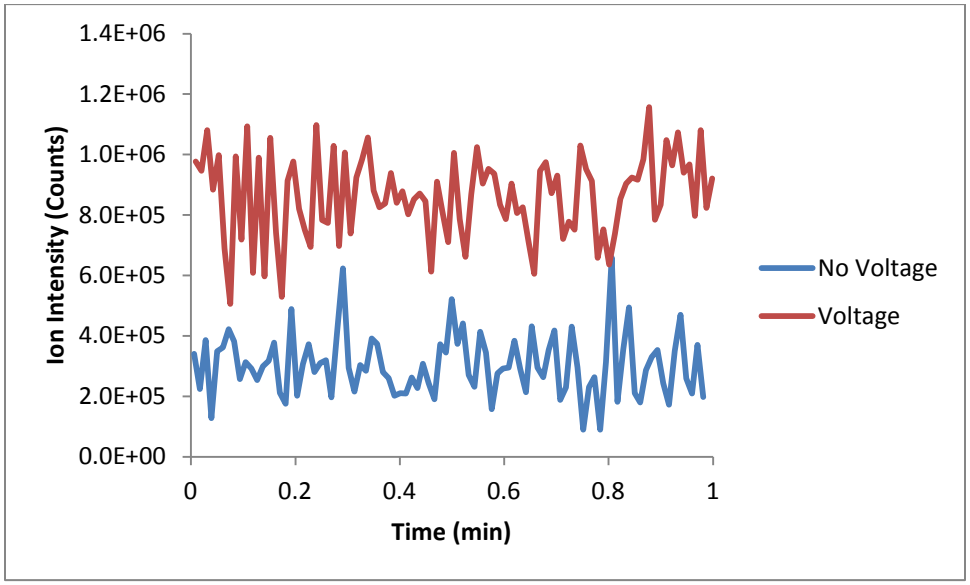

Figure 3-10 Ion signal from rivulet ESSI on glass using 100 nM RBB in 80:20 methanol/water solution with and without an applied voltage over the course of 1 min.

The experiment was repeated on slides made of Teflon, Delrin, and copper. Like glass, the other materials produced a signal without an applied voltage. Delrin and Teflon signals were comparable to that of glass, but the ion intensity from copper was lower than that of the other three, both with an applied potential and without. With an applied potential, the copper slide produced a smaller gain in RBB intensity than the corresponding non-conductive materials. The poor performance of conductive surfaces has been documented with traditional DESI.[10] It was later shown that non-conductive surfaces underwent a capacitive charge build up under the effects of DESI and that metal surfaces quickly dissipated charge.[13] If the surface was also grounded, the charge dissipation was nearly instantaneous. The authors noted that signal from grounded surfaces was not completely eliminated. They proposed that the neutralized solvent clusters from the grounded surface fused with charged droplets from the DESI source.[10]

I performed a similar grounding experiment to test whether a grounded surface would change the effectiveness of the rivulet ESSI on copper. A grounding line was attached to the edge of a copper slide while sampling with rivulet ESSI. This was done twice, once with a potential and once without. Figure 3-11 shows the results of applying a ground at 20 s into each run and removing the ground after 40 s.

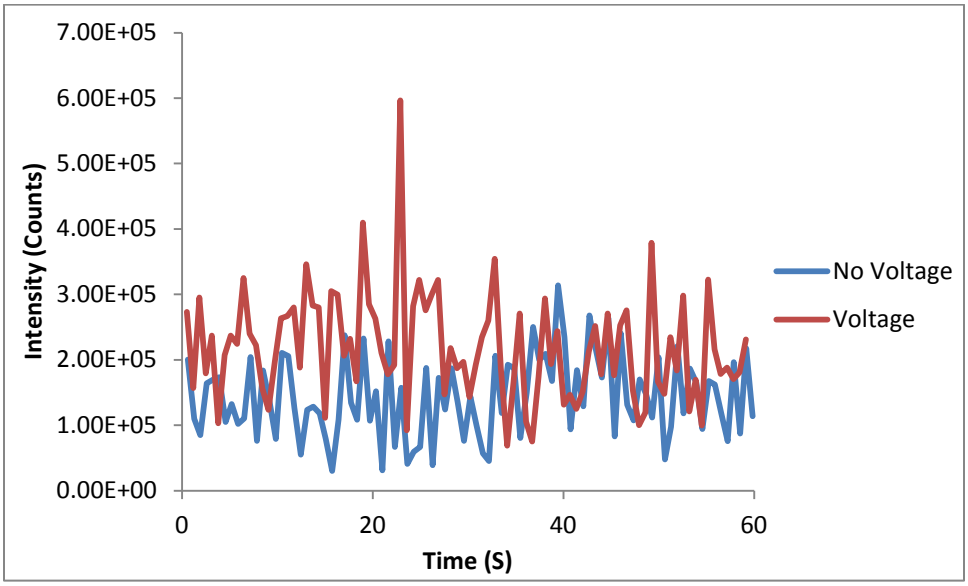

Figure 3-11 Rivulet ESSI ion signal of RBB on a copper surface that is grounded from 20-40 s.

The grounding of the copper slide caused no change in RBB signal. The lack of distinguishable difference suggests that charge build up when no ground is applied is negligible. Rivulet ESSI shows similar behavior to standard DESI in this regard. No difference in signal can be seen even when the copper slide is allowed to 'float' freely for the first and last 20 s of the experiment. The charge that would build up on a copper slide is evenly distributed on the copper slide. Sample detection on conductive metals such as palladium foil and gold film have been reported.[13] The current between a DESI source and the surface is very small, leaving the amount of charge transferred compared to the bulk of the slide relatively small. Thus,

grounding the copper slide has no effect because the thicker copper slide is already effectively acting as a ground.

The variability in signal with the non-conducting slides and the lack of an effect on the copper slide could be interpreted as surface independent ionization created directly from the ion source. While it is impossible to quantify how much analyte is transferred from the source itself and not from rivulet desorption, the poor performance of the copper surface indicates that a majority of the signal is coming from the surface and not from droplets generated by the rivulet ESSI source

The rivulet ESSI experiment provides additional evidence that a charged solvent on a surface can generate ions that are transported from the surface. When a conductive surface is used, the solvent loses its charge and is ineffective at creating ions; this behavior is exactly the same as in traditional DESI. Insulating surfaces keep the charge localized in the solvent, which increases in charge density as it evaporates, resulting in fragmentation due to charge repulsion. Conductive surfaces prevent charge build up by neutralizing the potential in the DESI solvent.

3.3.5 Dual Capillary DESI

Making DESI measurements with the solvent capillary in contact with the surface eliminates secondary droplets formed from thin film momentum transfer as possible ion sources.
The dc-DESI setup was designed to isolate the rivulets as a source of ionization by removing the spray itself and any of the droplets generated from the nebulizing gas flowing concentrically with the solvent. Instead of operating on the surface, as in rivulet ESSI and rivulet DESI, the dual

capillary setup preserves the orientation of the DESI nebulizing gas and employs a second solvent capillary for solvent delivery.

Proper alignment was required to generate signal from the dual capillary setup. If the nebulizing gas was not properly aligned with the solvent as it issued from the solvent capillary, there was no solvent dispersion and the analyte was not detected. Slight variations in alignment caused the solvent capillary to rapidly vibrate, creating a high pitched sound. This vibration did not inhibit the spread of the solvent on the surface, and still resulted in the generation of ions from the analyte, but was undesirable because it did not definitively show that the spray creation on the surface was generated without splashing.

When the analyte was contained within the solvent, a very strong signal from the RBB was seen from the mass spectrometer. This experiment was similar to rivulet ESSI done earlier, but removed the possibility of ion generation from droplets generated from the source tip. The only possible source for the ions was the sprayed analyte on the surface. It was suggested in the droplet generation modeling paper by the Cooks group that surface ionization is an unlikely candidate for ionization. Our findings indicate that surface desorption and ionization independent of splashing must be considered.

When the analyte is sampled from the surface by dual capillary DESI, proper positioning of the capillary with respect to the sample becomes an issue. Not only is capillary vibration still an issue, but analyte removal requires constant repositioning of the analyte slide. Despite these difficulties, it is readily apparent that a surface analyte can be sampled by dc-DESI. Desorption of the analyte from the surface is the ultimate indication that a sample can be dissolved, desorbed, and transported from the surface by the solvent moving across the surface. Such

evidence must be considered when modeling the mechanism for DESI. Figure 3-12 shows the ion signal intensity of a RBB spot using dc-DESI.

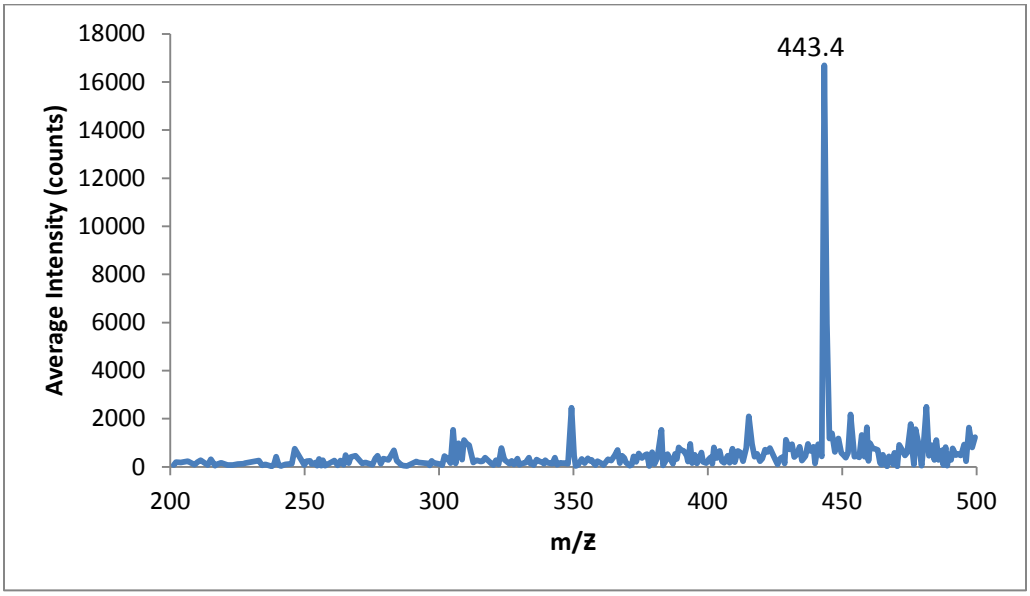

Figure 3-12 Average ion signal over 2 min when sampling a spot of RBB using dc-DESI.

Taken over 2 min and fairly weak compared to traditional DESI, Figure 3-12 clearly shows the presence of RBB through dc-DESI. The reason for the lower average signal is due to the sporadic nature of the sampling over time with relatively large peaks erratically appearing during sampling. Figure 3-13 shows the ion signal of RBB during dc-DESI.

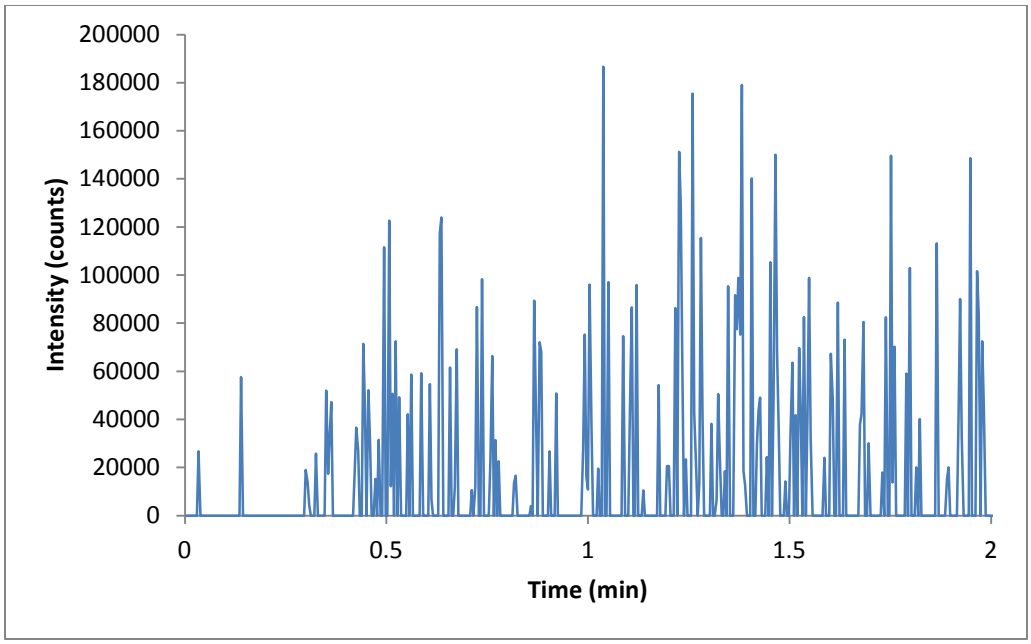

Figure 3-13 Ion signal of RBB during a 2 min run using dc-DESI. The sporadic signal contributes to the lower average signal, but individual peaks have magnitudes closer to DESI

When the slide attached to the solvent capillary was moved, the alignment below the nebulizing capillary was broken. In standard DESI, the microscope stage can be moved to prolong signal collection and compensate for analyte removal. To prolong sample time with dc-DESI, it was necessary to move the sample slide independently from the solvent capillary slide so that the position of the solvent capillary remained unchanged. This resulted in many sharp jumps in the ion current (including dead times) as the slide was repositioned during the analysis. Some of the individual peaks in Figure 3-13 approach 2.0 x 10^5 counts, which is comparable to traditional DESI. The footprint of dc-DESI appears similar to that of traditional DESI, varying only slightly by an elongation along the spray axis with longer rivulets, similar to the change caused by a reduction in spray angle. With dc-DESI, the solvent is exposed to a nebulizing gas from above, causing it to spread, dissolving the analyte as it runs along the slide. Figure 3-14 shows the displacement of RBB on the surface of a glass slide during a run.

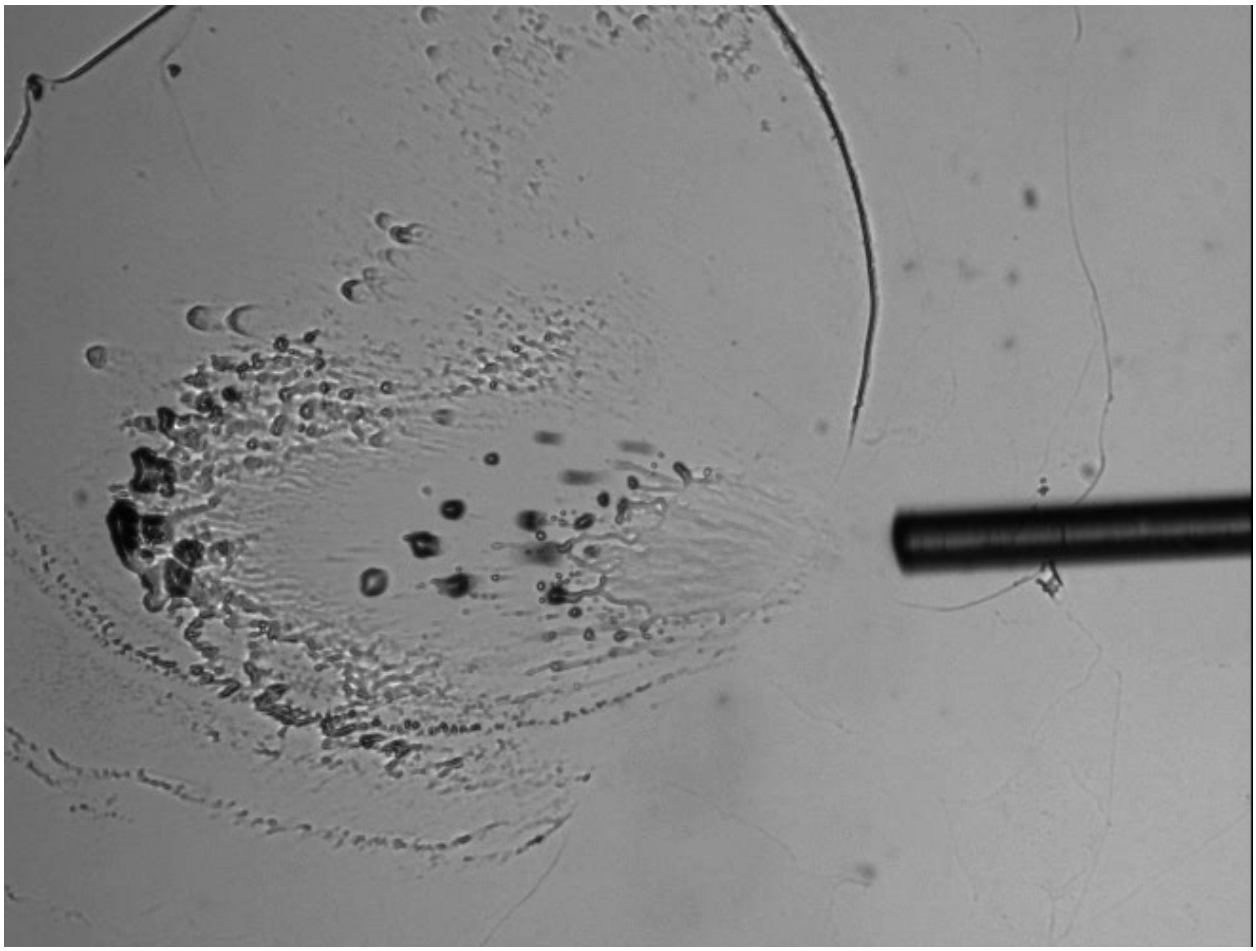

Figure 3-14 Image of dc-DESI on a 'coffee spot' of RBB. 2x magnification, 80:20 methanol/ water.

3.3.6 An Alternate Mechanism – The Rivulet Dissociation Mechanism

The results from the surface work on DESI using the inverted microscope provide additional insight into analyte transport and ionization from a surface with DESI. The three experiments demonstrated that desorption and ionization can occur through rivulets without secondary droplet formation. The thin film droplet splashing model cannot explain the results of the experiments summarized in this chapter and in Chapter 2. I propose a second mechanism for DESI called the rivulet dissociation model.

Rivulet Dissociation Mechanism

The rivulet dissociation mechanism takes into account the observations seen in the experiments presented in Chapter 2 as well as those presented in this chapter. Solvent leaves the capillary at high speed and comes in contact with the surface. Soluble, non-covalently bound molecules are dissolved in the solvent as it passes over the sample. Rapid evaporation causes the solvent to break into rivulets as it travels across the surface. The high speed nebulizing gas accelerates evaporation, causing the rivulets to shrink quickly. The reduction in surface area causes a charge build up and repulsion resulting in rivulet fracture and droplet formation. Droplets then undergo ESI like ionization to produce ions that are detected by the mass spectrometer with much of the analyte depositing back on the surface.

The rivulet dissociation mechanism is comparable to the ESI ionization model. Despite the ESI mechanism not being fully understood, parallels in transport and ionization can be drawn. The major difference between the two is the presence of the surface. When operating on a non-conductive surface, rivulets in DESI and suspended droplets in ESI are electrically isolated from each other, preventing neutralization of the charge. Thus, the surface effectively acts in the same role as the open air does in separating droplets and creating an environment where charge density increases with evaporation to the point of droplet or rivulet breakdown.

Despite the surface of DESI and the gas phase in ESI acting in comparable manner, the surface adds additional factors that must be accounted for. Charge distribution occurs across the surface of the solvent. Unlike droplets in ESI which travel unimpeded, imperfections on a surface can disturb the standard evaporation and fission process causing ‘premature’ fracturing. This can be seen in Figure 3-9 the rivulet breaks apart as it passes over the sample,

breaking into far more droplets than an unimpeded rivulet. Charged liquids carry the charge evenly distributed on the surface. Under the rivulet dissociation mechanism, surfaces which promote dissolution of analyte and disrupt rivulet flow, such as Teflon, should produce better results. The increase in rivulet breakdown due to surface interference is strong evidence for the droplet dissociation mechanism.

Analyte detection without an applied voltage is also consistent with the rivulet dissociation mechanism as well. The high velocity nebulizing gas causes the solvent to rapidly evaporate. At high enough concentrations, the rivulet stream disintegrates leaving the majority of the analyte deposited on the surface with some of it leaving the surface as fine droplets. The rapid evaporation and break down of an individual rivulet is enough to act as nebulizer, creating solvated ion clusters. These clusters would then produce some ions through the same mechanism involved in sonic spray ionization.

3.4 Conclusions

The Cooks group proposed the momentum transfer mechanism as the primary DESI mechanism for desorption electrospray ionization. In the Cooks' model, high velocity charged droplets generated by the DESI source collide with a thin solvent film containing a dissolved analyte and create secondary droplets. Cooks' group proposes that analyte ionization occurs within these secondary droplets by the same mechanism that creates ions in ESI.

Our experiments indicate that analyte desorption is unlikely to occur under many circumstances. Using an inverted microscope, we have shown that little analyte remains in the thin film for momentum transfer to be a significant factor for desorption. We have shown with our barrier experiments that secondary droplets are not necessary for analyte detection. These

experiments were crucial for our hypothesis that rivulets were involved in transport and ionization of the analyte on a surface.

Our rivulet experiments were designed to eliminate droplet splashing as a possible route for desorption to occur when operating with DESI. Despite operating under conditions where secondary droplets could not be produced, we were still able to detect our samples using rivulets. I propose the rivulet dissociation mechanism based on these findings.

3.5 References

1. Nemes, P.; Marginean, I.; Vertes, A., Spraying Mode Effect on Droplet Formation and Ion Chemistry in Electrosprays. *Analytical Chemistry* **2007,** *79* (8), 3105-3116.
2. Costa, A. B.; Cooks, R. G., Simulation Of Atmospheric Transport and Droplet-Thin Film Collisions in Desorption Electrospray Ionization. *Chemical Communications* **2007**, 3915-3917.
3. Costa, A. B.; Graham Cooks, R., Simulated Slashes: Elucidating the Mechanism of Desorption Electrospray Ionization Mass Spectrometry. *Chemical Physics Letters* **2008,** *464* (1-3), 1-8.
4. Takats, Z.; Wiseman, J. M.; Gologan, B.; Cooks, R. G., Electrosonic Spray Ionization. A Gentle Technique for Generating Folded Proteins and Protein Complexes in the Gas Phase and for Studying Ion Molecule Reactions at Atmospheric Pressure. *Analytical Chemistry* **2004,** *76* (14), 4050-4058.
5. Wood, M. C.; Busby, D. K.; Farnsworth, P. B., Microscopic Imaging of Glass Surfaces under the Effects of Desorption Electrospray Ionization. *Analytical Chemistry* **2009,** *81* (15), 6407-6415.
6. Pasilis, S. P.; Kertesz, V.; Van Berkel, G. J., Surface Scanning Analysis of Planar Arrays of Analytes with Desorption Electrospray Ionization-Mass Spectrometry. *Analytical Chemistry* **2007,** *79* (15), 5956-5962.
7. Kertesz, V.; Van Berkel, G. J., Improved imaging resolution in desorption electrospray ionization mass spectrometry. *Rapid Communications in Mass Spectrometry* **2008,** *22* (17), 2639-2644.
8. Ifa, D. R.; Wiseman, J. M.; Song, Q.; Cooks, R. G., Development of Capabilities for Imaging Mass Spectrometry Under Ambient Conditions with Desorption Electrospray Ionization (DESI). *International Journal of Mass Spectrometry* **2007,** *259* (1-3), 8-15.
9. Green, D. W.; Perry, R. H., Perry's Chemical Engineers' Handbook (8th Edition). McGraw-Hill Professional Publishing: Blacklick, OH, USA, 2007.
10. Takáts, Z.; Wiseman, J. M.; Cooks, R. G., Ambient Mass Spectrometry using Desorption Electrospray Ionization (DESI): Instrumentation, Mechanisms and Applications in Forensics, Chemistry, and Biology. *Journal of Mass Spectrometry* **2005,** *40* (10), 1261-1275.

11. Green, F. M.; Salter, T. L.; Gilmore, I. S.; Stokes, P.; O'Connor, G., The Effect of Electrospray Solvent Composition on Desorption Electrospray Ionisation (DESI) Efficiency and Spatial Resolution. *Analyst* **2010,** *135* (4), 731-737.
12. Kaftan, F.; Kofroňová, O.; Benada, O.; Lemr, K.; Havlíček, V.; Cvačka, J.; Volný, M., Scanning Electron Microscopic Imaging of Surface Effects in Desorption and Nano-desorption Electrospray Ionization. *Journal of Mass Spectrometry* **2011,** *46* (3), 256-261.
13. Volný, M.; Venter, A.; Smith, S. A.; Pazzi, M.; Cooks, R. G., Surface Effects and Electrochemical Cell Capacitance in Desorption Electrospray Ionization. *Analyst* **2008,** *133*, 525-531.

4 Future Work and Conclusions

We have created a powerful combination by coupling the DESI source and mass spectrometer with an inverted microscope. This combination has been the only published approach to real time imaging of the DESI spray on a surface. DESI experiments with a microscope are limited to transparent surfaces, but despite this limitation there are still many useful experiments that need to be done.

Despite what has been done by our research group and others, there is a continuing need to better understand the DESI source. Herein I describe potential experiments that include the characterization of the source through additional imaging experiments. These experiments require this combination of the DESI source with an inverted microscope. In addition to source characterization, I suggest experiments that focus on the surface, namely, modified DESI surfaces and chemical imaging efficiency studies.

4.1 Source Comparison

4.1.1 Introduction

As noted in Chapter 3, the sizes of the capillaries used in DESI source construction have varied among different research groups. This variation has led to expected differences in 'optimal settings' used in experiments by these groups. To simplify the discussion, I will group the controllable parameters into two separate groups. Any parameters that can be adjusted without rebuilding the source are soft variables. Parameters that cannot be adjusted without a reconstruction, such as changing the inner and outer capillary dimensions, are 'hard' variables.

Understandably, the soft variables have been researched far more extensively than the hard variables, due to the ease with which they can be adjusted. However, it is difficult to compare the results of optimizing the soft variables without considering the differences the hard variables introduce into the overall setup. The importance of the hard variables was recognized early on, and a paper[1] by the Van Berkel group included a discussion of size of the annulus between the capillaries. Some research of the hard variables' influence on the soft variables and their combined effects on the spray has been published. The Cooks group studied the differences in spot size using solvent capillaries with 1, 10, 25, and 50 μm inner diameters:[2] the larger the inner capillary, the larger the spot size. These findings were, however, later clarified[3] when it was discovered that resolution in imaging was not affected by the diameter of the solvent capillary alone and was attributed to a much more complex interaction that also included the size of the nebulizing capillary.

The need to clarify the original study of the relation of spot size to capillary diameter highlights the difficulty in comparing the DESI source construction parameters. Even when an experiment is carefully designed to control a single parameter in the source construction, it is tedious to perform densitometry experiments[2] or resolution testing[3] to determine its effect. Here again the microscope can play an important role in characterizing the differences in the spray among sources constructed with different sizes of capillary.

Table 4-1 lists the capillary dimensions used in research papers by various groups and some of the corresponding soft variables that were chosen with those dimensions.

Research Group	Inner Capillary ID (μm)	Inner Capillary OD (μm)	Outer Capillary ID (μm)	Tip Height mm	Flow Rate μL/min	Angle Degrees	Nebulizing Gas (varies)
Cooks[4]	100	150	250	1	3	35	350 m/s
Farnsworth[5]	75	150	250	1.5	2-3	55	150 psi
Fernandez[6]	50	147	250	1.0-2.0	5	55	365 mL/m
Green[7]	50	320	*	1.5-2.0	1	60	6 L/m
Hopfgartner[8]	305	470	600	0.5-1.0	5-10	60	0.5 L/s or 20 b
Muddiman[9]	50	150	250	2	2	45	120 psi
Van Berkel[1]	100	360	500	0.5-1.0	5	50	2.4 L/sec or 275 m/s
Zhang[10]	100	150	250	2	5	60	1 atm

Table 4-1 List of DESI source variables involved with construction and operation of the DESI source from various research groups. *Not provided.

Table 4-1 is useful because it provides the basis for an initial comparison of soft parameters used for optimal performance at a given set of capillary sizes. The table itself does not contain a complete list of parameters and is not intended to be comprehensive. The variation in reporting conditions used with the nebulizing gas highlights the complexity of the task as some are reported as velocity, flow rate, or back pressure. While the linear velocity is the most useful for comparison of sources, it is also the most difficult to determine as it must be measured with a complex apparatus.

Additionally, the distance the inner capillary extends beyond the outer capillary is not always reported, but often ranges between 0.1-1.0 mm. Further complicating the comparison of source construction and geometries is the fact that the soft variables chosen for optimal signal are influenced by solvent composition. As discussed in Section 3.3.2.3 the volatility of the

solvent makes it difficult to separate the contributions of capillary height and nebulizing gas pressure to the spray profile. Because individual settings are interdependent, the single parameter optimizations done in the past (which did not take into account source construction) were overly simplistic and should be considered to be source specific.

Thus far, signal optimization has been the method used to compare DESI settings. While functionally useful, it does not adequately allow comparison between two different sources. A signal response from one source may be comparable to another source without actually performing at optimal settings. Spray images taken using the microscope can supplement the information gained from signal optimization and help reduce the number of variables present by clarifying the nature of the spray on the surface. I predict that the conditions among different sources that give similar spray profiles will produce similar signals in the mass spectrometer. Even if a test of this hypothesis gives negative results, it will indicate different mechanisms in different sources. By comparing changes in the spray between two sources and the corresponding signal, we can also investigate which components of the spray make the most important contribution to the signal (such as rivulet generation, film composition, and removal rate).

4.1.2 Experimentation

The following is a brief list of some of the potential experiments that could be performed for study of the hard variables. Although the combination of parameters can be extensive, initial experimentation should remain fairly simple. Each of the following experiments could be performed under different conditions, but for initial research and discussion of each, I propose a single variation and discuss the potential experiments with regard to operation.

The suggested conditions for source comparison can be found in Table 4-2. My previous work was done with a solvent capillary and a small nebulizing capillary. To perform the comparison, a second DESI source would be constructed using the exact same setup with the exception of a larger outer capillary. The effective annulus for the nebulizing gas would be double the size of the first. The following sections contain experiments that would provide additional insight into the dependence of flow rate on capillary dimensions and are suggested to be used in conjunction with the proposed parameters in Table 4-2.

		Length (µm)	Area (m^2)	Annulus Size (m^2)
Inner Capillary	OD	150	$7.07*10^{-8}$	
Small Outer Capillary	ID	250	$1.96*10^{-7}$	$1.25*10^{-7}$
Large Outer Capillary	ID	320	$3.22*10^{-7}$	$2.51*10^{-7}$

Table 4-2. List of parameters proposed for the source comparison experiments. Two separate sources would be constructed, each with the same size inner capillary.

4.1.2.1 Mass Flow vs. Back Pressure

It would be very simple and informative to compare the two proposed sources using a mass flow control on both and then removing the mass flow control and comparing the DESI sources using back pressure. It would be necessary to measure the linear velocity with a technique such as Doppler particle analysis (see Section 1.3.3.2 for details) to compare the two sprays. With the two sources, a correlation could be generated between changes in pressure and mass flow with linear velocity.

4.1.2.2 Protrusion Distance

The distance the inner capillary protrudes from the outer capillary affects the spray profile. This effect is likely dependent on the dimensions of the capillaries in addition to the protrusion

distance. Generally, the farther the inner capillary protrudes from the outer, the more elongated the spray profile becomes. If the elongation is due to more solvent present from less evaporation, the effects on the profile of different sized annular regions at constant pressure should be similar, and would be reflected in the absolute signal in the experiment.

4.1.2.3 Height Experiment

The rivulet experiment documented the changes to our DESI spray profile as the source was lowered toward the surface. Typically, sources made from larger capillaries are operated at greater distances and higher flow rates. Because spray height usually has a curved response with a local maximum in signal, a comparison of height vs. signal would be very informative. Along with imaging at various heights, the experiment might be enhanced by also varying solvent flow rates to compensate for evaporation. This would provide answers to questions such as: Are the local maxima at spray height dependent on the nature of the spray or simply a function of the amount of solvent delivered to the surface? Do similar spray profiles (produced at different heights) by the individual sources produce similar signal? I expect that if different sources produced similar spray profiles and similar rivulet behavior, then they would produce a similar signal. Such a comparison could help create a new set of identifiers for comparing DESI parameters.

4.1.2.4 Solvent Experiment

As explained in Sections 3.3.2.2 and 3.3.2.3 the volatility of a solvent changes the behavior of the source at different operating parameters. Sometimes large differences in solvent composition are reported for the same source with different analytes.[2] The optimal solvent is

undoubtedly dependent on analyte solubility, but may also depend on source construction. If volatility of a solvent plays an important role in the delivery of the solvent, then the proposed variation in nebulizing capillary diameter listed in Table 4-2 should also make a difference. A perfectly adequate solvent for one source may evaporate too quickly to be useful on another source (without adjusting many other parameters to compensate).

4.1.2.5 Others

The four experiments listed above provide a useful starting point for comparing hard parameters. These two nebulizing capillary sizes constitute only a small fraction of the possible combinations that could be compared between hard and soft variables. It is likely that a trend will emerge when testing these parameters that will clarify which parts of the DESI setup contribute the most to the signal. These results could be used to further optimize DESI sampling based on the analyte.

4.2 Doppler Experiments

As noted in the previous section, the source construction determines the behavior of the nebulizing gas. Unlike the other parameters listed in Table 4-1, the method for reporting the nebulizing gas setting has varied among research groups. The differences are the result of controlling the nebulizing gas flow by adjusting the back pressure or by directly controlling it with a mass flow controller. Because mass flow and back pressure cannot easily be compared, a different parameter such as linear velocity would be a better measure as it is taken independently of source construction. Unfortunately, linear velocity cannot be calculated independently from the source dimensions. In the cases[1, 4] where the linear velocity has been

reported, it is not stated how the data were acquired, but linear velocity has been acquired experimentally with phase Doppler particle analysis (PDPA).[11]

A microscopic investigation of DESI is an important part of understanding the DESI source, but it is not enough to characterize the behavior of the nebulizing gas. The nebulizing gas effects on the DESI source as a whole have not been addressed. As discussed in the previous section, differences in source construction create differences in the spray profile. In addition to imaging the profile, the nature of the droplets created by DESI should be studied as a function of the source construction. This can be done by a Doppler particle analysis. Unlike the previous Doppler experiment, the images on the surface can be used to identify correlations between the spray profile and droplet generation.

Not only can Doppler analysis be used to construct a more accurate image of how droplets are generated from the spray, but it can also be used to test the rivulet dissociation mechanism proposed in Chapter 3. We have created circumstances in which droplet splashing cannot create secondary droplets for analyte transfer. It would be informative to see (using PDPA) if droplet generation also occurs from large rivulets. If droplets are not generated from rivulets (such as ion ejection), the mechanism for transport via rivulets needs to be examined. If droplets are generated from rivulets (such as fragmentation), it is possible that the ions detected by the previous measurements made by the Cooks group were not indicative of splashing, but of droplets generated from the rivulets.

Either case presents an opportunity for better understanding the DESI mechanism. These Doppler experiments may also be enhanced by using a simple barrier as was done in both previous experiments. It would be beneficial to reproduce the Doppler work[11] done by the

Cooks group and then add a barrier to the source and see the number of droplets removed from the system based on the barrier's location. This quantity and location of secondary droplet generation could also be measured by spraying glass slides with small orifices centered at the point the spray impinges on the slide. Presumably, a large orifice would decrease the available area and result in fewer droplets. A calibration curve of droplet generation could then be constructed using orifices of increasing size.

4.3 Alternate Surfaces

I began work on alternate surfaces after the initial paper on glass surfaces in *Analytical Chemistry*. The area has potential, but working with surfaces proved far more complex than I anticipated. I feel that this area of work has great potential, but without a better understanding of surface chemistry and without the proper equipment, it is not possible. I explain here what work has been done and what still needs to be done to complete the work.

4.3.1 Introduction

Our previous imaging work was performed on glass surfaces. While glass is one of the most common substrates to use, and the most common transparent surface, it is very different from other DESI surfaces such as Teflon. The hydrophobic nature of Teflon is attractive as a DESI substrate because it provides a useful surface for spotting polar solvents. When spotting on Teflon with a polar solvent, a droplet forms that does not spread out across the surface as it does on glass. As the solvent evaporates, the dissolved analyte is concentrated in a small spot, which greatly improves the detection limit of a sample over a similar spot on glass.

Unfortunately, our setup is not capable of online imaging of DESI on Teflon. Because Teflon is one of the most common DESI surfaces, it is important to consider alternatives for imaging projects that can provide insight into the differences between glass and surfaces similar to Teflon. The two factors that are most likely to contribute to these differences in the DESI mechanism are the polarity of the surface and the texture. The texture of the Teflon surface is difficult to reproduce and would result in a poor imaging surface even with a transparent material. The non-polar nature of the Teflon surface is easier to produce than the texture, and is found in a variety of other substances like plastics or materials that have been functionalized with long carbon chains.

Quartz slides functionalized with C18 were chosen to be the best candidate for comparison to my previous imaging work done on glass slides. This was done for a number of reasons. Quartz microscope slides were readily available for purchase and the functionalization of quartz was both well known and fairly simple. The C18 coated surfaces I created were transparent for imaging, easily cleaned, and extremely hydrophobic with contact angles above 110°. I expected that real time imaging of C18 coated and uncoated slides would reveal differences in the spray footprint caused by the substitution of a hydrophobic surface for the untreated glass surfaces. I also expected the change in surface to contribute to differences in desorption and ionization.

4.3.2 Previous work

4.3.2.1 Surface Preparation

Quartz microscope slides (25 x 75 x 1 mm) were purchased from Quartz Scientific Incorporated.

Each quartz slide was cleaned in piranha solution, rinsed with water, methanol, ethanol, and toluene. Each slide was then submerged in a 0.75% v/v Trichlorochloro-octydecyl-silane/toluene solution for 48 h. The slides were then removed, rinsed with water and methanol and rubbed with Kimwipes to remove any white films that had formed on the surface. The coated surfaces were then characterized on a contact angle goniometer. Each slide had a contact angle between 112-116°.

4.3.2.2 Dye Coating

While the preparation of the C18 slides was fairly simple, due to research on functionalizing fused silica columns, very little information existed on creating non-covalent coatings on non-polar surfaces. The dyes that had been used for imaging on glass were fairly polar and readily soluble in water and methanol. As expected, dipping a C18 coated slide into a concentrated solution of these dyes did not result in much dye covering the surface. This 'coating' was barely visible and was not useful for imaging.

Non-polar dyes exist, and would produce a better coating on a C18 surface when used for dipping with a different solvent. A non-polar dye and solvent pair would not work well on a glass surface, making it impossible for comparison of polar and non-polar surfaces. Additionally, DESI is performed with polar solvents that would not be very effective in dissolving or desorbing the non-polar dye from the surface, a necessary requirement for DESI ionization.[12] The possibility of using a molecular dye that was large enough to have both polar and non-polar ends was considered. Acridine orange was tested as a possible candidate, but did not work with DESI on either surface.

Spotting the surface with dye and allowing it to evaporate created a 'coffee ring' shape where the majority of the deposited analyte gathered at the edges of the spot. This method was effective for detection of the analyte from the surface (similar to both glass and Teflon), but was not effective for imaging. The coffee ring spots were too thick for fluorescence and showed almost no change during sampling. Additionally, rivulets on the C18 surface were difficult to see with the microscope as they were both smaller and traveled faster across the surface. To image the rivulets, RBB was dissolved into a 50:50% water/methanol solution and sprayed on a C18 slide. Figure 4-1 is an image of a 10 s time averaged fluorescent image of the DESI spray on C18.

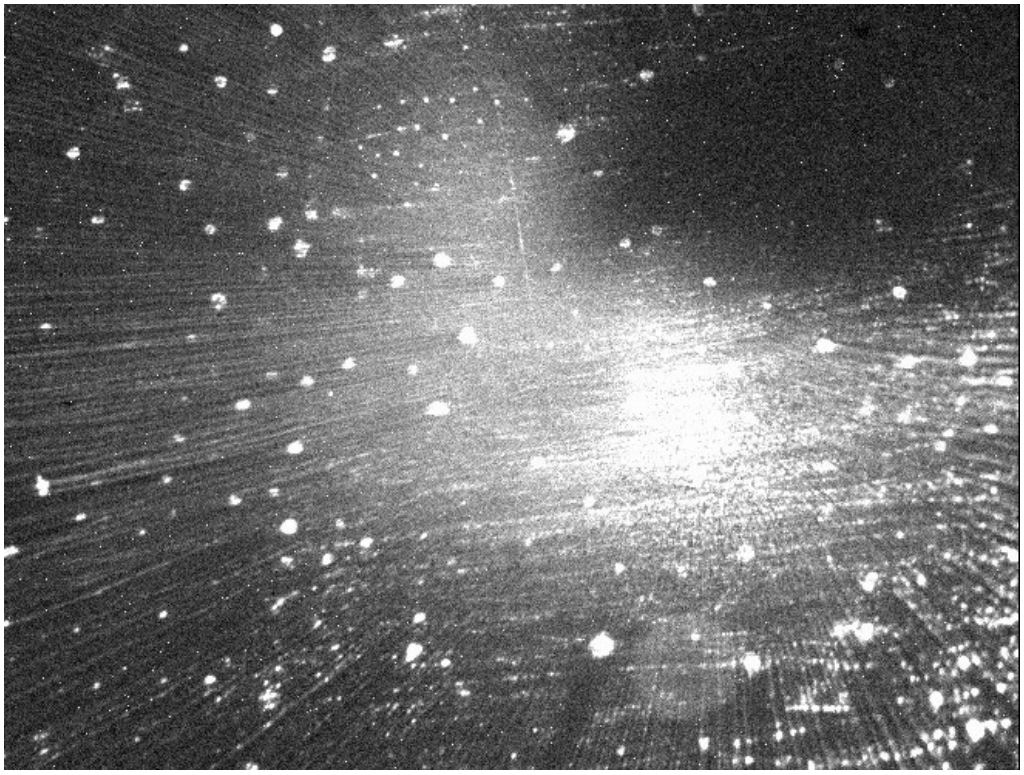

Figure 4-1 Fluorescence image of the DESI spray containing RBB on C18 coated quartz. Exposure for 10s with no gain, contrast adjusted to show the rivulets, 4x magnification.

Figure 4-1 shows a stark difference from DESI on glass surfaces. One of the chief differences exists in the rivulets. Due to hydrophobic interaction between the surface and the solvent, far more rivulets form. These rivulets are much smaller in size and travel faster than those produced on untreated glass, resulting in straighter paths and a much larger footprint. Because of their smaller size, it is difficult to image the DESI spray with short exposure times.

Green et al. published a paper on reproducible coatings using a vacuum coater with Rhodamine B dye.[7] Our research group did not have the funds to purchase a vacuum coater, but we felt that it would be possible to perform a vapor deposition on the coated slides with a custom setup. RBB dye was placed inside of a glass container and covered with a metal plate. The metal plate had a slit cut in it that was roughly 10 x 50 mm. The quartz slides were placed on top of the open slit above the RBB dye and then covered with a beaker containing ice water. The entire setup was then placed on a hot plate and heated for 10 min at 225 °C. The RBB melted, evaporated, and deposited where it came in contact with the cooled slide.

This method of coating produced a fairly homogenous coating of RBB on the surface, but was not without defects. One of the major problems was that the slide would usually coat with a gradient. The reproducibility of the coatings suffered correspondingly, which limited the comparison between two slides. In some cases, the coatings were very thick and not easily removed by DESI. When the method was repeated on glass, I found that the slides did not coat at the same rate. Figure 4-2 is a picture taken of two slides coated together using the vapor deposition setup. The left slide has a C18 layer and the right slide is made of glass. Faced with the fact that the RBB deposition varies between C18 coated and uncoated slides, as well as the other difficulties presented above, I elected to leave the project for future work.

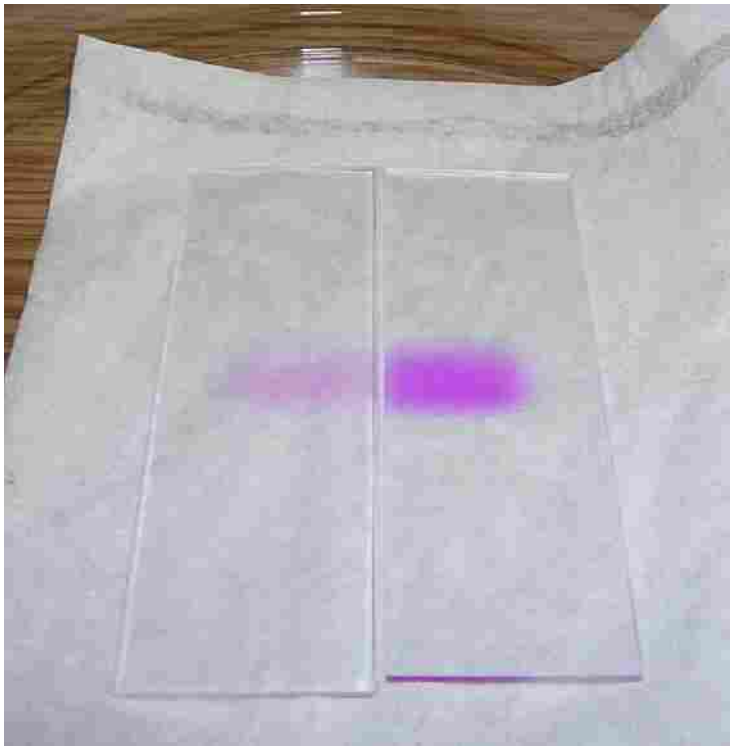

Figure 4-2 Vapor deposition coating performed simultaneously on two slides. The C18 coated slide (left) has far less dye on it than the standard glass slide (right).

4.3.3 Future Non-polar Surface Work

To hasten the work on non-polar surfaces, a vacuum coater should be acquired that is capable of creating coatings on microscope slides. The vacuum coater would be used to create RBB coatings on both C18 and glass slides. Even though the slides do not coat at the same rate, the reproducibility in coatings could be used to generate calibration curves for each surface type using fluorescence and microscopic imaging.

With proper coating, the experiments from the first chapter could be repeated with the C18 coated surfaces. Thick coatings of CV could be used for high speed imaging and

simultaneous experiments, and RBB would be used for shutter experiments. Both dyes could be used for rivulet experiments. These methods could be extended to other surfaces such as PMMA and PDMS to see if differences existed due to varying polarity of the surface.

4.4 Specialized Surfaces

An understanding of DESI on plastic surfaces can naturally be extended to the realm of machined plastics. The rivulet dissociation mechanism, in particular, opens up many interesting possibilities for specialized surfaces with DESI.

4.4.1 Microfluidic Work

Microfluidic devices are a rapidly growing area of separations. Most detection done on microfluidic devices is done through fluorescence imaging. Because most of the biological molecules used in microfluidic separations are not fluorescent, fluorescent labels or tags must be attached to the analyte prior to separation. While highly sensitive, fluorescent labels are not without problems. Some molecules do not 'tag' well and some labels take as much as 24 h to bind to the molecules of interest.

In recent years, microfluidic devices have been coupled with electrospray ionization for an alternate form of detection.[13] The electrospray ion source is highly compatible with microfluidic chips because both are solvent based. When coupled to a microfluidic device, the mass spectrometer acts as a detector for the separations, avoiding the need to label proteins with fluorescent tags. Like ESI, DESI could be coupled with microfluidic devices for online detection without the use of fluorescence.

Because DESI is also a solvent based technique, the possibility of combining it with microfluidics should be explored. Microfluidic separations do not occur on the surface, but take advantage of special fluid/surface interactions that occur in small channels with applied voltages. These channels, however, are connected between wells that are open to the surface. The size and shape of these wells provide an ideal point for detection of components contained therein. Typically, the analyte does not reach the wells in a microfluidic separation. Despite the fact that these wells normally do not contain analyte, it would be of interest to determine if DESI is capable of detecting sample from within the wells. Based on the results of such a study, it may be valuable to know the limitations and possible uses of DESI in conjunction with microfluidic devices.

4.4.2 Channel Work

Almost all DESI discussed in this dissertation has involved sampling from flat surfaces. The rivulet dissociation mechanism provides an interesting alternative to the droplet ejection model and can be exploited to take advantage of ionization from rivulets through the use of machined surfaces. One of the results of operating DESI on a flat surface is the 'washing' of the analyte downstream from the spray location. This process results in complete removal of the sample over time. It should be possible to design a modified surface that limits the amount of analyte washed downstream and that promotes the concentration down field to prolong signal and improve detection limits.

The simultaneous experiment revealed analyte migration from outside the spray profile. This migration was most likely caused by droplets falling outside the central region. This migration resulted in prolonged signal despite removal of the CV dye from the central elliptical

region. This behavior might be exploited to direct the dye movement to a single location through alterations to the surface. Figure 4-3A is an illustration of a conceptual 'well' that could be machined into glass or plastic that would reduce the amount of analyte that is washed outside of the spray footprint. The bowl shape of the well would cause excess solvent with dissolved analyte to move towards the central elliptical region. The pointed end of the well would direct the rivulets into a single location, concentrating the analyte in the center of the channel as the rivulets evaporated. By providing a single location for the concentration of the analyte, the channel would prolong the solvent interaction with the analyte. Due to the speculative nature of the behavior of the solvent in the well, it would be difficult to predict the correct size. It would be informative to experiment with various sizes of well compared to the size of the spray footprint.

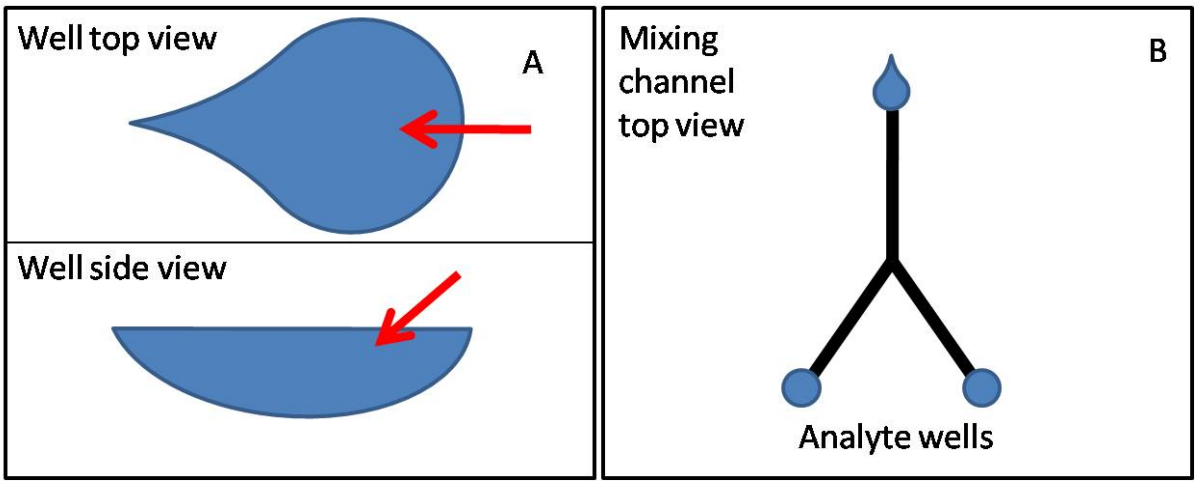

Figure 4-3 (A) Conceptual design for specially machined surface wells with the DESI spray originating from the right of the image. The well is pointed to concentrate displaced analyte downstream for continued sampling by rivulets. The well is also bowl shaped to reduce the washing effect and drive solvent to the middle. The red arrow reflects the direction of the spray (B) Machined channels designed to promote analyte mixing for kinetic studies.

Using the microscope, the effects of shape and size on sample migration and total effective sampling could be examined. Through an iterative process, the design of the wells could be changed to explore the contributions of deeper wells or additional points at the end of the well.

Experimentation with specialized surfaces could lead to interesting side projects outside the realm of analytical chemistry. One such area is kinetic investigation of mixing solutions in which DESI is used as a detector for mixing two solutions. The quantity of analyte used in microfluidics may below the detection limits of DESI. At a slightly larger scale, such as the mesofluidic range, the machined channels could be used in conjunction with pumps and a DESI source for miniature mixing chambers. Figure 4-3B shows a conceptual image of such a mixing chamber. Such a reaction vessel could be used continuously in conjunction with DESI. While such a chamber could be created with an electrospray system, the system would need to be subject to a continuous voltage across the channel. This constant voltage could promote unwanted electrochemistry in the system which must be accounted for.[14] While DESI does create a localized charge, the entire system would not be subject to the same potential as it would under ESI. Using traditional pumping methods and the DESI source as a detector, a microfluidic (or mesofluidic) device may be a useful tool for kinetic experiments.

4.5 Chemical Imaging

4.5.1 Introduction

As discussed in Chapter 1, DESI has been shown to be a valuable tool for chemical imaging. By combining the DESI source with the microscope, we have an extra advantage for investigating the capabilities of DESI through real time chemical imaging of samples. While imaging will

require transparent samples to make use of the microscope, these studies will help clarify the resolution of the DESI source in imaging studies. Both the Cooks and Van Berkel groups have published studies on improving the resolution of chemical imaging with DESI.[3, 15] While these studies were performed on flat printed surfaces, neither of publication took into account the contour of the surface itself when considering resolution. This is important because many samples imaged chemically have not been perfectly flat. Published DESI imaging of biological tissues such as the mapping of antifungal chemicals in seaweed[16] and of proteins in rat spinal tissues[17] are very likely to be influenced by the contour of the surface. Because we have shown that rivulets play an important role in ionization, rivulet formation and direction should be considered when dealing with all non-flat surfaces.

To study the contribution of contour on imaging resolution, machined surfaces could be created to test the actual imaging capability of the system. This would provide a valuable resource for the current DESI imaging community by clarifying the actual imaging power of DESI on natural samples.

4.5.2 Imaging Experiment

4.5.2.1 Hardware Modifications

For chemical imaging, our system needs to be adapted in several ways:

1. The microscope needs to be fitted with an automated stage that can perform the rastering necessary for proper chemical imaging.[18]
2. We need a computer with software capable of constructing 2D images from MS data generated by the Xcalibur software package.

3. A modification must be made to our DESI transfer line so that it does not make contact with the surface being imaged.

4.5.2.2 Sample Preparation

To test the effects of surface contours on DESI performance, special surfaces will need to be prepared. These samples will need to be machined to precise specifications. In addition, a method for precisely printing or coating the surface with an analyte needs to be found. The following theoretical experiments are dependent on such samples. Both the Cooks and the Van Berkel resolution papers have used printers than can produce lines as narrow as 100 µm. To test the effects of surface contour on resolution, channels with these dimensions must be created on our sample surfaces.

Even with artificially-created channels it will be necessary to precisely coat the slides with the sample analyte. It may be possible to image a single analyte, so long as it is possible to exclude it from either the channel or the surface. An ideal situation would be one where a single analyte can be placed within the narrow channel while a second analyte is placed on the surface.

4.5.2.3 Single Groove Surface

The simplest of the contour imaging experiments could be performed on a surface with a single groove cut in it. The channel would contain an analyte such as RBB. Images would be created by scanning across the channel in various directions and comparing the reported resolution to the coating thickness, which would be dependent on the channel dimensions. This process could then be repeated with the analyte on the surface and none in the channel.

4.5.2.4 Variable Width Channels

I have seen minor flaws in coatings that alter the flow direction of a single rivulet. The width of a channel most likely has an effect on the resolution of the DESI spray. To compare the effect of channel width on resolution, I would prepare a single surface with multiple channels of increasing width. I would then scan across the channels and record the resolution achieved with a DESI scan.

4.5.2.5 Variable Depth Channels

If the channels were too deep for the rivulets to effectively escape, the resolution would be affected. To determine the effect of channel depth on resolution, I would prepare a single surface with multiple channels of increasing depth. I would then scan across the channels and record the resolution.

4.5.2.6 Surface Variations

Because chemical imaging of tissues is performed on heterogeneous surfaces, it is unlikely that the surface–solvent interaction will be exactly the same across the entire surface of an imaged sample. Section 4.3.2.2 discusses the differences between the behavior of the DESI spray on a hydrophobic surface and its behavior on untreated glass. To study the effects of the surface polarity on imaging resolution, a narrow strip of C18 could be functionalized onto a quartz slide, and then coated with an analyte using a vacuum coating system. When chemically imaged, such a surface should produce a featureless image when corrections for coating differences on C18 vs. quartz are applied. If the image is not featureless, then the polarity of the surface needs to be considered as well for chemical imaging.

4.6 Conclusions

Research by various groups has been performed to characterize the DESI source through parameter optimization. The Farnsworth group has now also characterized the source by imaging the spray on glass surfaces. There still remain many experiments that can utilize this unique combination of inverted microscope and DESI source. The studies proposed here provide many opportunities to further clarify the DESI mechanism and improve certain areas of application through real time and chemical imaging of surfaces.

4.7 References

1. Van Berkel, G. J.; Ford, M. J.; Deibel, M. A., Thin-Layer Chromatography and Mass Spectrometry Coupled Using Desorption Electrospray Ionization. *Analytical Chemistry* **2005,** *77* (5), 1207-1215.
2. Takáts, Z.; Wiseman, J. M.; Cooks, R. G., Ambient Mass Spectrometry using Desorption Electrospray Ionization (DESI): Instrumentation, Mechanisms and Applications in Forensics, Chemistry, and Biology. *Journal of Mass Spectrometry* **2005,** *40* (10), 1261-1275.
3. Ifa, D. R.; Wiseman, J. M.; Song, Q.; Cooks, R. G., Development of Capabilities for Imaging Mass Spectrometry Under Ambient Conditions with Desorption Electrospray Ionization (DESI). *International Journal of Mass Spectrometry* **2007,** *259* (1-3), 8-15.
4. Cotte-Rodríguez, I.; Takáts, Z.; Talaty, N.; Chen, H.; Cooks, R. G., Desorption Electrospray Ionization of Explosives on Surfaces: Sensitivity and Selectivity Enhancement by Reactive Desorption Electrospray Ionization. *Analytical Chemistry* **2005,** *77* (21), 6755-6764.
5. Wood, M. C.; Busby, D. K.; Farnsworth, P. B., Microscopic Imaging of Glass Surfaces under the Effects of Desorption Electrospray Ionization. *Analytical Chemistry* **2009,** *81* (15), 6407-6415.
6. Nyadong, L.; Green, M. D.; De Jesus, V. R.; Newton, P. N.; Fernandez, F. M., Reactive Desorption Electrospray Ionization Linear Ion Trap Mass Spectrometry of Latest-Generation Counterfeit Antimalarials via Noncovalent Complex Formation. *Analytical Chemistry* **2007,** *79* (5), 2150-2157.
7. Green, F. M.; Stokes, P.; Hopley, C.; Seah, M. P.; Gilmore, I. S.; O'Connor, G., Developing Repeatable Measurements for Reliable Analysis of Molecules at Surfaces Using Desorption Electrospray Ionization. *Analytical Chemistry* **2009,** *81* (6), 2286-2293.
8. Leuthold, L. A.; Mandscheff, J.-F.; Fathi, M.; Giroud, C.; Augsburger, M.; Varesio, E.; Hopfgartner, G., Desorption Electrospray Ionization Mass Spectrometry: Direct Toxicological Screening and Analysis of Illicit Ecstasy Tablets. *Rapid Communications in Mass Spectrometry* **2006,** *20* (2), 103-110.

9. Bereman, M. S.; Williams, T. I.; Muddiman, D. C., Carbohydrate Analysis by Desorption Electrospray Ionization Fourier Transform Ion Cyclotron Resonance Mass Spectrometry. *Analytical Chemistry* **2007,** *79* (22), 8812-8815.
10. Ma, X.; Zhao, M.; Lin, Z.; Zhang, S.; Yang, C.; Zhang, X., Versatile Platform Employing Desorption Electrospray Ionization Mass Spectrometry for High-Throughput Analysis. *Analytical Chemistry* **2008,** *80* (15), 6131-6136.
11. Venter, A.; Sojka, P. E.; Cooks, R. G., Droplet Dynamics and Ionization Mechanisms in Desorption Electrospray Ionization Mass Spectrometry. *Analytical Chemistry* **2006,** *78* (24), 8549-8555.
12. Green, F. M.; Salter, T. L.; Gilmore, I. S.; Stokes, P.; O'Connor, G., The Effect of Electrospray Solvent Composition on Desorption Electrospray Ionisation (DESI) Efficiency and Spatial Resolution. *Analyst* **2010,** *135* (4), 731-737.
13. Sung, W.-C.; Makamba, H.; Chen, S.-H., Chip-based Microfluidic Devices Coupled with Electrospray Ionization-mass Spectrometry. *ELECTROPHORESIS* **2005,** *26* (9), 1783-1791.
14. Kertesz, G. J. V. B.; Vilmos, Using the Electrochemistry of the Electrospray Ion Source. *Analytical Chemistry* **2007,** *79* (15), 5510-5520.
15. Kertesz, V.; Van Berkel, G. J., Improved imaging resolution in desorption electrospray ionization mass spectrometry. *Rapid Communications in Mass Spectrometry* **2008,** *22* (17), 2639-2644.
16. Lane, A. L.; Nyadong, L.; Galhena, A. S.; Shearer, T. L.; Stout, E. P.; Parry, R. M.; Kwasnik, M.; Wang, M. D.; Hay, M. E.; Fernandez, F. M.; Kubanek, J., Desorption Electrospray Ionization Mass Spectrometry Reveals Surface-mediated Antifungal Chemical Defense of a Tropical Seaweed. *Proceedings of the National Academy of Sciences* **2009,** *106* (18), 7314-7319.
17. Girod, M.; Shi, Y.; Cheng, J.-X.; Cooks, R. G., Desorption Electrospray Ionization Imaging Mass Spectrometry of Lipids in Rat Spinal Cord. *Journal of the American Society for Mass Spectrometry* **2010,** *21* (7), 1177-1189.
18. Kertesz, V.; Van Berkel, G. J., Scanning and Surface Alignment Considerations in Chemical Imaging with Desorption Electrospray Mass Spectrometry. *Analytical Chemistry* **2008,** *80* (4), 1027-1032.

5 Appendix

Glossary of Abbreviations

BNC - Bayonet Neill–Concelman
C18 – Carbon 18
CCD – Charged coupled device
CV – Crystal Violet
DART – Direct analysis in real time
dc-DESI – Dual capillary DESI
DESI – Desorption electrospray ionization
ELDI – Electrospray-assisted laser desorption ionization
ESI – Electrospray Ionization
ESSI – Electrosonic spray ionization
FS – Fused silica
GI – Geometry independent
ID – Inner diameter
MALDESI – Matrix assisted laser desorption electrospray ionization
MALDI – Matrix assisted laser desorption ionization
MS – Mass Spectrometry
OD – Outer diameter
PCI – Peripheral component interconnect
PDPA – phase Doppler particle analysis
PEEK – Polyether ether ketone
PFA – perfluoroalkoxy
PML – Precision Machining Laboratory
PP – Polypropylene
ppm – parts per million
psi – Pounds per square inch
RBB – Rhodamine B Base
SSI – Sonic spray ionization
SIM – Selected ion monitoring
SIMS – Secondary ion mass spectrometry
TLC – Thin layer chromatography